Theoretical Oceanography
Lecture Notes Master AO-W27

Martin Schmidt

[1] *Leibniz Institute for Baltic Sea Research Warnemünde,*
Seestraße 15, D - 18119 Rostock, Germany,
Tel. +49-381-5197-121, e-mail: martin.schmidt@io-warnemuende.de

The general outline of this lesson is based on the lessons of Wolfgang Fennel and the book "Analytical theory of forced oceanic waves".

April 2, 2014

Contents

Chapter 1

Responses of a stratified ocean to wind forcing

1.1. Basic equations and approximations

1.1.1. The linearized Boussinesq approximation

The aim of this section is the simplification of the non-linear hydrodynamic equations toward a linearized version suitable for analytical solution.

We recall the equations of motion for an incompressible fluid on an rotating sphere,

$$\rho\frac{d}{dt}\overrightarrow{v} + 2\rho\overrightarrow{\Omega}\times\overrightarrow{v} = \rho\overrightarrow{g} - \nabla P + \eta_{vis}\Delta\overrightarrow{v} + \overrightarrow{F}^{ext}, \tag{1.1}$$

$$\frac{d}{dt}\rho = \frac{\partial}{\partial t}\rho + \overrightarrow{v}\cdot\nabla\rho = 0, \tag{1.2}$$

$$\nabla\cdot\overrightarrow{v} = 0. \tag{1.3}$$

These equations are completed by advection-diffusion equations for the potential or conservative temperature and salinity and the equation of state

$$\rho = \rho(T, S, P). \tag{1.4}$$

These equations of motion are non-linear and difficult to solve. Generally, this is only possible with numerical methods.

From observations we know, that the ocean state variables $\mathbf{u}$, T and S are changing slowly and vary only slightly around some "average state. We are interested in the deviations from this "average state, which is usually much smaller than the state variable itself. This helps us to develop systematic approximations to simplify our equations. Later, after introducing also simplifications for the ocean geometry, even analytical solution can be gained, which are of great value to understand the basic principles of ocean dynamics.

In the previous lessons we considered mostly elevations of the ocean surface. Now we elevate also internal surfaces, i.e. isopycnals.

Hence, let us start the consideration with an "ocean at rest. The variables corresponding to this special state are denoted with a subscript '0'. For an ocean at rest a vertical stratification is established and the remaining equation of motion reads

$$\rho\overrightarrow{g} = \nabla P = \nabla p_0 \tag{1.5}$$

The gravity force is balanced by the vertical pressure gradient and the horizontal pressure gradient vanishs. This implies, that the density depends on the vertical coordinate only,

$$\frac{\partial}{\partial z}p_0 = -g\rho_0(z), \qquad \frac{\partial}{\partial x}p_0 = 0, \qquad \frac{\partial}{\partial y}p_0 = 0, \qquad \frac{\partial}{\partial t}\rho_0 = 0. \tag{1.6}$$

The equilibrium density does not change with time, which is a consequence of the adiabatic approximation made in the continuity equation, which excludes thermal expansion.

We want to consider ocean responses to forces elevating isobars from this state of rest. As long as the elevation is small, the main density variation is still vertical and density and pressure variations are a small perturbation:

$$\rho(x,y,z,t) = \rho_0(z) + \rho'(x,y,z,t), \tag{1.7}$$
$$p(x,y,z,t) = p_0(z) + p'(x,y,z,t). \tag{1.8}$$

Hence, with

$$\rho = \rho_0\left(1 + \frac{\rho'}{\rho_0}\right), \tag{1.9}$$

we have found a quantity suitable to linearize and, hence, to simplify the equations of motion. With

$$\frac{1}{\rho}\left(\rho\vec{g} - \nabla p\right) = \frac{1}{\rho}\left(\rho_0\vec{g} + \rho'\vec{g} - \nabla p_0 - \nabla p'\right) = \frac{1}{\rho}\left(\rho'\vec{g} - \nabla p'\right) \approx \frac{1}{\rho_0}\left(\rho'\vec{g} - \nabla p'\right), \tag{1.10}$$

the equations of motion can be linearized with respect to density perturbations,

$$\frac{d}{dt}\vec{v} + 2\vec{\Omega} \times \vec{v} = \frac{\rho'}{\rho_0}\vec{g} - \frac{1}{\rho_0}\nabla p' + \nu\Delta\vec{v} + \frac{1}{\rho_0}\vec{F}^{ext}. \tag{1.11}$$

Velocity is of the same order as the density perturbation. Hence, the linearized equation of continuity becomes

$$\frac{\partial}{\partial t}\rho' + w\frac{\partial}{\partial z}\rho_0 = 0, \tag{1.12}$$

changes in the density distribution are solely caused by vertical elevation of isopycnals.

Introducing the buoyancy,

$$b = -g\frac{\rho'}{\rho_0}, \tag{1.13}$$

as a measure for the perturbation of the density field and the Brunt-Väisälä frequency,

$$N^2 = -\frac{g}{\rho_0}\frac{\partial}{\partial z}\rho_0, \tag{1.14}$$

as a measure for stratification, the equations of motions linearized with respect to density perturbations reads

$$\frac{d}{dt}u - fv + \frac{\partial}{\partial x}p = \eta_{vis}\Delta u + F_x^{ext}, \tag{1.15}$$

$$\frac{d}{dt}v + fu + \frac{\partial}{\partial y}p = \eta_{vis}\Delta v + F_y^{ext}, \tag{1.16}$$

$$\frac{d}{dt}w + \frac{\partial}{\partial z}p - b = \eta_{vis}\Delta w + F_z^{ext}, \tag{1.17}$$

$$\frac{\partial}{\partial t}b + wN^2 = 0. \tag{1.18}$$

$$\nabla \cdot \overrightarrow{v} = 0. \tag{1.19}$$

The symbol p is introduced for the pressure perturbation divided by the equilibrium density, $p = p'/\rho_0$, not to be mistaken for the total pressure P in Eq. 1.1. In the vertical equation a term of the order

$$p\frac{N^2}{g} \tag{1.20}$$

is dropped. Note also the neglect of the vertical component of the Coriolis force.

This is a set of five equations defining five dynamic quantities, the zonal, meridional vertical velocity u, v and w, the elevation of isopycnals described by the buoyancy b and the pressure perturbation p.

1.1.2. The hydrostatic balance

We introduce the hydrostatic balance as a commonly used approximation for the vertical momentum equation. The reduces the set of prognostic variables. We give two types of scale arguments to identify the limits of the hydrostatic balance.

In many cases the vertical acceleration $\frac{d}{dt}w$ is small compared with the other terms in the system Eqs. 1.19. This leads us to the hydrostatic balance,

$$\frac{\partial}{\partial z}p - b \approx 0. \tag{1.21}$$

The pressure perturbation is defined solely from the elevation of isopycnals. This is a considerable simplification of our set of equations, which is very common in oceanography, but also in atmosphere physics.

Before we use it, we should investigate the limits for the applicability of this approximation. To this end we consider the Fourier transformed of the (linearized) vertical momentum equation and the buoyancy equation. With

$$A(t) = \int_{-\infty}^{+\infty} \frac{d\omega}{2\pi} e^{-i\omega t} A(\omega), \tag{1.22}$$

we find

$$-i\omega w + \frac{\partial}{\partial z}p - b = 0, \tag{1.23}$$

$$-i\omega b + N^2 w = 0. \tag{1.24}$$

and combining both equations,

$$\left(N^2 - \omega^2\right) w - i\omega\frac{\partial}{\partial z}p = 0. \tag{1.25}$$

High frequency corresponds to fast processes, low frequency and the limit $\omega \to 0$ to slowly changing or steady states. Hence, the hydrostatic approximation acts like a filter restricting the solution to frequencies $\omega^2 \ll N^2$. Hence, this approximation is a good choice when looking for slowly varying processes with frequencies below or near the inertial frequency, f. These will be of main interest in the next sections. In the Baltic Sea the Brunt-Väisälä frequency is much larger then the inertial frequency,

$$f \approx 10^{-4}\mathrm{s}^{-1} \tag{1.26}$$

$$N \approx 10^{-2}\mathrm{s}^{-1}, \tag{1.27}$$

and the hydrostatic approximation is well justified for $\omega^2 \leq f^2$.

A more general discussion of the hydrostatic approximation could be based on scale arguments. Assume that the characteristic scale of vertical and horizontal velocity are W and U, the corresponding length scales are H and L. Buoyancy and pressure have scales B and P, earth rotation F. The buoyancy equation implies the scale equation

$$\frac{B}{T} + \frac{BU}{L} + \frac{BW}{H} + N^2 W = 0. \tag{1.28}$$

If the time scale T is small enough that neither horizontal advection UT nor vertical advection WT exceeds the horizontal or the vertical length scale L and H respectively, non-linear terms are small,

$$\frac{UT}{L} \ll 1 \tag{1.29}$$

$$\frac{WT}{H} \ll 1. \tag{1.30}$$

In this case the scale B reads

$$B = N^2 WT. \tag{1.31}$$

Using similar arguments for the vertical momentum equation in combination with Eq. 1.31 gives

$$\frac{W}{T} + FU + \frac{P}{H} + N^2 WT = 0. \tag{1.32}$$

From the horizontal momentum equations an expression for the pressure scale can be gained,

$$P = FUL. \tag{1.33}$$

This corresponds to the geostrophic balance. Hence, the pressure term is by a factor L/H large than the Coriolis term. This is the reason why the Coriolis term in the vertical equation is not considered. Finally, for time scales $T \gg N^{-1}$ the first term in Eq. 1.32 is small and the remaining balance is

$$\frac{P}{H} + N^2 WT = 0. \tag{1.34}$$

This gives an estimate for the scale of the vertical velocity,

$$W = U\frac{L}{H}\frac{F}{N}\frac{1}{NT}. \tag{1.35}$$

This relation goes beyond the aspect ratio found in most text books. The vertical velocity is much smaller than the horizontal velocity not only for a small aspect ratio, but also for $N^2 \gg F^2$ and time scale exceeding $1/N$.

1.1.3. The treatment of turbulence

Applying approximations like the Boussinesq approximation, linearizion and hydrostatic approximation filters out a large part of the solution spectrum, especially the irregular small scale motion mostly called "turbulence". With the aim to describe large scale motion this seems to be a great advantage and simplification. However, this way also the mechanism for wind forcing and bottom friction would be lost. We show a systematic way to overcome this dilemma.

Um die nichtlineare Kopplung zwischen kleinskalige und großskalige Prozessen zu untersuchen, führen wir eine (etwas willkürliche Zerlegung) aller dynamischer Größen a in einen großskaligen Anteil $\bar{a}$ und einen kleinskaligen Anteil a' ein,

$$a = \bar{a} + a'. \tag{1.36}$$

Dabei soll $\bar{\ }$ eine Projektion auf den großskaligen Anteil (etwa eine Mittelung) bedeuten. Der Operator $\bar{\ }$ muß dann idempotent sein,

$$\bar{\bar{a}} = \bar{a} \tag{1.37}$$

und es gelte

$$\overline{a'} = 0. \tag{1.38}$$

Mit Hilfe der Reynolds-Regeln (Postulate)

$$\overline{cu} = c\bar{u} \tag{1.39}$$

$$\overline{u+v} = \bar{u} + \bar{v} \tag{1.40}$$

$$\overline{u\bar{v}} = \bar{u}\bar{v} \tag{1.41}$$

$$\overline{\bar{u}v'} = 0 \tag{1.42}$$

$$\overline{\bar{u}\bar{v}} = \bar{u}\bar{v}. \tag{1.43}$$

Nach Anwendung des Operators $\bar{\ }$ lauten die horizontalen Impulsgleichungen

$$\frac{\partial\bar{u}}{\partial t} + \bar{u}\frac{\partial\bar{u}}{\partial x} + \bar{v}\frac{\partial\bar{u}}{\partial y} + \bar{w}\frac{\partial\bar{u}}{\partial z} - f\bar{v} + \frac{\partial\bar{p}}{\partial x} = \frac{\partial}{\partial x}\overline{u'u'} - \frac{\partial}{\partial y}\overline{v'u'} - \frac{\partial}{\partial z}\overline{w'u'}. \tag{1.44}$$

Für die drei Impulsgleichungen haben die mittleren Beiträge der turbulenten, kleinskaligen Bewegung zu den großskaligen dieselbe Form, wie der (molekulare) stress-Tensor und werden daher oft als *Reynolds stress* bezeichnet.

Für die Terme mit $\overline{a'b'}$ kann ebenfalls eine Gleichung abgeleitet werden, die jedoch auf der rechten Seite Terme der Form $\overline{a'b'c'}$ enthält. Dadurch erhält man eine Hierarchie von Gleichungen für die Mittelwerte immer höherer Produkte der kleinskaligen dynamischen Felder.

Diese Hierarchie kann durch zusätzliche Annahmen abgebrochen werden.

- Die einfachste Näherung ist die Vernachlässigung dieser Terme, man erhält die Eulerschen Gleichungen.

- Eine Verbesserung erhält man durch Einführung empirischer turbulenter Diffusionskoeffizienten. Diese Näherung wird nachfolgend diskutiert.

- Berechnung höherer Mittelwerte, d.h. der turbulenten kinetischen Energie und ihrer Dissipationsrate (k-ε-Theorie).

Die Parametrisierung durch turbulente Diffusionskoeffizienten erfolgt in Analogie zu den dissipativen Termen in den Navier-Stokes-gleichungen,

$$-\overline{u'u'} = 2A_H \frac{\partial \bar{u}}{\partial x} \tag{1.45}$$

$$-\overline{v'v'} = 2A_H \frac{\partial \bar{v}}{\partial y} \tag{1.46}$$

$$-\overline{w'w'} = 2A_V \frac{\partial \bar{w}}{\partial z} \tag{1.47}$$

$$-\overline{u'v'} = -\overline{v'u'} = A_H \left(\frac{\partial \bar{v}}{\partial x} + \frac{\partial \bar{u}}{\partial y} \right) \tag{1.48}$$

$$-\overline{u'w'} = -\overline{w'u'} = A_V \frac{\partial \bar{u}}{\partial z} + A_H \frac{\partial \bar{w}}{\partial x} \tag{1.49}$$

$$-\overline{v'w'} = -\overline{v'u'} = A_V \frac{\partial \bar{v}}{\partial z} + A_H \frac{\partial \bar{w}}{\partial y}. \tag{1.50}$$

Betrachten wir das Integral der Impulsgleichungen über ein bestimmtes Volumen, dessen eine Grenze die Meeresoberfläche oder der Meeresboden sein soll, so ist unmittelbar klar, daß der Wert des turbulenten Reibungstensors an der Oberfläche als Randbedingung vorgegeben werden muß. Diese wird in Analogie zu der Randbedingung der molekularen Reibung geschrieben. Der turbulente, vertikale Impulsfluß ist gleich der an der Oberfläche angreifenden (turbulenten) Schubspannung $\overline{\tau}$,

$$-\overline{u'w'} = \frac{\overline{\tau}^{(x)}}{\rho_0)} \quad \text{für} \quad z = 0, \tag{1.51}$$

$$-\overline{v'w'} = \frac{\overline{\tau}^{(y)}}{\rho_0)} \quad \text{für} \quad z = 0. \tag{1.52}$$

Wenn die Berandung die Meeresoberfläche ist, ist $\overline{\tau}$ die gemittelte Windschubspannung, wenn die Berandung der Meeresboden ist, ist $\overline{\tau}$ die Schubspannung durch Bodenreibung. Die Windschubspannung läßt sich durch die Windgeschwindigkeit W parametrisieren

$$\frac{\tau^{(x,y)}}{\rho_0} = C_{10} \frac{\rho_A}{\rho_0} W^{(x,y)} |W|. \tag{1.53}$$

Die Größe C_{10} heißt drag-Koeffizient. Eine analoge Parametrisierung kann am Boden formuliert werden.

Mit obiger Parametrisierung des turbulenten Reibungstensors durch die Stromscherung der großskaligen Bewegung wird der Impulseintrag durch Wind mit der vertikalen Stromscherung verknüpft. Das ist problematisch und führt teilweise zu unrealistischen Ergebnissen. Unter dem Einfluß des Windes werden vor allem kleinskalige Bewegungen (Turbulenz) angeregt, z.B. Oberflächenwellen die sich brechen und kleinskalige interne Wellen erzeugen. Ein Beispiel für die Kopplung an großskalige Bewegungen ist die Stokesdrift, die zwar mit einer vertikalen Stromscherung einhergeht, aber nicht mit turbulenten Vermischungskoeffizienten zusammenhängt.

Die kinetische Energie der turbulente Bewegung kann abwärts propagieren. Dabei erfolgt Durchmischung, d.h. es ist Arbeit gegen die Schichtung zu leisten, die kinetische turbulente Energie wird dissipiert und in Wärme bzw. potentielle Energie umgewandelt. Dieser ständige Energieverlust der turbulenten Bewegung führt dazu, daß der turbulente durchmischte Bereich auf eine Deckschicht der Dicke H_{mix} beschränkt bleibt.

Entscheidend für die horizontale Impulsgleichung ist nicht die Impulsflußdichte selbst sonderen deren Divergenz (der Anteil der in die großskalige Bewegung pro Zeiteinheit übergeht). Diese Größe ist sehr schwer meßbar und auch theoretisch schwer zugänglich. Wichtig ist ihr Integral, der Impulsfluß durch die Oberfläche (gegeben durch die Oberfächenrandbedingung). Unterhalb der Mischungstiefe wird sie sehr klein. Da sie im Sinne einer Urache-Wirkung Beziehung von den großskaligen Stromfeldern kaum abhängt, kann die Divergenz der Impulsflußdichte als von außen aufgeprägte Volumenkraft $\mathbf{X}$ aufgefaßt werden. Ihre Tiefenabhängigkeit folgt nicht aus der großskaligen Bewegung und wird extra festgelegt werden. Ein einfacher Ansatz wäre der einer in der durchmischten Deckschicht konstanten Divergenz der Impulsflußdichte:

$$X = -\frac{\partial}{\partial z}\overline{u'w'} = \frac{\tau^{(x)}}{\rho_0}\frac{\theta\left(z+H_{mix}\right)}{H_{mix}} \tag{1.54}$$

$$Y = -\frac{\partial}{\partial z}\overline{v'w'} = \frac{\tau^{(y)}}{\rho_0}\frac{\theta\left(z+H_{mix}\right)}{H_{mix}}. \tag{1.55}$$

Das vertikale Integral ergibt gerade den Impulsfluß durch die Oberfläche.

Nach Parametrisierung der turbulenten Diffusionsterme können die Boussinesq-gleichungen wie folgt geschrieben werden:

$$\frac{\partial \bar{u}}{\partial t} + \bar{\mathbf{u}}\cdot\nabla\bar{u} - f\bar{v} + \frac{\partial \bar{p}}{\partial x} = A_H\Delta\bar{u} + \frac{\partial}{\partial z}A_V\frac{\partial}{\partial z}\bar{u} + X \tag{1.56}$$

$$\frac{\partial \bar{v}}{\partial t} + \bar{\mathbf{u}}\cdot\nabla\bar{v} + f\bar{u} + \frac{\partial \bar{p}}{\partial y} = A_H\Delta\bar{v} + \frac{\partial}{\partial z}A_V\frac{\partial}{\partial z}\bar{v} + Y \tag{1.57}$$

$$-\bar{b} + \frac{\partial \bar{p}}{\partial z} = 0 \tag{1.58}$$

$$\frac{\partial \bar{b}}{\partial t} + \bar{\mathbf{u}}\cdot\nabla\bar{b} + N^2\bar{w} = D \tag{1.59}$$

$$\frac{\partial \bar{u}}{\partial x} + \frac{\partial \bar{v}}{\partial y} + \frac{\partial \bar{w}}{\partial z} = 0. \tag{1.60}$$

Ergänzt werden diese Gleichungen durch Diffusionsgleichungen für T und s, die den Term D in der bouyancy-Gleichung bestimmen. Hier tauchen in den horizontalen Gleichungen beide Parametrisierungen des Reynoldsstresses auf. Dabei soll mit **X** allein der Impulseintrag durch den Wind beschrieben werden der in der durchmischten Deckschicht entscheidend ist. Mit A_V werden alle übrigen kleinskaligen Prozesse (barokline Instabilität, Brechnung interner Wellen o.ä.) die unterhalb der durchmischten Deckschicht zur turbulenten Diffusion von Impuls beitragen, parametrisiert. Diese Unterscheidung kann zu unsinnigen Resultaten führen, wenn nicht beachtet wird, daß die Oberflächenrandbedingung für den gesamten Reynoldsstress gilt. Wenn also **X** die Windschubspannung an der Oberfläche beschreibt, muß der Impulsfluß durch die Oberfläche infolge des diffusiven Terms mit A_V verschwinden, d.h. es muß gelten $u_z = 0$ für $z = 0$. Das ist streng nicht möglich, die im nächsten Abschnitt besprochene rigid-lid Näherung führt jedoch zu konsistenten Ergebnissen.

1.1.4. Boundary conditions

Kinematic boundary conditions

To solve partial differential equations boundary conditions are needed. Sea floor and coastlines are like rigid walls where no flow may pass through. At the moving sea surface vertical velocity and time tendency of the elevation are related.

At fixed boundaries like coasts or the sea floor, the velocity component perpendicularly to the boundary vanishes. Exceptions are under-water sources and sinks like ground water inflow or hydrothermal deep sea sources, so called “black smokers”. A general form of the boundary condition reads

$$\vec{v} \cdot \vec{n} = 0, \tag{1.61}$$

where $\vec{n}$ is the normal vector to the boundary. For our purpose a more explicit form is preferred. The sea floor is described by the equation

$$z + H(x, y) = 0. \tag{1.62}$$

Application of the operator $\frac{d}{dt}$ yields

$$w + u\frac{\partial}{\partial x} + v\frac{\partial}{\partial y}H(x, y) = 0, \quad z = -H. \tag{1.63}$$

For a flat bottom we find

$$w = 0, \quad z = -H. \tag{1.64}$$

In the limit of a vertical boundary the velocity perpendicularly to this boundary vanishes.

If the position of the boundary depends on time like for a moving sea surface,

$$z - \eta(x, y, t) = 0, \tag{1.65}$$

a similar method can be used. Application of the operator $\frac{d}{dt}$ yields

$$w - \frac{\partial}{\partial t}\eta - u\frac{\partial}{\partial x}\eta - v\frac{\partial}{\partial y}\eta = 0, \quad z = \eta, \tag{1.66}$$

or more general

$$(\vec{v} - \vec{v_s}) \cdot \vec{n} = 0, \quad z = \eta, \tag{1.67}$$

where $\vec{v_s}$ denotes the velocity of the moving surface.

This is an equation of simple shape. but non-linear and difficult to handle. Remember in the complex discussion of the surface boundary condition for wind driven gravity waves.

A second surface boundary condition applies for the pressure, the pressure at the sea surface is continuous,

$$P = P_A, \quad z = \eta, \tag{1.68}$$

where P_A is the air pressure. P_A is considered to be constant here. Applying again the the operator $\frac{d}{dt}$ and sorting orders of 'primed' terms yields

$$\frac{dP}{dt} \approx \frac{\partial}{\partial t} p' + w \frac{\partial}{\partial z} p_0 = 0, \quad z = \eta, \tag{1.69}$$

and with the hydrostatic equation at rest

$$\frac{\partial}{\partial t} p' = w \rho_0 g \quad z = \eta. \tag{1.70}$$

This is still a nonlinear problem, because the sea level η is unknown and must be determined from the pressure equation. For simplicity small sea level elevations can be assumed and the boundary conditions apply approximately at $z = 0$, the sea level at rest,

$$w = \frac{\partial}{\partial t} \eta = \frac{\partial}{\partial t} \frac{p}{g} \quad z = 0 \tag{1.71}$$

$$p = g\eta \quad z = 0 \tag{1.72}$$

Writing this as an equation for the pressure alone gives

$$\frac{\partial}{\partial t} \frac{p}{g} = -\frac{1}{N^2} \frac{\partial}{\partial z} \frac{\partial}{\partial t} p \quad z = 0. \tag{1.73}$$

Dynamic boundary conditions

Dynamic boundary conditions specify the momentum transfer (momentum flux) at ocean-land or ocean atmosphere boundaries.

1.1.5. Elimination of the buoyancy equation

Elimination of the buoyancy reduces the set of variables to 4. Three variables are defined by its time tendency, the horizontal velocity components and the pressure. The vertical velocity is diganosed from the divergency of the horizontal velocity components.

We eliminate the buoyancy from the equations. The vertical velocity reads

$$w = -\frac{1}{N^2} \frac{\partial}{\partial t} b \tag{1.74}$$

$$= -\frac{1}{N^2} \frac{\partial}{\partial z} \frac{\partial}{\partial t} p. \tag{1.75}$$

$$\frac{\partial}{\partial t} u - fv + \frac{\partial p}{\partial x} = A_H \Delta u + \frac{\partial}{\partial z} A_V \frac{\partial}{\partial z} u + X \tag{1.76}$$

$$\frac{\partial}{\partial t} v + fu + \frac{\partial p}{\partial y} = A_H \Delta \bar{v} + \frac{\partial}{\partial z} A_V \frac{\partial}{\partial z} \bar{v} + Y \tag{1.77}$$

$$\frac{\partial \bar{u}}{\partial x} + \frac{\partial \bar{v}}{\partial y} = \mathcal{Z} \frac{\partial}{\partial t} p. \tag{1.78}$$

The operator $\mathcal{Z}$ stands for

$$\mathcal{Z} = \frac{\partial}{\partial z} \frac{1}{N^2} \frac{\partial}{\partial z}. \tag{1.79}$$

1.2. Solution techniques for an ocean with a flat bottom

1.2.1. Separation of coordinates, the vertical eigenvalue problem

Die Eigenwertgleichung

Eine unmittelbare Konsequenz des ebenen Bodens ist die Separierbarkeit der vertikalen und horizontalen Koordinaten. Ein gewisses Problem stellen dabei die vertikalen Diffusionsterme dar. Wir werden sie zunächst vernachlässigen und später diskutieren.

Wir nehmen eine Lösung der Form

$$u(xyzt) = \tilde{u}(xyt)F(z), \tag{1.80}$$
$$v(xyzt) = \tilde{v}(xyt)F(z), \tag{1.81}$$
$$p(xyzt) = \tilde{p}(xyt)F(z) \tag{1.82}$$

an. Um eine Gleichung für die vertikalen Funktionen F zu gewinnen, betrachten wir die vertikalen Gleichungen. Die buoyancy b kann eliminiert werden, mit Hilfe der Kontinuitätsgleichung folgt dann

$$\frac{\partial}{\partial t} p \mathcal{Z} F = F \left(\frac{\partial \tilde{u}}{\partial x} + \frac{\partial \tilde{v}}{\partial y} \right), \tag{1.83}$$

bzw.

$$\frac{\mathcal{Z}F}{F} = \frac{\frac{\partial \tilde{u}}{\partial x} + \frac{\partial \tilde{v}}{\partial y}}{\frac{\partial}{\partial t} p}. \tag{1.84}$$

Der Operator $\mathcal{Z}$ steht für

$$\mathcal{Z} = \frac{\partial}{\partial z} \frac{1}{N^2(z)} \frac{\partial}{\partial z}. \tag{1.85}$$

Die linke Seite hängt nur von z ab, die rechte Seite ist nur einen Funktion der horizontalen Koordinaten, d.h. beide Seiten müssen konstant sein. Damit lautet die Gleichunge für F

$$\mathcal{Z}F(z) + \lambda^2 F(z) = 0 \tag{1.86}$$

mit den Randbedingungen (folgen unmittelbar aus den RB für den Druck)

$$F'(0) + \frac{N^2(0)}{g} F(0) = 0 \tag{1.87}$$
$$F'(-H) = 0. \tag{1.88}$$

Das ist ein sogenanntes Sturm -Liouville'sches Eigenwertproblem. Die Dgl. besitzt abzählbar unendlich viele Lösungen (Eigenfunktionen) $F_n(z)$ mit Eigenwerten λ_n. Die Eigenschaften der Eigenfunktionen und Eigenwerte sind gut bekannt. Insbesondere sind die Eigenfunktionen eine vollständige Basis eines Hilbertraumes, d.h. alle Funktionen (die gewisse gutartige Eigenschaften haben müssen), können nach Funktionen F_n entwickelt werden. Die Funktionen F_n sind orthogonal

$$\frac{1}{H}\int_{-H}^{0} dz F_m(z)F_n(z') = \delta_{mn}. \tag{1.89}$$

Beweisidee: Nehme die Dgl. für F_n und F_m, subtrahiere beide und nutze die Randbedingungen aus.

Die Entwicklung einer Funktion $f(z)$ hat die Form

$$f(z) = \sum_n a_n F_n(z). \tag{1.90}$$

Die Koeffizienten können mit obiger Orthogonalitätsrelation sofort bestimmt werden:

$$a_n = \frac{1}{H}\int_{-H}^{0} dz F_n(z)f(z). \tag{1.91}$$

Anschaulich kann man diese Entwicklung so verstehen, daß die Funktion $f(z)$ auf die Basisvektoren F_n projiziert wird. Die Koeffizienten a_n sind dann einfach diejenigen Anteile von $f(z$, die in die Richtung von F_n zeigen. $f(z)$ kann als

$$f(z) = \int_{-H}^{0} dz' f(z')\left(\frac{1}{H}\sum_n F_n(z)F_n(z')\right) \tag{1.92}$$

geschrieben werden. Damit bei der Zerlegung kein Anteil von $f(z)$ verloren geht, muß die Summe $\sum_n F_n(z)F_n(z')$ die Eigenschaften einer Dirac'schen Deltadistribution besitzen:

$$\frac{1}{H}\sum_n F_n(z)F_n(z') = \delta(z-z'). \tag{1.93}$$

(Vollständigkeit der Eigenfunktionen) Die Vollständigkeit und die Konvergenzeigenschaften von Reihenentwicklungen nach F_n wird durch die Parsevalsche Gleichung ausgedrückt.

$$\frac{1}{H}\int_{-H}^{0} dz f^2(z) = \sum_{mn} a_m a_n \frac{1}{H}\int_{-H}^{0} dz F_m(z)F_n(z). \tag{1.94}$$

Wegen der Orthogonalität verbleiben nur Terme mit $m = n$ in der Summe,

$$\frac{1}{H}\int_{-H}^{0} dz f^2(z) = \sum_n a_n^2. \tag{1.95}$$

Konstante Brunt-Väisälä-Frequenz

Wir untersuchen das vertikale Eigenwertproblem für das spezielle analytisch lösbare Beispiel einer konstanten BVF.

$$N(z) = const. \tag{1.96}$$

Die allgemeine Lösung der Dgl. ist

$$F(z) = A\sin(\lambda N z) + B\cos(\lambda N z). \tag{1.97}$$

Die Konstanten A, B und λ werden aus den Randbedingungen bestimmt. Einsetzen von F_n in die Randbedingungen liefert:

$$A\lambda N + B\frac{N^2}{g} = 0 \tag{1.98}$$

$$A\cos(\lambda NH) + B\sin(\lambda NH) = 0. \tag{1.99}$$

Dieses Gleichungssystem hat nur dann eine nichttriviale Lösung für A und B, wenn die Koeffizientendeterminante verschwindet, d.h.

$$\tan(\lambda NH) = \frac{N}{g\lambda}. \tag{1.100}$$

Diese Eigenwertgleichung hat abzählbar unendlich viele Lösungen, die Eigenwerte λ_n.
Näherungen:

Es gibt eine Lösung, für die $\lambda NH \ll 1$ ist. Dann kann nämlich die linke Seite entwickelt werden und es folgt der Eigenwert

$$\lambda_0^2 = \frac{1}{gH}. \tag{1.101}$$

Die Bedingung für die Gültigkeit dieser Approximation ist

$$H \ll \frac{3g}{N^2} \approx 10^5\text{m}, \tag{1.102}$$

d.h, sie ist (fast) überall im Ozean unbeschränkt gültig. Die Größenordnung von N ist 10^{-3} .. 10^{-2}s^{-1}. Ist andererseits λ sehr groß, ist die Eigenwertbedingung näherungsweise

$$\tan(\lambda NH) = 0, \tag{1.103}$$

und

$$\lambda_n = \frac{n\pi}{NH}. \tag{1.104}$$

Die Bedingung für die Gültigkeit dieser Näherung ist

$$H \ll \frac{n\pi g}{N^2} \approx n10^5\text{m}, \tag{1.105}$$

und ist damit verträglich mit der Näherung für λ_0. Mit

$$\frac{\lambda_0^2}{\lambda_n^2} = \frac{N^2 H}{n^2\pi^2 g} \approx 10^{-6}\frac{H}{n^{-2}} \tag{1.106}$$

folgt, daß λ_0 ein bis drei Größenordnungen kleiner als λ_n ist.

Die zu den Eigenwerten gehörenden Eigenfunktionen können jetzt bestimmt werden, indem A oder B mit Hilfe der Randbedingungen eliminiert wird. Es verbleibt noch eine frei wählbare Konstante, die durch Normierung festgelegt werden kann. (Das ist nicht unbedingt nötig, vereinfacht aber später die Rechnung.)

Die normierten Eigenfunktionen lauten

$$F_n(z) = \sqrt{\frac{2}{1 + \frac{\sin(2\lambda_n NH)}{2\lambda_n NH}}}\cos\left(\lambda_n N(z+H)\right). \tag{1.107}$$

Eine Vereinfachung der Normierungskonstante ergibt sich mit

$$\frac{\sin(2\lambda_n NH)}{2\lambda_n NH} \approx 1 \quad \text{für} \quad n=0 \tag{1.108}$$

$$\frac{\sin(2\lambda_n NH)}{2\lambda_n NH} \approx 0 \quad \text{für} \quad n=1. \tag{1.109}$$

Für $n = 0$ kann der Kosinus entwickelt werden und man erhält näherungsweise:

$$F_0(z) \approx 1 - \frac{N^2 H}{g}\left(\frac{z}{H} + \frac{1}{2}\left(\frac{z}{H}\right)^2\right), \tag{1.110}$$

$$F_n(z) \approx \sqrt{2}(-1)^n \cos\left(n\pi\frac{z}{H}\right). \tag{1.111}$$

F_0 hängt kaum von z ab und heißt barotrope Eigenfunktion, F_n variiert stark mit z und heißt barokline Eigenfunktion. (Die Begriffe bedürfen einer besseren Definition, später.) Es soll vorweggenommen werden, daß die Inversen der Eigenwerte $c_n = \lambda_n^{-1}$ die Rolle von Phasengeschwindigkeiten spielen, mit der sich die einzelnen vertikalen Moden der Gesamtlösung ausbreiten. Aus dem berechneten Beispiel ist ersichtlich, daß sich barotrope Signale 100 bis 1000 mal schneller ausbreiten als barokline. Für die westliche Ostsee typische Ausbreitungsgeschwindigkeiten $H = 50m$ sind

$$c_0 \approx 20\,\mathrm{ms}^-1 \tag{1.112}$$

$$c_1 \approx 0.2\,\mathrm{ms}^-1. \tag{1.113}$$

Dieser große Geschwindigkeitsunterschied berechtigt oftmals zu der Näherung, daß barotrope Signale sich (im Vergleich zu baroklinen) unendlich schnell ausbreiten $\lambda_0 = 0$. Der Eigenwert $\lambda_0 = 0$ ergibt sich, wenn die Meeresoberfläche als starr (rigid lid) angenommen wird (w=0). Diese Näherung ist immer dann sinnvoll anwendbar, wenn nach stationären Lösungen gesucht wird und die schnellen Prozesse von untergeordneter Bedeutung sind. Die vereinfachte Oberflächenrandbedingung lautet dann

$$\frac{\partial F}{\partial z} = 0 \quad \text{für} \quad z = 0. \tag{1.114}$$

Die barotrope Eigenfunktion wird

$$F_0(z) = 1. \tag{1.115}$$

Die quantitativen Änderungen der baroklinen Eigenfunktionen sind meist vernachlässigbar, der Gewinn durch Einfachheit ist oft beträchtlich.

Wir testen jetzt die Zerlegung einer Funktion nach diesen Eigenfunktion am Beispiel von

$$f(z) = \frac{\theta(z + H_{mix})}{H_{mix}}, \tag{1.116}$$

einer Näherung für den Impulseintrag in eine durchmischte Deckschicht der Dicke H_{mix}. θ ist eine Sprungfunktion

$$\theta(x) = \begin{cases} 1 & \text{für} \quad x > 0 \\ 0 & \text{für} \quad x < 0 \end{cases} \tag{1.117}$$

Die Entwicklungskoeffizienten a_n lauten

$$a_n = \frac{1}{H}\int_{-H}^{0} dz \frac{\theta\,(z + H_{mix})}{H_{mix}} F_n(z) = \frac{1}{H}\int_{-H_{mix}}^{0} dz \frac{F_n(z)}{H_{mix}}. \tag{1.118}$$

Die Ausführung der Integrale ist elementar und wir erhalten

$$a_0 = \frac{1}{H} \tag{1.119}$$

$$a_n = \frac{\sqrt{2}}{H}(-1)^n \frac{\sin\left(n\pi \frac{H_{mix}}{H}\right)}{n\pi \frac{H_{mix}}{H}}. \tag{1.120}$$

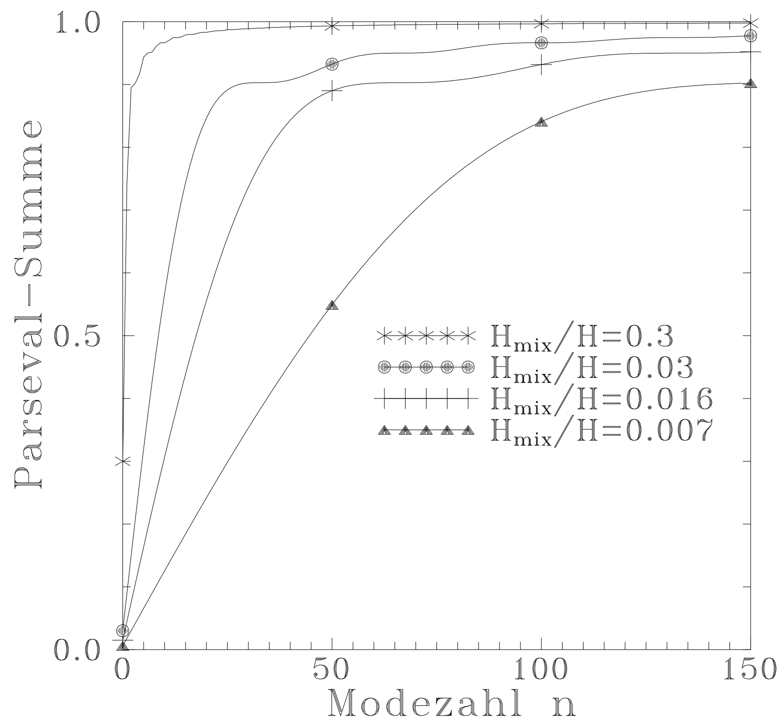

Figure 1.1. Parsevalsche Summe der Zerlegung einer Sprungfunktion nach vertikalen Eigenfunktionen

Die Konvergenzeigenschaften der Reihe können mit der Parsevalschen Gleichung beschrieben werden. Die Abbildung zeigt Partialsummen der Parsevalschen Gleichung als Funktion der Anzahl der einbezogenen vertikalen Eigenfunktionen. Dabei zeigt sich, daß unter Umständen bereits sehr wenige Moden ausreichen können während in anderen Fällen eine sehr große Zahl von Eigenfunktionen aufsummiert werden muß, bis eine befriedigende Konvergenz erreicht wird. Je feiner die vertikale Struktur der zu entwickelnden Funktion im Vergleich zur Gesamttiefe, desto mehr Eigenfunktionen werden zur Darstellung benötigt.

Näherungslösungen des vertikalen Eigenwertproblems

Ein konstante BVF ist untypisch, die Regel sind komplizierte Funktionen, die keine analytische Behandlung zulassen. Nachfolgend soll auf eine analytische Näherungsmethode (WKB-Methode) und eine numerische Lösungsmethode eingegangen werden.

Die WKB-Methode

Die WKB-(Wentzel-Kramers-Brillouin)-Methode entstammt der quantenmechanischen Streutheorie und ist dort anwendbar, wo die Welleneigenschaften der gestreuten Quantenobjekte in den Hintergrund tritt, d.h. bei hohen Relativenergien. Ein optisches Analogon ist der Übergang von der Wellenoptik zur Näherung der Strahlenoptik (Eikonalgleichung) der immer dann möglich ist, wenn Beugungseffekte vernachlässigt werden können.

Die Rechnung wird übersichlicher, wenn wir eine neue Funktion

$$Z(z) = \frac{1}{N^2}\frac{\partial F}{\partial z} \tag{1.121}$$

definieren. $F(z)$ kann aus $Z(z)$ durch Integration oder durch Differentiation und Ausnutzen der Eigenwertgleichung von F berechnet werden. Die Eigenwertgleichung für Z lautet

$$\frac{\partial^2}{\partial z^2}Z + \lambda^2 N^2 Z = 0. \tag{1.122}$$

Wir machen den Ansatz, daß $S(z)$, $A(z)$ und $B(z)$ eine schwach mit z variierende Funktion sei und Z die Form

$$Z(z) = A(z)\sin(\lambda S(z)) + B(z)\cos(\lambda S(z)) \tag{1.123}$$

habe. Einsetzen in die Eigenwertgleichung liefert

$$\begin{aligned} & A''\sin(\lambda S) + B''\cos(\lambda S) \\ + \; & \lambda\left(S''\left(A\cos(\lambda S) - B\sin(\lambda S)\right) + 2S'\left(A'\cos(\lambda S) - B'\sin(\lambda S)\right)\right) \\ - \; & \lambda^2\left(S'^2 - N^2\right)\left(A\sin(\lambda S) + B\cos(\lambda S)\right) = 0. \end{aligned} \tag{1.124}$$

Wenn die Eigenwerte groß sind (der barotrope Mode kann also nicht in WKB-Näherung beschrieben werden) können die Terme mit A'' und B'' vernachlässigt werden. Die verschiedenen Ordnungen von λ ergeben drei Gleichungen:

$$S'^2 = N^2 \tag{1.125}$$

$$S''A = -2S'A' \tag{1.126}$$

$$S''B = -2S'B'. \tag{1.127}$$

Damit folgt sofort

$$S(z) = \int_H^z dz' N(z') \tag{1.128}$$

$$A(z) = A_0\sqrt{N}^{-1} \tag{1.129}$$

$$B(z) = B_0\sqrt{N}^{-1}. \tag{1.130}$$

Die Eigenfunktionen F ergeben sich (wieder unter der Voraussetzung großer Eigenwerte) zu

$$F(z) = -\frac{\sqrt{N}}{\lambda}\left(A_0 \cos(\lambda S(z)) - B_0 \sin(\lambda S(z))\right). \tag{1.131}$$

Die Bestimmung von λ erfolgt wie im Falle $N = const$. Aus den Randbedingungen folgt die Eigenwertgleichung

$$\tan\left(\lambda H \bar{N}\right) = \frac{N(0)}{g\lambda}, \tag{1.132}$$

die wieder näherungsweise eine Lösung der Form

$$\lambda_n = \frac{n\pi}{H\bar{N}} \tag{1.133}$$

hat. Dabei ist $\bar{N}$ die vertikal gemittelte BVF

$$\bar{N} = \frac{1}{H}\int_{-H}^{0} dz N(z). \tag{1.134}$$

Für $N = const$ erhält man die bekannten Lösungen aus dem vorhergehenden Abschnitt. Die genäherten baroklinen Eigenfunktionen sind

$$F_n(z) = (-1)^n \left(2\frac{N(z)}{\bar{N}}\right)^{\frac{1}{2}} \cos\left(n\pi \frac{\int_{-H}^{z} dz' N(z')}{H\bar{N}}\right). \tag{1.135}$$

Damit gestattet die WKB-Methode die Berechnung von baroklinen Eigenwerten und Eigenfunktionen für beliebig komplizierte Verläufe der BVF. Insbesondere können experimentell bestimmte Profile der BVF mit geringem numerischen Aufwand untersucht werden.

Numerische Lösungen

Die Nutzung von Bibliotheken und Standardmethoden zur numerischen Eigenwertberechnung stößt auf die Schwierigkeit, daß in der Regel eine analytische Formulierung der Differentialgleichung erforderlich ist. Das ist bei experimentell (oder aus der Analyse eines numerischen Modells) gewonnenen Profilen der BVF in der Regel nicht der Fall.

Wir untersuchen das Eigenwertproblem

$$\frac{d^2 Z}{dz^2} + \lambda^2 N^2 Z = 0 \tag{1.136}$$

mit den Randbedingungen

$$Z(z) = 0 \quad \text{für} \quad z = 0, -H. \tag{1.137}$$

Der Einfachheit halber benutzen wir die rigid-lid-Näherung.

Die Differentialgleichungen werden durch Differenzengleichungen approximiert. Entwickeln wir eine Funktion $f(z)$ an der Stelle z_n in eine Taylorreihe an der Stelle z_{n+1} und z_{n-1}

$$f(z_{n+1}) \approx f(z_n) + f'(z_n)\Delta z_{n+1} + f''(z_n)\frac{\Delta z_{n+1}^2}{2} \tag{1.138}$$

$$f(z_{n-1}) \approx f(z_n) - f'(z_n)\Delta z_n + f''(z_n)\frac{\Delta z_n^2}{2} \tag{1.139}$$

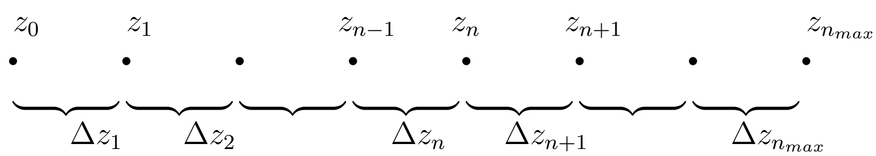

so kann die erste Ableitung eliminiert werden $(f(z_n) = f_n)$

$$f_n'' \approx 2\frac{f_{n+1}\Delta z_n + f_{n-1}\Delta z_{n+1} - f_n(\Delta z_{n+1} + \Delta z_n)}{\Delta z_{n+1}\Delta z_n(\Delta z_{n+1} + \Delta z_n)} \tag{1.140}$$

Das ergibt $n_{max} - 1$ Gleichungen. Zusammen mit den Randbedingungen hat man damit $n_{max} + 1$ Gleichungen:

$$\left(A_{nm} + \lambda^2\delta_{n,m}\right) Z_m = 0 \quad n = 1..n_{max} - 1 \tag{1.141}$$

$$Z_0 = 0 \tag{1.142}$$

$$Z_{n_{max}} = 0. \tag{1.143}$$

Die Matrixelemente lauten

$$A_{nm} = \delta_{n+1,m}\frac{2}{N_n^2\Delta z_{n+1}(\Delta z_{n+1} + \Delta z_n)} \tag{1.144}$$

$$+ \delta_{n-1,m}\frac{2}{N_n^2\Delta z_n(\Delta z_{n+1} + \Delta z_n)} \tag{1.145}$$

$$- \delta_{n,m}\frac{2}{N_n^2\Delta z_{n+1}\Delta z_n}. \tag{1.146}$$

Diese Gleichungen können einfach programmiert und mit einem Bibliothekseigenwertprogramm gelöst werden. Für kleine Matrizen sind auch analytische Verfahren (MATHEMATICA) interessant.

Als Test wird das Eigenwertproblem für $N = const$ numerisch gelöst. Die Tabelle zeigt im Vergleich das exakte Ergebnis und die mit verschiedenen Stützstellenzahlen gewonnenen Näherungen.

n	$n^2\pi^2$	$n_{max} = 3$	$n_{max} = 4$	$n_{max} = 5$	$n_{max} = 6$
1	9.87	9.00	9.30	9.54	9.64
2	39.47	27.00	32.00	34.55	36.00
3	88.83	-	54.62	65.45	72.00
4	157.91	-	-	90.45	108.00
5	246.74	-	-	-	134.35

Für eine kleine Zahl von Stützstellen werden nur die niedrigsten Eigenwerte zuverlässig approximiert, während die höheren Eigenwerte Abweichungen von bis zu 50% aufweisen. Die Konvergenz mit wachsender Anzahl von Stützstellen ist relativ langsam.

Die Abbildungen zeigen die numerisch berechneten ersten vier Eigenfunktionen für ein exponentielles Profil der BVF.

Separation der vertikalen Koordinate ohne vertikaler Reibung

Wir führen jetzt die Separation der vertikalen Koordinate in den Boussinesq- Gleichungen durch. Ein exakte Separation ist nur bei verschwindender vertikaler Reibung

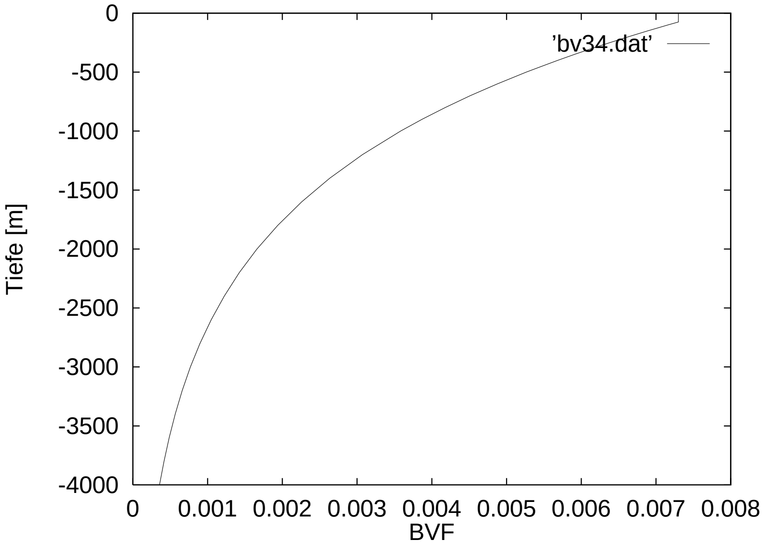

Figure 1.2. Profil der Brunt-Väsiälä-Frequenz

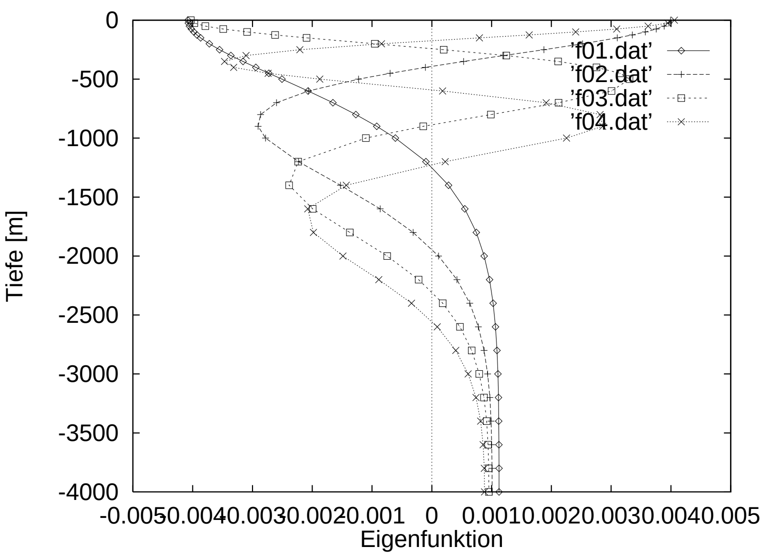

Figure 1.3. Die ersten vier baroklinen Eigenfunktionen $F_n(z)$

möglich. Dieser Fall wird zuerst diskutiert. Es ist zweckmäßig, die vertikale Geschwindigkeit und die bouyancy zu eliminieren. Die verbleibenden Gleichungen lauten:

$$\frac{\partial}{\partial t}u - fv + \frac{\partial p}{\partial x} = X \tag{1.147}$$

$$\frac{\partial}{\partial t}v + fu + \frac{\partial p}{\partial y} = Y \tag{1.148}$$

$$\frac{\partial u}{\partial x} + \frac{\partial v}{\partial y} - \mathcal{Z}\frac{\partial}{\partial t}p = 0. \tag{1.149}$$

Die Randbedingungen für die vertikale Bewegung konnten in der hydrostatischen Näherung als Randbedingung für den Druck geschrieben werden:

$$\frac{\partial}{\partial t}\left(p + \frac{g}{N^2}\frac{\partial p}{\partial z}\right) = 0 \quad \text{für} \quad z = 0, \tag{1.150}$$

$$\frac{\partial}{\partial t}\frac{\partial p}{\partial z} = 0 \quad \text{für} \quad z = -H \tag{1.151}$$

Wir multiplizieren die Gleichungen mit einer Eigenfunktion F_n und integrieren über z. Für alle Terme mit Ausnahme des Druckterms in der Kontinuitätsgleichung erhält man zwanglos die Koeffizienten

$$a_n = \frac{1}{H}\int_{-H}^{0} dz a(z) F_n(z). \tag{1.152}$$

Für den Druckterm ergibt sich nach zweimaliger partialler Integration

$$\frac{\partial}{\partial t}\frac{1}{H}\int_{-H}^{0} dz F_n(z)\mathcal{Z}p = \frac{\partial}{\partial t}\left(F_n(z)\frac{1}{N^2}\frac{\partial p}{\partial z}\bigg|_{-H_0}^{0} - \frac{1}{N^2}p\frac{\partial F_n}{\partial z}\bigg|_{-H_0}^{0} + \frac{1}{H}\int_{-H}^{0} dz p\mathcal{Z}F_n\right). \tag{1.153}$$

An dieser Stelle zeigt sich die Zweckmäßigkeit der etwas künstlichen Randbedingungen für F. Mit Hilfe der Randbedingungen für p und F verschwinden die ersten beiden Terme. Der letzte kann mit Hilfe der Eigenwertgleichung umgewandelt werden,

$$\frac{1}{H}\int_{-H}^{0} dz p\mathcal{Z}F_n = -\lambda_n^2\frac{1}{H}\int_{-H}^{0} dz p F_n = -\lambda_n^2 p_n. \tag{1.154}$$

Die Boussinesq-Gleichungen lauten damit

$$\frac{\partial}{\partial t}u_n - f v_n + \frac{\partial p_n}{\partial x} = X_n \tag{1.155}$$

$$\frac{\partial}{\partial t}v_n + f u_n + \frac{\partial p_n}{\partial y} = Y_n \tag{1.156}$$

$$\frac{\partial u_n}{\partial x} + \frac{\partial v_n}{\partial y} + \frac{\partial}{\partial t}\lambda_n^2 p_n = 0. \tag{1.157}$$

Separation der vertikalen Koordinate bei vertikaler Reibung

Tritt in den horizontalen Impulsgleichungen ein vertikaler Reibungsterm

$$\frac{\partial}{\partial z}A_V\frac{\partial}{\partial z}(u, v) \tag{1.158}$$

auf, so ist eine Separation der Variablen nicht mehr möglich, da die Anwendung des Operators

$$\frac{\partial}{\partial z}A_V\frac{\partial}{\partial z} \tag{1.159}$$

auf Eigenfunktionen F_n allgemein nicht auf die Eigenfunktion zurückführt. Das hat zur Folge, daß das vertikale Eigenwertproblem Reibung explizit berücksichtigen müßte.

Für theoretische Untersuchungen ist der genaue Verlauf $A_V(z)$ oft nicht ausschlaggebend und man kann ohne Beschränkung der Allgemeinheit einen Ansatz in der Form

$$A_V(z) \approx A \frac{1}{N^2(z)} \tag{1.160}$$

machen (Fjeldstad). In diesem Falle folgt

$$\frac{\partial}{\partial z} A_V \frac{\partial}{\partial z} F_n(z) = -A\lambda_n^2 F_n(z) \tag{1.161}$$

so daß die Separation der vertikalen Koordinate wieder möglich ist. Jeder vertikale Mode wird dann mit einer eigenen Reibungskonstanten $A_n = A\lambda_n^2$ bedämpft. Da die Eigenwerte mit n stark anwachsen, werden in dieser Näherung die Moden mit hohem n stärker bedämpft als der barotrope Mode oder die ersten baroklinen Moden.

Wird wie im vorherigen Abschnitt die Entwicklung nach Eigenfunktionen durchgeführt, so treten Terme

$$\begin{aligned} \frac{1}{H}\int_{-H}^{0} dz F_n(z) A \mathcal{Z} u = A \Bigg(& F_n(z) \frac{1}{N^2} \frac{\partial u}{\partial z}\Bigg|_{-H_0}^{0} - \frac{1}{N^2} u \frac{\partial F_n}{\partial z}\Bigg|_{-H_0}^{0} \\ & + \frac{1}{H}\int_{-H}^{0} dz u \mathcal{Z} F_n \Bigg) . \end{aligned} \tag{1.162}$$

auf. Während u_z durch die Windschubspannung bzw. die Bodenreibung gegeben ist, kann keine Randbedingung für u angegeben werden. Die Randbedingung für F, die auf den Druck zugeschnitten ist, läßt diesen Term nicht verschwinden. Ein Ausweg ist die rigid-lid-Näherung. Die Wasseroberfläche wird als starrer Deckel angenommen ($w(0) = 0$). Die entsprechende Randbedingungen für den Druck und F_n lauten

$$\frac{\partial}{\partial t} \frac{\partial p}{\partial z} = 0 \quad \text{für} \quad z = 0, \tag{1.163}$$

$$\frac{\partial F_n}{\partial z} = 0 \quad \text{für} \quad z = 0. \tag{1.164}$$

Damit ist wiederum eine vollständige Separation möglich. Da in der rigid-lid-Näherung für den barotropen Eigenwert $\lambda_0 = 0$ gilt, wird der barotrope Mode nur bedämpft, wenn Bodenreibung explizit berücksichtigt wird.

Wenn die Windschubspannung separat über eine Volumenkraft $\mathbf{X}$ parametrisiert wird, muß an der Oberfläche $u_z = 0$ gelten, um nicht einen weiteren Impulsfluß durch die Oberfläche zuzulassen, der u.U. zu unsinnigen Resultaten führen würde.

Nach dem Separieren der vertikalen und horizontalen Koordinaten (vertikale Reibung wird in Fjeldstad-Näherung behandelt) lautet das zu lösende Gleichungssystem

$$-i\bar{\omega}_n u_n - f v_n + \frac{\partial p_n}{\partial x} = X_n \tag{1.165}$$

$$-i\bar{\omega}_n v_n + f u_n + \frac{\partial p_n}{\partial y} = Y_n \tag{1.166}$$

$$\frac{\partial u_n}{\partial x} + \frac{\partial v_n}{\partial y} - i\omega\lambda_n^2 p_n = 0. \tag{1.167}$$

$\bar{\omega}_n$ ist Abkürzung für

$$\bar{\omega}_n = \omega + iA_n. \tag{1.168}$$

Die vertikale Reibung führt in der hier gewählten Näherung einfach zum Auftreten eines Imaginärteils in der Frequenz (Dämpfung). Eine weitere Vereinfachung ergibt sich, wenn die bisher vernachlässigte Diffusion von Wärme und Salz einbezogen wird. Für viele Zwecke ist es ausreichend, dieses durch die Einführung eines entsprechenden Dämpfungsterms in der bouyancy-Gleichung zu tun und für die Diffusionskonstante den gleichen Wert wie für den Impulsaustausch zu wählen. Die Kontinuitätsgleichung lautet dann

$$\frac{\partial u_n}{\partial x} + \frac{\partial v_n}{\partial y} - i\bar{\omega}\lambda_n^2 p_n = 0. \tag{1.169}$$

1.2.2. Reduction of the system of equations

To solve the forced Boussinesq equations we transform the system 1.157 into a single equation for one variable. This could be either the pressure, the vertical velocity or one of the horizontal velocity components.

The v-equation

Aiming an investigation of upwelling, where a coastal boundary condition plays a critical role, we use one of the horizontal velocity components, say v. For a short notation we drop the subscript “n” and use subsrcipts “t”, “x” and “y” for partial derivatives,

$$u_t - fv + p_x = X \qquad \text{I} \tag{1.170}$$
$$v_t + fu + p_y = Y \qquad \text{II} \tag{1.171}$$
$$p_t = -\lambda^{-2}(u_x + v_y) \qquad \text{III} \tag{1.172}$$

To eliminate u from Eq. (II) we derive (II) again with respect to time and replace u_t with the help of (I).

$$v_{tt} + f(fv - p_x + X) + p_{ty} = Y_t. \tag{1.173}$$

To eliminate p we use (III). To this end we derive (II) again with respect to time and (III) with respect to x and y,

$$v_{ttt} + f(fv_t - p_{tx} + X_t) + p_{tty} = Y_{tt}, \tag{1.174}$$
$$p_{tx} = -\lambda^{-2}(u_{xx} + v_{xy}), \tag{1.175}$$
$$p_{tty} = -\lambda^{-2}(u_{txy} + v_{tyy}), \tag{1.176}$$
$$\tag{1.177}$$

to get

$$v_{ttt} + f^2 v_t + f(\lambda^{-2}(u_{xx} + v_{xy})) - \lambda^{-2}(u_{txy} + v_{tyy}) = Y_{tt} - fX_t. \tag{1.178}$$
$$\tag{1.179}$$

Cross-differentiating and subtracting (I) and (II) gives

$$u_{ty} - v_{tx} - f(u_x + v_y) = X_y - Y_x, \tag{1.180}$$

and again with respect to x

$$u_{txy} - f(u_{xx} + v_{xy}) \quad = \quad X_{xy} - Y_{xx} + v_{txx}. \tag{1.181}$$

This gives the final equation for v

$$v_{ttt} + f^2 v_t - \lambda^{-2}\Delta_h v_t \quad = \quad Y_{tt} - fX_t + \lambda^{-2}(X_{xy} - Y_{xx}). \tag{1.182}$$

Assuming that the equation for v is solved, u and p can be calculated,

$$u_{tt} - \lambda^{-2}u_{xx} \quad = \quad fv_t + \lambda^{-2}v_{xy} + X_t, \tag{1.183}$$
$$p_{tt} - \lambda^{-2}p_{xx} \quad = \quad -\lambda^{-2}(fv_x + v_{ty} + X_x). \tag{1.184}$$

The pressure-equation

Similarly, an equation for the pressure can be derived. Cross differentiation of (I) and (II) gives

$$u_{tx} + v_{ty} - f(v_x - u_y) + \Delta_h p \quad = \quad X_x + Y_y, \tag{1.185}$$
$$u_{ty} - v_{tx} - f(u_x + v_y) \quad = \quad X_y - Y_x. \tag{1.186}$$

The relative vorticity $v_x - u_y$ can be eliminated,

$$u_{ttx} + v_{tty} + f^2(u_x + v_y) + \Delta_h p_t \quad = \quad X_{tx} + Y_{ty} - f(X_y - Y_x). \tag{1.187}$$

With the help of equation (III) and its second time derivative the horizontal velocity divergency is replced by the pressure,

$$-\lambda^2(p_{ttt} + f^2 p_t) + \Delta_h p_t \quad = \quad X_{tx} + Y_{ty} - f(Y_x - X_y). \tag{1.188}$$

Again, assuming p to be known from a solution of the pressure equation, velocities can be calculated,

$$u_{tt} + f^2 u \quad = \quad -fp_y - p_{tx} + X_t + fY, \tag{1.189}$$
$$v_{tt} + f^2 v \quad = \quad fp_x - p_{ty} + Y_t - fX. \tag{1.190}$$

The pressure equation reveals directly, how pressure changes can be induced within the open ocean:

- by a divergent wind field changing with time,

- by a rotational wind.

Otherwise the pressure time tendency remains zero all the time, if the initial pressure perturbation is zero.

1.3. Free waves

1.3.1. Spectrum, phase and group velocity

Assuming for a moment, that the wind forcing (X, Y) is zero. In this case the equations for the velocity and the pressure have the same form. Considering only the x-dimension, the solution is wave like,

$$p(x,t) = p_0(k,\omega)e^{ikx-i\omega t}, \tag{1.191}$$

the total solution is a superposition for all wave numbers k and all frequencies ω. However, ω and k are not independent variables but are linked by a dispersion relation. This is found by inserting the ansatz for p into the pressure equation:

$$-i\omega\left(\lambda^2(\omega^2 - f^2) - k^2\right) = 0. \tag{1.192}$$

This equation has the solutions:

$$\omega = 0, \tag{1.193}$$

$$\omega = \pm\sqrt{f^2 + k^2\lambda^{-2}}. \tag{1.194}$$

Hence, there exists either a constant pressure perturbation or there are waves with frequencies above the inertial frequency. Remebering the discrete spectrum of the vertical eigenvalues λ_n, the frequency of waves spreading within a stratified and rotating ocean reads

$$\omega_n = \pm f\sqrt{1 + k^2R_n^2}. \tag{1.195}$$

The quantity

$$R_n = (\lambda_n f)^{-1} \tag{1.196}$$

is called Rossby radius. Phase and group velocity are

$$c_p = \frac{\omega_n}{k} = \frac{1}{\lambda_n}\sqrt{1 - \frac{f^2}{\omega_n^2}}^{-1} \tag{1.197}$$

$$c_g = \frac{1}{\lambda_n}\sqrt{1 - \frac{f^2}{\omega_n^2}} \tag{1.198}$$

For high frequency phase and group velocity become independent of f (hence of rotation) and are constants (non-dipersive). Near the inertial frequency the phase velocity is large, the group velocity tends to zero. Hence, there are only uniform motions (small wave number or large wave length) of the ocean for $\omega = f$.

The group velocity c_g is the velocity of signal propagation by waves. Eq. (1.198) reveals $1/\lambda_n$ as an upper limit for the wave speed.

1.3.2. Initial pressure perturbation

Now we consider the spreading of an initial pressure perturbation. We are only interested in the basic priciples and consider an ocean uniform in y-direction.

First we consider details of the initial conditions. Assuming an initial pressure gradient in x-direction and zero velocity, from the continuity equation (III) it follows that the initial pressure time derivative also vanishes.

$$p(x,0) = p_0(x), \tag{1.199}$$
$$p_t(x,0) = 0. \tag{1.200}$$

$$p_{tt} = -\lambda^{-2}(u_{tx} + v_{ty}), \tag{1.201}$$
$$= -\lambda^{-2}\left(f(v_x - u_y) - p_{xx} - p_{yy}\right). \tag{1.202}$$
$$\tag{1.203}$$

Hence, since the ocean is at rest initially,

$$p_{tt}(x,0) = \lambda^{-2}p_{xx}. \tag{1.204}$$

Now we are going to solve the homogeneous pressure equation by means of Fourier transforms. Defining

$$p(x,\omega) = \int_0^\infty dte^{i\tilde{\omega}t}p(x,t), \tag{1.205}$$
$$\tilde{\omega} = \omega + i\varepsilon. \tag{1.206}$$

We have added an infinitesimal imaginary part to ω to ensure the convergence of the integral also for a constant pressure.

Applying the Fourier transformation to the pressure equations requires integration by parts (suppress the x argument):

$$\int_0^\infty dte^{i\tilde{\omega}t}p_t(t) = -p(0) - \int_0^\infty dti\tilde{\omega}e^{i\tilde{\omega}t}p(t), \tag{1.207}$$
$$= -p(0) - i\tilde{\omega}p(\omega) \tag{1.208}$$

$$\int_0^\infty dte^{i\tilde{\omega}t}p_{ttt}(t) = -p_{tt}(0) - \int_0^\infty dti\tilde{\omega}e^{i\tilde{\omega}t}p_{tt}(t), \tag{1.209}$$
$$= -p_{tt}(0) - i\tilde{\omega}\left(-p_t(0) - i\tilde{\omega}\int_0^\infty dte^{i\tilde{\omega}t}p_t(t)\right), \tag{1.210}$$
$$= -p_{tt}(0) - i\tilde{\omega}\left(i\tilde{\omega}p(0) - \tilde{\omega}^2p(\omega)\right) \tag{1.211}$$

Next we apply a Fourier transformation in space,

$$p(k,\omega) = \int_{-\infty}^\infty dxe^{-ikx}p(x,\omega). \tag{1.212}$$
$$\tag{1.213}$$

To ensure the convergence of this integral we must require that p vanishs for $x \to \pm\infty$.

Putting all together we end up with a inhomogeneous equation for the pressure,

$$i\tilde{\omega}\left[-\lambda^2(\tilde{\omega}^2 - f^2) + k^2\right]p(k,\omega) = p(0)\lambda^2(\tilde{\omega}^2 - f^2) \tag{1.214}$$

or

$$p(k,\omega) = -\frac{p(0)(\tilde{\omega}^2 - f^2)}{i\tilde{\omega}\left(\tilde{\omega}^2 - f^2 - k^2\lambda^{-2}\right]} \tag{1.215}$$

The denominator is well known. Its zeros define the dispersion relation of waves as given in the previous section.

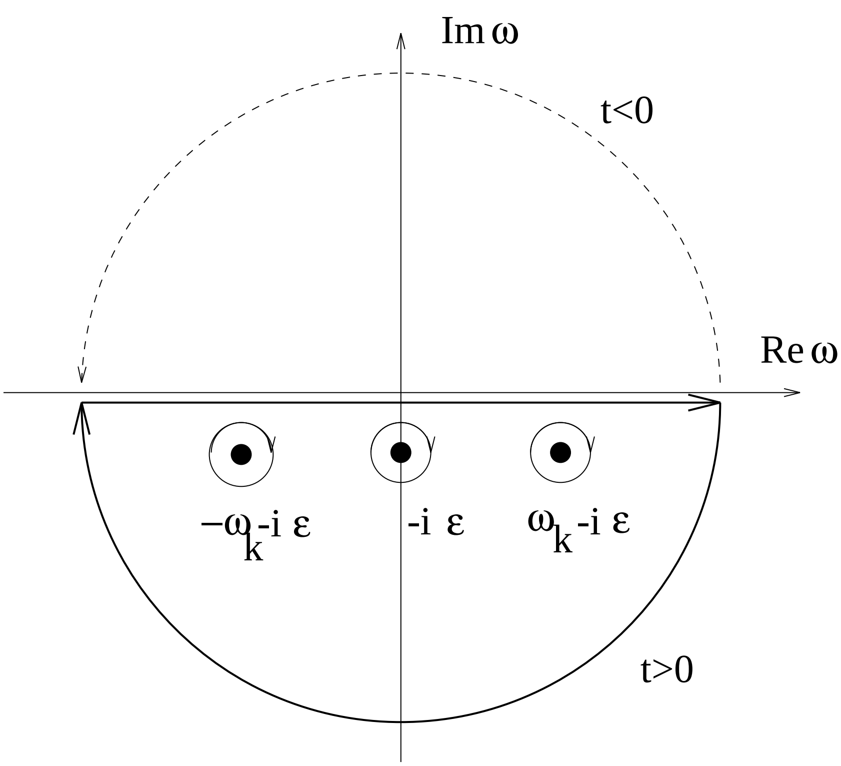

Figure 1.4. The integration path in der complex ω plane. For $t < 0$ the path is closed in the upper half plane and no poles are enclosed, for $t > 0$ the poles in the lower plane are located within the enclosed area.

The solution in the real space requires the inverse Fourier transformation,

$$p(x,t) = \int_{-\infty}^{\infty}\frac{d\omega}{2\pi}\int_{-\infty}^{\infty}\frac{dk}{2\pi}e^{ikx - i\tilde{\omega}t}p(k,\omega). \tag{1.216}$$

This can be done with help of Cauchy's integral theorem,

$$\oint \frac{d\omega}{2\pi i}\frac{f(\omega)}{\omega - \omega_0} = f(\omega_0). \tag{1.217}$$

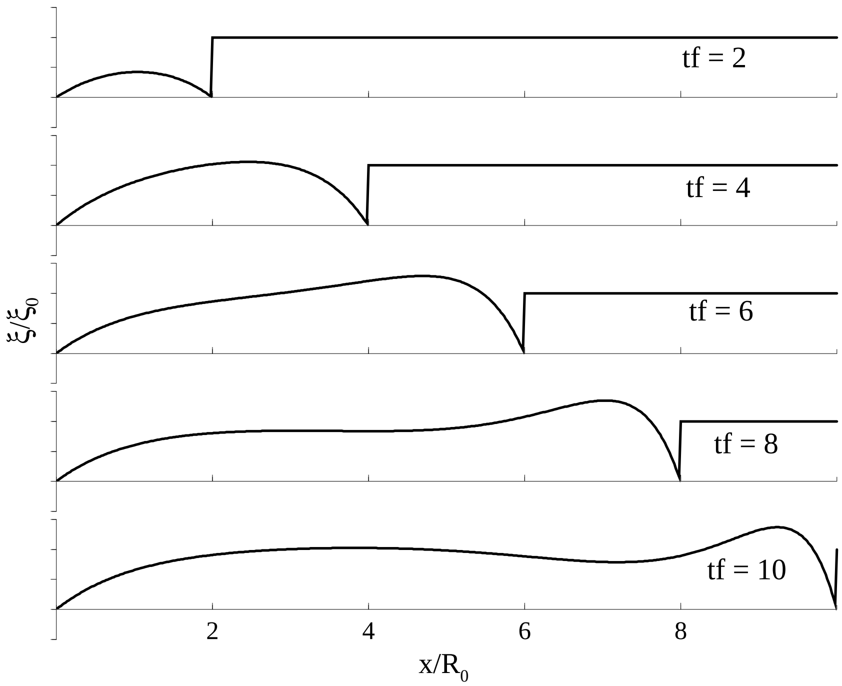

Figure 1.5. Response des Wasserstandes auf eine Wasserstandsstufe bei $x = 0$

The integration path in the complex plane is anti-clockwise and must encircle the point $\omega = \omega_0$. It is required, that $f(\omega)$ is an analytical function in the area enclosed by the integration path, singularities outside not enclosed by the integration path do not matter.

The denominator of Eq. (1.215) has the form

$$\frac{1}{i\tilde{\omega}\,(\tilde{\omega}^2 - \omega_k^2])} \tag{1.218}$$

$$\omega_k = \sqrt{f^2 + k^2\lambda^{-2}} \tag{1.219}$$

It can be rewritten as follows,

$$\frac{1}{i\tilde{\omega}\,(\tilde{\omega}^2 - \omega_k^2])} = \frac{1}{2i\omega_k^2}\left(-\frac{2}{\omega} + \frac{1}{\omega - \omega_k} + \frac{1}{\omega + \omega_k}\right) \tag{1.220}$$

Carrying out the ω integral

$$p(k,t) = \int_{-\infty}^{\infty} \frac{d\omega}{2\pi} e^{-i\tilde{\omega}t} p(k,\omega) \tag{1.221}$$

$$= \int_{-\infty}^{\infty} \frac{d\omega}{2\pi i} \frac{p(0)e^{-i\tilde{\omega}t}(\tilde{\omega}^2 - f^2)}{2\omega_k^2} \left(-\frac{2}{\tilde{\omega}} + \frac{1}{\tilde{\omega} - \omega_k} + \frac{1}{\tilde{\omega} + \omega_k}\right) \tag{1.222}$$

$$= -\theta(t) \oint \frac{d\omega}{2\pi i} \frac{p(0)e^{-i\tilde{\omega}t}(\tilde{\omega}^2 - f^2)}{2\omega_k^2} \left(-\frac{2}{\omega + i\varepsilon} + \frac{1}{\omega - \omega_k + i\varepsilon} + \frac{1}{\omega + \omega_k + i\varepsilon}\right) \tag{1.223}$$

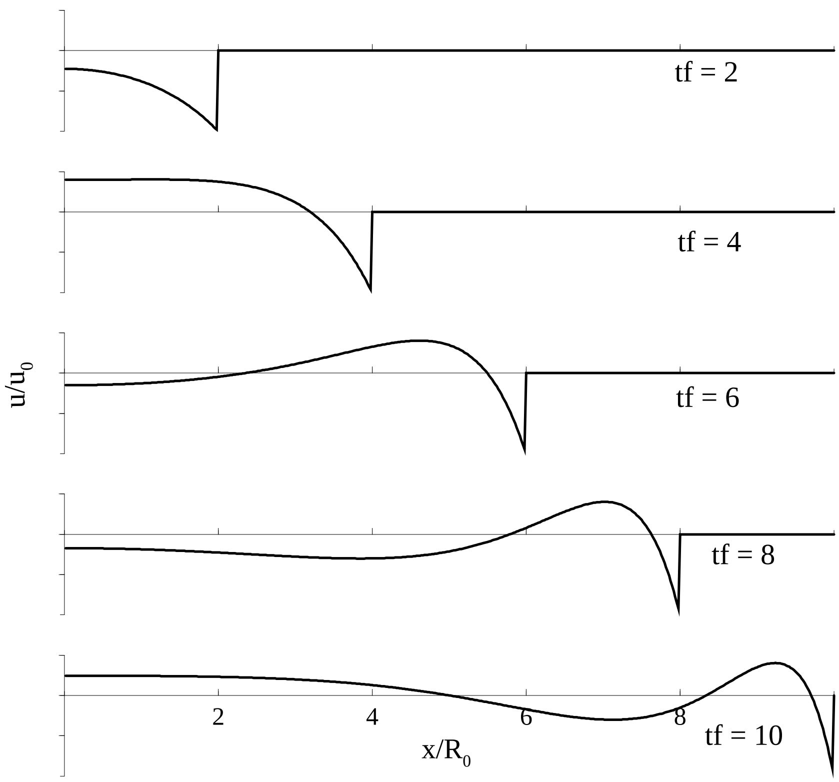

Figure 1.6. u-Komponente der Response auf eine Wasserstandsstufe bei $x = 0$

The closed integration path is shown in Fig. 1.4. It shows the importance of accounting ε carefully, to find the correct integration path. Note that for $t > 0$ the exponential diverges for $\omega \to i\infty$ (upper half plane), but tends to zero exponentially for $\omega \to -i\infty$ (lower half plane). Hence, we close in the lower half plane for $t > 0$ and in the upper half plane for $t < 0$. Since no singularity is enclosed in the upper half plane, the solution is zero for $t < 0$. This is a satisfying result, there is no action into the past as required by the causality principle. Here we lear, that the infinitesimal ε represents the causality principle in the mathematical treatment of this initial value problem.

$p(k,t)$ reads now

$$p(k,t) \quad = \quad p_0(k)\theta(t)\left(1 + \frac{k^2}{\lambda^2\omega_k^2}(\cos\omega_k t - 1)\right) \tag{1.224}$$

The k-integral for p cannot be carried out analytically. As an alternative we may consider the continuity equation and find

$$u(k) \quad = \quad -\frac{1}{ik}\frac{\partial}{\partial t}p(k) \tag{1.225}$$

$$\quad = \quad \frac{1}{ik}p_0(k)\frac{k^2}{\omega_k}\sin\omega_k t \tag{1.226}$$

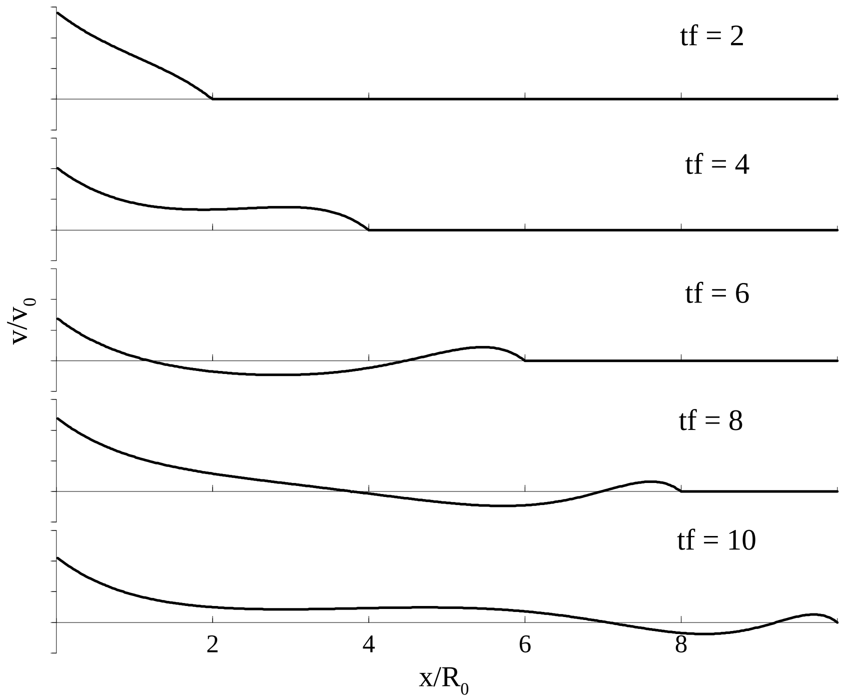

Figure 1.7. v-Komponente der Response eine Wasserstandsstufe bei $x = 0$

Assuming a step like initial pressure perturbation $p_0(x) = p_0 sig(x)$ the Fourier transformed is

$$\begin{aligned} p_0(k) &= \int_{-\infty}^{+\infty} dx \mathrm{e}^{ikx} p_0 \mathrm{sgn}(x) \\ &= -p_0 \frac{2ik}{k^2 + \varepsilon^2}. \end{aligned} \tag{1.227}$$

In this case the inverse Fourier transformed for u is

$$\begin{aligned} u(xt) &= \int_{-\infty}^{+\infty} \frac{dk}{2\pi} \mathrm{e}^{ikx} \frac{2p_0}{\omega_k} \sin \omega_k t \\ &= -p_0 \lambda \theta(t - \lambda|x|) J_0 \left(f\sqrt{t^2 - x^2\lambda^2} \right) \end{aligned} \tag{1.228}$$

p can be found from u_x, v by integrating the momentum equation.

For large time, $tf \gg \frac{|x|}{R}$, the asymptotic approximation of the Bessel functionen can be used. For u it follows

$$u(xt) \approx -\lambda p_0 \sqrt{\frac{2}{\pi f t}} \cos\left(ft - \frac{\pi}{4} \right), \tag{1.229}$$

oscillations take place with the inetrtial frequency f and are decreasing like $\sqrt{(t)}$. The integrals over the Bessel function can be carried out

$$v \rightarrow p_0 \lambda \mathrm{e}^{-\frac{|x|}{R}}, \tag{1.230}$$

$$p \rightarrow p_0 \mathrm{sgn}(x) \left(1 - \mathrm{e}^{-\frac{|x|}{R}} \right). \tag{1.231}$$

This is the geostrophic balance.

This example reveals a basic difference between adjustment processes in the rotating or non-rotating ocean. In the rotating case there remains a part of the initial perturbation balanced by a geostrophic current.

To be more specific, we consider the case, that only the first vertical mode is excitet. In this case the pressure is $p = g\eta$ and $\lambda^{-1} = \sqrt{gH}$. We have also to multiply with $F_0 \approx 1/\sqrt{H}$. For an initial step of height $\eta(0,x) = \eta_0 sig(x)$ the solution reads

$$v = \frac{\eta_0}{H} c_0 \mathrm{e}^{-\frac{|x|}{R}}, \tag{1.232}$$

$$p = p_0 \mathrm{sgn}(x) \left(1 - \mathrm{e}^{-\frac{|x|}{R_0}}\right). \tag{1.233}$$

$$c_0 = \lambda_0^{-1} = \sqrt{gH} \tag{1.234}$$

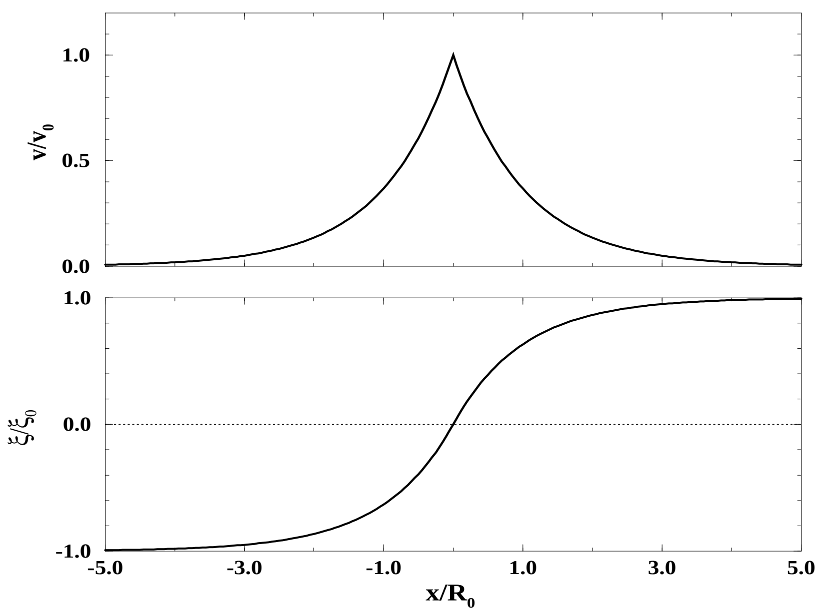

Figure 1.8. Sea level and geostrophically balanced currents for large time.

The change of the potential energy between the initial state and the asymptotic state is

$$\Delta E_{pot} = 2\frac{\rho g}{2}\eta_0^2 \int_0^\infty dx \left(1 - \left(1 - e^{-\frac{x}{R_0}}\right)^2\right) \tag{1.235}$$

$$= \frac{3}{2} g\eta_0^2 R_0. \tag{1.236}$$

The final kinetic energy is

$$\Delta E_{kin} = 2\frac{\rho g}{2}\eta_0^2 \int_0^\infty dx e^{-\frac{2x}{R_0}} \tag{1.237}$$

$$= \frac{1}{2} g \eta_0^2 R_0. \tag{1.238}$$

Hence, an important part of the released energy is radiated away with the inertial waves, but 1/3 remains trapped in the geostropic current field near the initial perturbation.

1.4. Forcing an unbounded ocean

1.5. The influence of a coast - coastal upwelling

1.5.1. Inhomogeneous boundary value problems - Green's functions

We consider the example of a f-plane ocean, which is initially at rest and forced by a wind field starting at $t = 0$. The ocean is bounded by a coastline which orients zonally. The we transform the equation for v into the Fourier space. The transformation with respect to the time is simple, because all variables are zero initially. Also the transformation of the zonal variable x is simple because the v is assumed to be finite for $x \to \pm\infty$,

$$p(x,t) = \int_{-\infty}^{\infty} \frac{d\omega}{2\pi} \int_{-\infty}^{\infty} \frac{dk}{2\pi} e^{ikx - i\tilde{\omega}t} p(k,\omega). \tag{1.239}$$

Our start equation reads

$$-i\tilde{\omega} \left(f^2 - \tilde{\omega}^2 + \lambda^{-2} \left(k^2 - \frac{\partial^2}{\partial y^2} \right) \right) v = -\tilde{\omega}^2 Y + i\tilde{\omega} f X + \lambda^{-2} \left(ikX_y + k^2 Y \right). \tag{1.240}$$

Remember, that v, λ, X and Y have an index n from the decomposition into vertical modes. A more suitable form for a soluution is

$$\left(\frac{\partial^2}{\partial y^2} + \alpha^2 \right) v = \mathcal{F}, \tag{1.241}$$

$$\mathcal{F} = \left(\lambda^2 f + \frac{k}{\tilde{\omega}} \frac{\partial}{\partial y} \right) X + \frac{i\left(\lambda^2 \tilde{\omega}^2 - k^2\right)}{\tilde{\omega}} Y, \tag{1.242}$$

$$\alpha^2 = \lambda^2 \left(\tilde{\omega}^2 - f^2 \right) - k^2 \tag{1.243}$$

The boundary value for v reads simply

$$v = 0 \quad \text{for} \quad y = 0, \tag{1.244}$$

$$v = 0 \quad \text{for} \quad y \to \infty, \tag{1.245}$$

there is no flow through the coastline and no flow is excited far away from the coast.

The general solution of this boundary value problem problem is a linear superposition of a solution of the homogeneous equation and a particular solution of the inhomogeneous equation, which conform with the boundary conditions.

We will use a systematic method to derive an expression for an arbitrary forcing function $\mathcal{F}$. To this end we consider a function $G(y, y')$ defined by the equation

$$\left(\frac{\partial^2}{\partial y'^2} + \alpha^2 \right) G(y,y') = \delta(y - y'). \tag{1.246}$$

Renaming the coordinate in the v-equation y by y' and multiplying this equation by G and the equation for G by v gives

$$G(y,y')\frac{\partial^2}{\partial y'^2}v(y') - v(y')\frac{\partial^2}{\partial y'^2}G(y,y') = \mathcal{F}(y')G(y,y') - \delta(y-y')v(y'). \tag{1.247}$$

As the next step we integrate over y' and use the property of the δ-distribution

$$\int_0^\infty dy' v(y')\delta(y-y') = v(y). \tag{1.248}$$

We restrict the domain of y to the ocean area, $y \geq 0$ and get

$$v(y) = \int_0^\infty dy' \mathcal{F}(y')G(y,y') - \int_0^\infty dy' G(y,y')\frac{\partial^2}{\partial y'^2}v(y') + v(y')\frac{\partial^2}{\partial y'^2}G(y,y'). \tag{1.249}$$

The expression with the second order derivatives can be simplified by partial integration

$$\int_0^\infty dy' \left(G(y,y')\frac{\partial^2}{\partial y'^2}v(y') - v(y')\frac{\partial^2}{\partial y'^2}G(y,y') \right) \tag{1.250}$$

$$= G(y,y')\frac{\partial}{\partial y'}v(y') - v(y')\frac{\partial}{\partial y'}G(y,y')\Big|_0^\infty. \tag{1.251}$$

To specify this term, four boundary values for v and four boundary conditions for G are needed. We are free to chose the boundary conditions for the Green's functions G as

$$G(y,y') = 0 \quad \text{for} \quad y' = 0, \tag{1.252}$$
$$G(y,y') = 0 \quad \text{for} \quad y \to \infty. \tag{1.253}$$

With this choice all terms in Eq. (1.251) vanish and the formal solution for v reads,

$$v(y) = \int_0^\infty dy' \mathcal{F}(y')G(y,y') = \mathcal{F} * G. \tag{1.254}$$

What is the purpose of this mathematical manipulations? The task of solving an inhomogeneous differential equation is traced back to the task of solving a homogeneous equation. This is a great simplification. Instead of dealing with a large variety of inhomogeneous equations for various forms of wind fields we have to solve a single homogeneous problem instead. A similar treatment is known classical electrodynamics, quantumstatistics or also from engeneering, where a so called "step function response" is considered to analyse the properties of electronic circuits or mechanical constructs.

1.5.2. Estimation of the Green's function

The differential equation of the Green's function has a δ-like right hand side. Hence, to construct G we try the ansatz

$$G(y,y') = \theta(y-y')g^>(y,y') + \theta(y'-y)g^<(y,y'). \tag{1.255}$$

The first derivative reads

$$\frac{\partial}{\partial y'}G(y,y') = -\delta(y-y')\left(g^>(y,y') - g^<(y,y')\right) \tag{1.256}$$

$$
\begin{aligned}
&+ \quad \theta(y-y')\frac{\partial}{\partial y'}g^{>}(y,y') + \theta(y'-y)\frac{\partial}{\partial y'}g^{<}(y,y'), && (1.257)\\
&= \quad -\delta(y-y')\left(g^{>}(y,y) - g^{<}(y,y)\right) && (1.258)\\
&+ \quad \theta(y-y')\frac{\partial}{\partial y'}g^{>}(y,y') + \theta(y'-y)\frac{\partial}{\partial y'}g^{<}(y,y') && (1.259)\\
&. && (1.260)
\end{aligned}
$$

Note, that the term $g^{>}(y,y) - g^{<}(y,y)$ is independent of y'. The second derivative is

$$
\begin{aligned}
\frac{\partial^2}{\partial y'^2}G(y,y') &= -\left(g^{>}(y,y') - g^{<}(y,y')\right)\frac{\partial}{\partial y'}\delta(y-y') && (1.261)\\
&- \delta(y-y')\left(\frac{\partial}{\partial y'}g^{>}(y,y') - \frac{\partial}{\partial y'}g^{<}(y,y')\right) && (1.262)\\
&+ \theta(y-y')\frac{\partial^2}{\partial y'^2}g^{>}(y,y') + \theta(y'-y)\frac{\partial^2}{\partial y'^2}g^{<}(y,y') && (1.263)
\end{aligned}
$$

Inserting into the differential equation for the Green's function gives the boundary conditions for $g^{>}$ and $g^{<}$ at $y = y'$,

$$
\begin{aligned}
g^{>}(y,y') - g^{<}(y,y') &= 0 \qquad y = y', && (1.264)\\
g^{>}_{y'}(y,y') - g^{<}_{y'}(y,y') &= -1 \qquad y = y'. && (1.265)
\end{aligned}
$$

Finally, $g^{>}$ and $g^{<}$ are solutions of the homogeneous equation,

$$
\begin{aligned}
\left(\frac{\partial^2}{\partial y'^2} + \alpha^2\right) g^{>}(y,y') &= 0 \qquad y > y', && (1.266)\\
\left(\frac{\partial^2}{\partial y'^2} + \alpha^2\right) g^{<}(y,y') &= 0 \qquad y < y'. && (1.267)
\end{aligned}
$$

These equations have an oscillating solution $\alpha^2 > 0$ and an exponential solution for $\alpha^2 < 0$.
We make now the ansatz

$$
\begin{aligned}
g^{<}(y,y') &= A(y)e^{i\alpha y'}, && (1.268)\\
g^{>}(y,y') &= B(y)\sin\alpha y'. && (1.269)
\end{aligned}
$$

$g^{>}(y,y')$ fulfills the boundary condition for $y' = 0$, $g^{>}(y,0) = 0$, $g^{<}(y,y')$ is finite for $y' \to \infty$ and vanishs exponentially for small fequency values, where $\alpha^2 < 0$. Now we apply the boundary conditions at $y = y'$,

$$
\begin{aligned}
A(y)e^{i\alpha y} - B(y)\sin\alpha y &= 0, && (1.270)\\
-i\alpha A(y)e^{i\alpha y} + \alpha B(y)\cos\alpha y &= 1, && (1.271)\\
& && (1.272)
\end{aligned}
$$

$$
\begin{pmatrix} e^{i\alpha y} & -\sin\alpha y \\ -i\alpha e^{i\alpha y} & \alpha\cos\alpha y \end{pmatrix}\begin{pmatrix} A(y) \\ B(y) \end{pmatrix} = \begin{pmatrix} 0 \\ -1 \end{pmatrix} \qquad (1.273)
$$

The determinant is

$$
det = \alpha e^{i\alpha y}\left(\cos\alpha y - i\sin\alpha y\right) = \alpha. \qquad (1.274)
$$

Remarkably this quantity is independent of y. This general property will not be discussed in detail here. For A and B we find

$$A(y) = \alpha^{-1} \begin{vmatrix} 0 & -\sin\alpha y \\ -1 & \alpha\cos\alpha y \end{vmatrix} = -\alpha^{-1}\sin\alpha y \tag{1.275}$$

$$B(y) = \alpha^{-1} \begin{vmatrix} e^{i\alpha y} & 0 \\ -i\alpha e^{i\alpha y} & -1 \end{vmatrix} = -\alpha^{-1}\alpha e^{i\alpha y} \tag{1.276}$$

This gives our finar result for the Green's function,

$$G(y,y') = -\frac{1}{\alpha}\left(\theta(y-y')e^{i\alpha y}\sin\alpha y' + \theta(y'-y)\sin\alpha y e^{i\alpha y'}\right) \tag{1.277}$$

or equivalently

$$G(y,y') = \frac{1}{2i\alpha}\left(e^{i\alpha|y-y'|} - e^{i\alpha(y+y')}\right) \tag{1.278}$$

Note the symmetry of the Green's function in y and y'. On the other hand, it does not depend on $y-y'$ alone. Hence, the homegenity of space is broken by the existence of the coast.

A more formal method to find the Green's function is the following:

- find two linearly independent solutions $u^{(1)}$ and $u^{(2)}$ of the homogeneous equation 1.267. One should fulfill the boundary condition for $y=\infty$ the other one $y=-\infty$. To achieve this, linear combinations of $u^{(1)}$ and $u^{(2)}$ can be used instead. Normalisation of $u^{(i)}$ is not necessary.

- Define

$$\begin{aligned} g^{>}(y,y') &= \frac{u^{(1)}(y)u^{(2)}(y')}{W} \\ g^{<}(y,y') &= \frac{u^{(1)}(y')u^{(2)}(y)}{W} \end{aligned} \tag{1.279}$$

With this choice the condition

$$g^{>}(y,y') - g^{<}(y,y') = 0 \qquad y = y' \tag{1.280}$$

is satisfied.

- From the second boundary condition

$$g^{>}_{y'}(y,y') - g^{<}_{y'}(y,y') = -1 \qquad y = y', \tag{1.281}$$

we find W,

$$W(y) = u^{(2)}(y)u^{(1)}_y(y) - u^{(1)}(y)u^{(2)}_y(y). \tag{1.282}$$

W is called the Wronskian of the functions $u^{(1)}$ and $u^{(2)}$. Using the homegeneous differential equation, it can be shown that

$$\frac{\partial}{\partial y}W(y) \;=\; 0, \tag{1.283}$$

hence, $W(y)$ does not depend on y.

For our example the Wronskian is easily found. However, for other differential equations, like for the equatorial ocean, where the solutions of the homogeneous equation are parabolic cylinder functions, it requires extended knowledge on the analytical theory of special functions. (See Miller or Abramowitz and Stegun)

1.5.3. The formal solution

Keeping in mind the meaning of the convolution integral

$$v(y) \;=\; G*\mathcal{F} = \int_0^\infty dy' G(y,y')\mathcal{F}(y'), \tag{1.284}$$

the formal solution for v reads

$$v(y) \;=\; G*\mathcal{F} \tag{1.285}$$

$$\;=\; \lambda^2 f G*X + \frac{k}{\tilde{\omega}}G*X_{y'} + \frac{i\left(\lambda^2\tilde{\omega}^2 - k^2\right)}{\tilde{\omega}}G*Y. \tag{1.286}$$

The form of the Green's function assures that v fulfills the boundary condition at $y=0$ and $y=\infty$. To find u, p and w we return to Eqs 1.184, here in as Fourier transformed equations

$$-(\omega^2 - \lambda^{-2}k^2)u \;=\; -i\tilde{\omega}fv + ik\lambda^{-2}v_y - i\tilde{\omega}X, \tag{1.287}$$

$$-(\omega^2 - \lambda^{-2}k^2)p \;=\; -\lambda^{-2}(ikfv - i\tilde{\omega}v_y + ikX). \tag{1.288}$$

or

$$u \;=\; \frac{i\tilde{\omega}(fv+X) - ik\lambda^{-2}v_y}{\omega^2 - \lambda^{-2}k^2}, \tag{1.289}$$

$$p \;=\; \frac{\lambda^{-2}\left(ik(fv+X) - i\tilde{\omega}v_y\right)}{\omega^2 - \lambda^{-2}k^2}. \tag{1.290}$$

Inserting v and v_y we find

$$u(k,y,\omega) \;=\; -f\lambda^2 G*Y + \frac{k}{\tilde{\omega}}G_y*Y + \frac{i}{\omega^2-\lambda^{-2}k^2}\left(\tilde{\omega}X + \lambda^2 f^2\tilde{\omega}G*X + kfG*X_{y'} - kG_y*(fX + \frac{k}{\tilde{\omega}}\lambda^{-2}X_{y'})\right) \tag{1.291}$$

$$p(k,y,\omega) \;=\; -f\frac{k}{\tilde{\omega}}G*Y + G_y*Y + \frac{i\lambda^{-2}}{\tilde{\omega}^2-\lambda^{-2}k^2}\left(kX + k\lambda^2 f^2 G*X + \frac{k^2}{\tilde{\omega}}fG*X_{y'} - \tilde{\omega}G_y*(\lambda^2 fX + \frac{k}{\tilde{\omega}}X_{y'})\right) \tag{1.292}$$

1.5.4. A first look at the spectrum

From out prvious studies we know singularities as essential for the Fourier transformation bach into the time domain. There are poles at

- $\tilde{\omega} = 0$, i.e., $\omega = -i\varepsilon$. For this pole the Fourier factor is constant and this part of the solution corresponds to a non-oscillating current field.
- $\tilde{\omega} = \pm k\lambda^{-1}$. In this case we have $\alpha_n^2 = -1/R_n^2$ (remember, $R_n = 1/(\lambda f)$ and the Green's functions reads

$$G(y, y')|_{\omega^2=\lambda^{-2}k^2} = -\frac{R}{2}\left(e^{-\frac{|y-y'|}{R}} - e^{-\frac{y+y'}{R}}\right). \tag{1.293}$$

- a branch point at $\alpha = 0$. For a given value of ω there are two values for the square root of α^2, $\alpha = \pm\sqrt{\lambda^2\left(\tilde{\omega}^2 - f^2\right) - k^2}$. Both solutions coincide at a single point $\alpha = 0$. This point acts as a branch point, i.e., when varying ω away from this point one has to decide which one of the two leafs in the complex α-plane is used. This has to be considered when carrying out cntour integrals in the complex ω-plane.

As it will be shown in more detail below, the localised Green's function results in wave pattern trapped at the coast. Onyl the zonal wind X (parallel to the coast) contributes to terms with poles at $\tilde{\omega} = \pm k\lambda^{-1}$, a wind field perpendicularly to the coast drives other flow pattern. In order to discuss the role of the Kelvin waves in more detail we assume $Y = 0$ for the moment.

To find the residues decomposition into partial frations is needed:

$$\frac{k}{\tilde{\omega}^2 - \lambda^{-2}k^2} = \frac{\lambda}{2}\left(\frac{1}{\tilde{\omega} - \frac{k}{\lambda}} - \frac{1}{\tilde{\omega} + \frac{k}{\lambda}}\right) \tag{1.294}$$

$$\frac{\tilde{\omega}}{\tilde{\omega}^2 - \lambda^{-2}k^2} = \frac{1}{2}\left(\frac{1}{\tilde{\omega} - \frac{k}{\lambda}} + \frac{1}{\tilde{\omega} + \frac{k}{\lambda}}\right) \tag{1.295}$$

$$\frac{1}{\tilde{\omega}\left(\tilde{\omega}^2 - \lambda^{-2}k^2\right)} = -\frac{\lambda^2}{k^2}\left(\frac{1}{\tilde{\omega}} - \frac{1}{2}\left(\frac{1}{\tilde{\omega} - \frac{k}{\lambda}} + \frac{1}{\tilde{\omega} + \frac{k}{\lambda}}\right)\right). \tag{1.296}$$

The result for u is

$$\begin{aligned} u &= \frac{i}{\tilde{\omega}} G_y * X_{y'} \\ &+ \frac{i}{2\left(\tilde{\omega} - \frac{k}{\lambda}\right)}\left(X + \lambda^2 f^2 G * X + \lambda f G * X_{y'} - \lambda f G_y * X - G_y * X_{y'}\right) \\ &+ \frac{i}{2\left(\tilde{\omega} + \frac{k}{\lambda}\right)}\left(X + \lambda^2 f^2 G * X - \lambda f G * X_{y'} + \lambda f G_y * X - G_y * X_{y'}\right) \end{aligned} \tag{1.297}$$

In the next step we write the expression in the form $u = X * ()$, which allows to discuss the terms with the Green's function separately. With the relations

$$X = x * \delta(y - y') \tag{1.298}$$

$$G * X_{y'} = G_{y'} * X \tag{1.299}$$

one finds

$$
\begin{aligned}
u &= \frac{i}{\tilde{\omega}} G_y * X_{y'} \\
&\quad + \frac{iX}{2\left(\tilde{\omega} - \frac{k}{\lambda}\right)} * \left(\delta(y-y') + \lambda^2 f^2 G - \lambda f \left(G_{y'} + G_y\right) + G_{y,y'}\right) \\
&\quad + \frac{iX}{2\left(\tilde{\omega} + \frac{k}{\lambda}\right)} * \left(\delta(y-y') + \lambda^2 f^2 G + \lambda f \left(G_{y'} + G_y\right) + G_{y,y'}\right) \qquad (1.300)
\end{aligned}
$$

For $\tilde{\omega} = \pm\frac{k}{\lambda}$ we have $\alpha^2 = -\frac{1}{R^2}$ (remember, $\lambda f = \frac{1}{R}$. For this special value for ω, the Green's function equation reads

$$
G_{yy} = \delta(y-y') + \frac{G}{R^2}. \qquad (1.301)
$$

Other useful relations are

$$
\begin{aligned}
G &= -\frac{R}{2}\left(e^{-\frac{|y-y'|}{R}} - e^{-\frac{y+y'}{R}}\right) \\
G_y &= sig(y-y')\frac{e^{-\frac{|y-y'|}{R}}}{2} - \frac{e^{-\frac{y+y'}{R}}}{2} \\
G_{y'} &= -sig(y-y')\frac{e^{-\frac{|y-y'|}{R}}}{2} - \frac{e^{-\frac{y+y'}{R}}}{2} \\
G_{y,y'} &= -\delta(y-y') + \frac{e^{-\frac{|y-y'|}{R}}}{2R} + \frac{e^{-\frac{y+y'}{R}}}{2R} \\
G_y + G_{y'} &= -e^{-\frac{y+y'}{R}} \qquad (1.302)
\end{aligned}
$$

Hence, for $\tilde{\omega} = \frac{k}{\lambda}$ we find

$$
\begin{aligned}
\delta(y-y') + \lambda^2 f^2 G - \lambda f \left(G_{y'} + G_y\right) + G_{y,y'} &= \frac{e^{-\frac{|y-y'|}{R}}}{2R} + \frac{e^{-\frac{y+y'}{R}}}{2R} + \frac{e^{-\frac{y+y'}{R}}}{R} - \frac{e^{-\frac{|y-y'|}{R}}}{2R} + \frac{e^{-\frac{y+y'}{R}}}{2R}, \\
&= \frac{2}{R} e^{-\frac{y+y'}{R}}. \qquad (1.303)
\end{aligned}
$$

For the second term $\tilde{\omega} = -\frac{k}{\lambda}$ we get

$$
\begin{aligned}
\delta(y-y') + \lambda^2 f^2 G + \lambda f \left(G_{y'} + G_y\right) + G_{y,y'} &= \frac{e^{-\frac{|y-y'|}{R}}}{2R} + \frac{e^{-\frac{y+y'}{R}}}{2R} - \frac{e^{-\frac{y+y'}{R}}}{R} - \frac{e^{-\frac{|y-y'|}{R}}}{2R} + \frac{e^{-\frac{y+y'}{R}}}{2R}, \\
&= 0. \qquad (1.304)
\end{aligned}
$$

Hence, only a Kelvin wave with $\tilde{\omega} = \frac{k}{\lambda}$ can propagate.

1.5.5. Adjustment to homogeneous wind forcing - coastal jets, upwelling and intertial waves

Now we consider a special example and assume a uniform wind field switched on at $t = 0$,

$$
X(xyzt) = \frac{u_*^2}{H_{mix}} \theta(z + H_{mix})\theta(t). \qquad (1.305)
$$

Fourier transformation and decomposition into vertical modes gives

$$X_n(kyz\omega) = \frac{u_*^2}{h_n} 2\pi\delta(k) \frac{i}{\omega + i\varepsilon}. \tag{1.306}$$

Subsequently we drop the mode index "n" again.

Using the property of the δ-distribution, $\delta(k)f(k) = \delta(k)f(0)$, the expressions for u, v and p become much simples,

$$u(k,y,\omega) = \frac{i}{\tilde{\omega}}\left(X + \lambda^2 f^2 G * X\right) \tag{1.307}$$

$$v(k,y,\omega) = \lambda^2 f G * X, \tag{1.308}$$

$$p(k,y,\omega) = -\frac{i}{\tilde{\omega}} G_y * fX, \tag{1.309}$$

and

$$\alpha^2 = \lambda^2\left(\tilde{\omega}^2 - f^2\right) \tag{1.310}$$

To transform these expression back into the space-time domain we perform first the convolation integrals. Since X is independent of y, the convolution integrals are simple integrals over the Green's function. Remember,

$$G(y,y') = -\frac{1}{\alpha}\left(\theta(y-y')e^{i\alpha y}\sin\alpha y' + \theta(y'-y)\sin\alpha y e^{i\alpha y'}\right). \tag{1.311}$$

$$\begin{aligned}\int_0^\infty dy' G(y,y') &= -\frac{1}{\alpha}\left(e^{i\alpha y}\int_0^y dy'\sin\alpha y' + \sin\alpha y\int_y^\infty dy' e^{i\alpha y'}\right)\\ &= \frac{1}{\alpha^2}\left(1 - e^{i\alpha y}\right)\end{aligned} \tag{1.312}$$

The y-derivative needed for the pressure reads

$$\int_0^\infty dy' G_y(y,y') = -\frac{i}{\alpha}e^{i\alpha y}. \tag{1.313}$$

Hence, we find expressions for pressure and currents in dependence on k, y and ω,

$$\begin{aligned}u(k,y,\omega) &= \frac{u_*^2}{h_n}2\pi\delta(k)\frac{-1}{\tilde{\omega}^2}\left(1 + \lambda^2 f^2\frac{1}{\lambda^2\left(\tilde{\omega}^2 - f^2\right)}\left(1 - e^{i\alpha y}\right)\right)\\ &= \frac{u_*^2}{h_n}2\pi\delta(k)\left(\frac{-1}{\tilde{\omega}^2 - f^2} + \frac{f^2 e^{i\alpha y}}{\tilde{\omega}^2\left(\tilde{\omega}^2 - f^2\right)}\right)\\ &= \frac{u_*^2}{h_n}2\pi\delta(k)\left(\frac{-1}{\tilde{\omega}^2 - f^2} - e^{i\alpha y}\left(\frac{1}{\tilde{\omega}^2} - \frac{1}{\tilde{\omega}^2 - f^2}\right)\right)\end{aligned} \tag{1.314}$$

$$\begin{aligned}v(k,y,\omega) &= \frac{u_*^2}{h_n}2\pi\delta(k)\frac{if}{\tilde{\omega}\left(\tilde{\omega}^2 - f^2\right)}\left(1 - e^{i\alpha y}\right)\\ &= \frac{u_*^2}{h_n}2\pi\delta(k)\frac{(-1)}{f}\left(\frac{i}{\tilde{\omega}} - \frac{i\tilde{\omega}}{\tilde{\omega}^2 - f^2}\right)\left(1 - e^{i\alpha y}\right)\end{aligned} \tag{1.315}$$

$$p(k,y,\omega) = \frac{u_*^2}{h_n} 2\pi\delta(k) \frac{f}{\tilde{\omega}^2 i\lambda\sqrt{\tilde{\omega}^2 - f^2}} e^{i\alpha y}. \tag{1.316}$$

To find the inverse Fourier transforms the singularities of the integrand must be considered.

- $\omega = -i\varepsilon$. The residues can be calculated using Cauchy's theorem. Here we use the following results:

$$\int_{-\infty}^{\infty} \frac{d\omega}{2\pi} e^{-i\omega t} \frac{i}{\omega+\varepsilon} = \theta(t), \tag{1.317}$$

$$\int_{-\infty}^{\infty} \frac{d\omega}{2\pi} e^{-i\omega t} \frac{(-1)}{(\omega+\varepsilon)^2} = \int_{-\infty}^{\infty} \frac{d\omega}{2\pi} e^{-i\omega t} \frac{\partial}{\partial\omega} \frac{1}{(\omega+\varepsilon)} = t \int_{-\infty}^{\infty} \frac{d\omega}{2\pi} e^{-i\omega t} \frac{i}{\omega+\varepsilon} \tag{1.318}$$

$$= t\theta(t). \tag{1.319}$$

Hence, these polse correspond to constant (switched on) or linearly growing flow amplitudes. We get

$$u_n(y,t) = \frac{u_*^2}{h_n} \theta(t) t e^{-\frac{y}{R_n}} \tag{1.320}$$

$$v_n(y,t) = \frac{u_*^2}{h_n f} \theta(t) \left(1 - e^{-\frac{y}{R_n}}\right) \tag{1.321}$$

$$p_n(y,t) = \frac{u_*^2}{h_n} R_n f \theta(t) t e^{-\frac{y}{R_n}} \tag{1.322}$$

Note that we have recovered the vertical mode index and will carry out the sum over vertical modes now. We have, as derived previously,

$$R_n = \frac{R_1}{n}, \qquad \lambda_n = \frac{n\pi}{NH} = \frac{1}{fR_n} \tag{1.323}$$

$$F_0 = \frac{1}{\sqrt{H}}, \qquad F_n = \sqrt{\frac{2}{H}} (-1)^n \cos\frac{\pi z}{H}. \tag{1.324}$$

The coefficients h_n for the z-dependency of the volume force are

$$\frac{1}{h_0} = \sqrt{\frac{1}{H}}, \qquad \frac{1}{h_n} = \sqrt{\frac{2}{H}} (-1)^n \frac{\sin\left(\frac{n\pi H_{mix}}{H}\right)}{\frac{n\pi H_{mix}}{H}}. \tag{1.325}$$

Hence, we find

$$u(y,z,t) = u_*^2 t \sum_{n=0}^{\infty} \frac{F_n}{h_n} e^{-\frac{y}{R_n}} = \frac{u_*^2 t}{H_{mix}} \left(\frac{H_{mix} e^{-\frac{y}{R_0}}}{H} + S^1(y,z) \right), \tag{1.326}$$

$$v(y,z,t) = -\frac{X}{f} + \frac{u_*^2}{f H_{mix}} \left(\frac{H_{mix} e^{-\frac{y}{R_0}}}{H} + S^1(y,z) \right), \tag{1.327}$$

$$w(y,z,t) = -\frac{u_*^2}{N^2} \sum_{n=1}^{\infty} \frac{F_n'}{\lambda_n h_n} e^{-\frac{y}{R_n}} = \frac{u_*^2}{N H_{mix}} S^2(y,z) \tag{1.328}$$

The last equation is gained from

$$w = -\frac{1}{N^2} p_{zt}. \tag{1.329}$$

This sums could be carried out numerically, especially, when the eigenfunctions F_n are calculated numerically. To find an analytical result for the constant N^2 case the formula

$$\begin{aligned} \sum_{n=1}^{\infty} \frac{\chi^n}{n} &= -\ln(1-\chi) = -\ln|1-\chi| - i\arg(1-\chi) \\ &= -\ln\sqrt{1-\chi-\chi^*+\chi\chi^*} - i\arctan\frac{Im(1-\chi)}{Re(1-\chi)} \end{aligned} \tag{1.330}$$

will be used. This motivates the subsequent operations to bring the summands into an appropriate form. We have to calculate both the sums

$$S^1 = H_{mix} \sum_{n=0}^{\infty} \frac{F_n}{h_n} e^{-\frac{y}{R_n}} \tag{1.331}$$

$$S^2 = -\frac{H_{mix}}{N} \sum_{n=0}^{\infty} \frac{F_n'}{\lambda_n h_n} e^{-\frac{y}{R_n}}. \tag{1.332}$$

With

$$\frac{F_n}{h_n} = \frac{2}{H}\cos\left(\frac{n\pi z}{H}\right)\frac{H}{n\pi H_{mix}}\sin\left(\frac{n\pi H_{mix}}{H}\right) \tag{1.333}$$

$$= \frac{2}{n\pi H_{mix}}\cos\left(\frac{n\pi z}{H}\right)\sin\left(\frac{n\pi H_{mix}}{H}\right), \tag{1.334}$$

and

$$-\frac{1}{N}\frac{F_n'}{\lambda_n h_n} = \frac{2}{H}\frac{n\pi}{H}\sin\left(\frac{n\pi z}{H}\right)\frac{HN}{Nn\pi}\frac{H}{n\pi H_{mix}}\sin\left(\frac{n\pi H_{mix}}{H}\right) \tag{1.335}$$

$$= \frac{2}{n\pi H_{mix}}\sin\left(\frac{n\pi z}{H}\right)\sin\left(\frac{n\pi H_{mix}}{H}\right), \tag{1.336}$$

Writing the trigonometric functions in exponential form we find,

$$H_{mix}\frac{F_n}{h_n} = \frac{1}{n\pi} Im\left(e^{in\phi_+} + e^{in\phi_+}\right) \tag{1.337}$$

$$-\frac{H_{mix}}{N}\frac{F_n}{h_n} = -\frac{1}{n\pi} Re\left(e^{in\phi_+} - e^{in\phi_+}\right), \tag{1.338}$$

with the abbreviations

$$\phi_+ = \frac{\pi}{H}\left(H_{mix} + z\right), \tag{1.339}$$

$$\phi_- = \frac{\pi}{H}\left(H_{mix} - z\right). \tag{1.340}$$

Hence, we have to calculate sums of the form

$$S = \frac{1}{\pi}\sum_{n=1}^{\infty}\frac{e^{-\frac{y}{R_n}}}{n}e^{in\phi} = \frac{1}{\pi}\sum_{n=1}^{\infty}\frac{\chi^n}{n}, \tag{1.341}$$

which is exactly the form Eq. 1.330. Hence, since S^1 is realted to the argument of the sum (imaginary part)

$$S^1 = -\frac{1}{\pi}\left(\arctan -\frac{e^{-\frac{y}{R_1}}\sin\phi_+}{1-e^{-\frac{y}{R_1}}\cos\phi_+} + \arctan -\frac{e^{-\frac{y}{R_1}}\sin\phi_-}{1-e^{-\frac{y}{R_1}}\cos\phi_-}\right) \tag{1.342}$$

$$= \frac{1}{\pi}\left(\arctan\frac{\sin\phi_+}{e^{\frac{y}{R_1}}-\cos\phi_+} + \arctan\frac{\sin\phi_-}{e^{\frac{y}{R_1}}-\cos\phi_-}\right). \tag{1.343}$$

S^2 is related to the difference of the two real parts (modulus) and reads

$$1-\chi-\chi^*+\chi\chi^* = 1-e^{-\frac{y}{R_1}}\left(e^{i\phi}-e^{-i\phi}\right)+e^{-\frac{2y}{R_1}} \tag{1.344}$$

$$= 2e^{-\frac{y}{R_1}}\left(\cosh\left(\frac{y}{R_1}\right)-\cos\phi\right), \tag{1.345}$$

and S^2 becomes

$$S^2 = \frac{1}{2\pi}\ln\frac{\cosh\left(\frac{y}{R_1}\right)-\cos\phi_+}{\cosh\left(\frac{y}{R_1}\right)-\cos\phi_-} \tag{1.346}$$

Now we can collect all terms to the final result for the non-oscillating contributions,

$$u(y,z,t) = \frac{u_*^2 t}{\pi H_{mix}}\left(\frac{\pi H_{mix}e^{-\frac{y}{R_0}}}{H} + \arctan\frac{\sin\phi_+}{e^{\frac{y}{R_1}}-\cos\phi_+} + \arctan\frac{\sin\phi_-}{e^{\frac{y}{R_1}}-\cos\phi_-}\right), \tag{1.347}$$

$$v(y,z,t) = -\frac{X}{f} + \frac{u_*^2}{f\pi H_{mix}}\left(\frac{\pi H_{mix}e^{-\frac{y}{R_0}}}{H} + \arctan\frac{\sin\phi_+}{e^{\frac{y}{R_1}}-\cos\phi_+} + \arctan\frac{\sin\phi_-}{e^{\frac{y}{R_1}}-\cos\phi_-}\right), \tag{1.348}$$

$$w(y,z,t) = \frac{u_*^2}{NH_{mix}2\pi}\ln\frac{\cosh\left(\frac{y}{R_1}\right)-\cos\phi_+}{\cosh\left(\frac{y}{R_1}\right)-\cos\phi_-} \tag{1.349}$$

This is a rather complex result. It needs some efforts to show that the coastal boundary condition is fulfilled. The best way to study the shape of these flow pattern is to write a short program for visualisation. This can be done with matlab

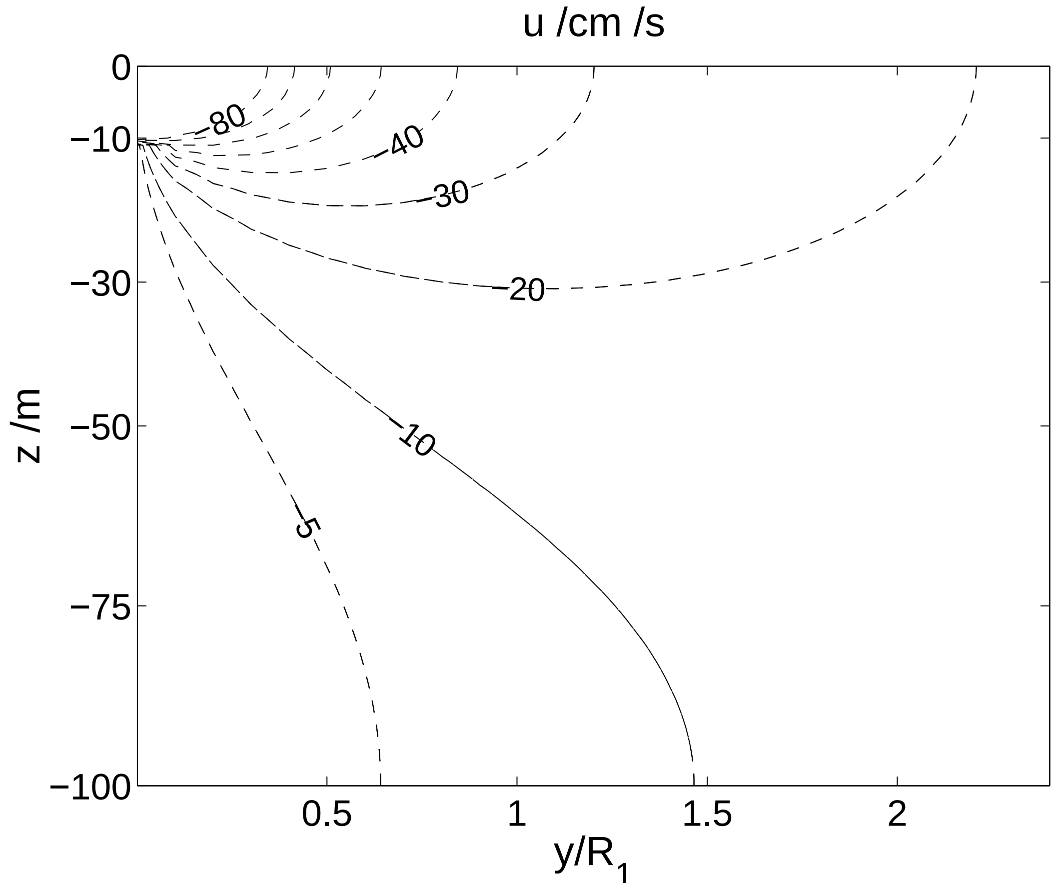

Figure 1.9. The coastal jet

or ferret or similar tools. Because the solution does not depend on x and has a simple time dependency, sections in the y-z plane are possibly the best choice.

For the visualisation we choose an easterly wind, hence, blowing in negative zonal direction. X carries a minus sign. As a result the zonal flow is driven westward too. Maximum speed is found at the surface and near the coast, it decreases downward and in off shore direction. This is the reason for the name "coastal jet".

- $\omega = \pm f - i\varepsilon$. Distant from the coast, $y \to \infty$ the exponentials tend to zero. This is so because of the small imaginary part of $\tilde{\omega}$. In this case we find

$$u_n(y,\omega) = \frac{u_*^2}{h_n}\frac{-1}{\tilde{\omega}^2 - f^2} \quad (1.350)$$

$$v_n(y,\omega) = \frac{u_*^2}{h_n}\frac{(-1)}{f}\left(\frac{i}{\tilde{\omega}} - \frac{i\tilde{\omega}}{\tilde{\omega}^2 - f^2}\right) \quad (1.351)$$

$$p_n(y,\omega) = 0 \quad (1.352)$$

The pressure perturbation vanishes. This is not surprising, far offshore a homgeneous wind drives only Ekman transport and inertial oscillations in the surface layer. Again with Cauchy's integral theorem we can solve the follwoing integrals,

$$\int_{-\infty}^{\infty} \frac{d\omega}{2\pi} e^{-i\omega t} \frac{-f}{\tilde{\omega}^2 - f^2} = \theta(t)\sin ft, \quad (1.353)$$

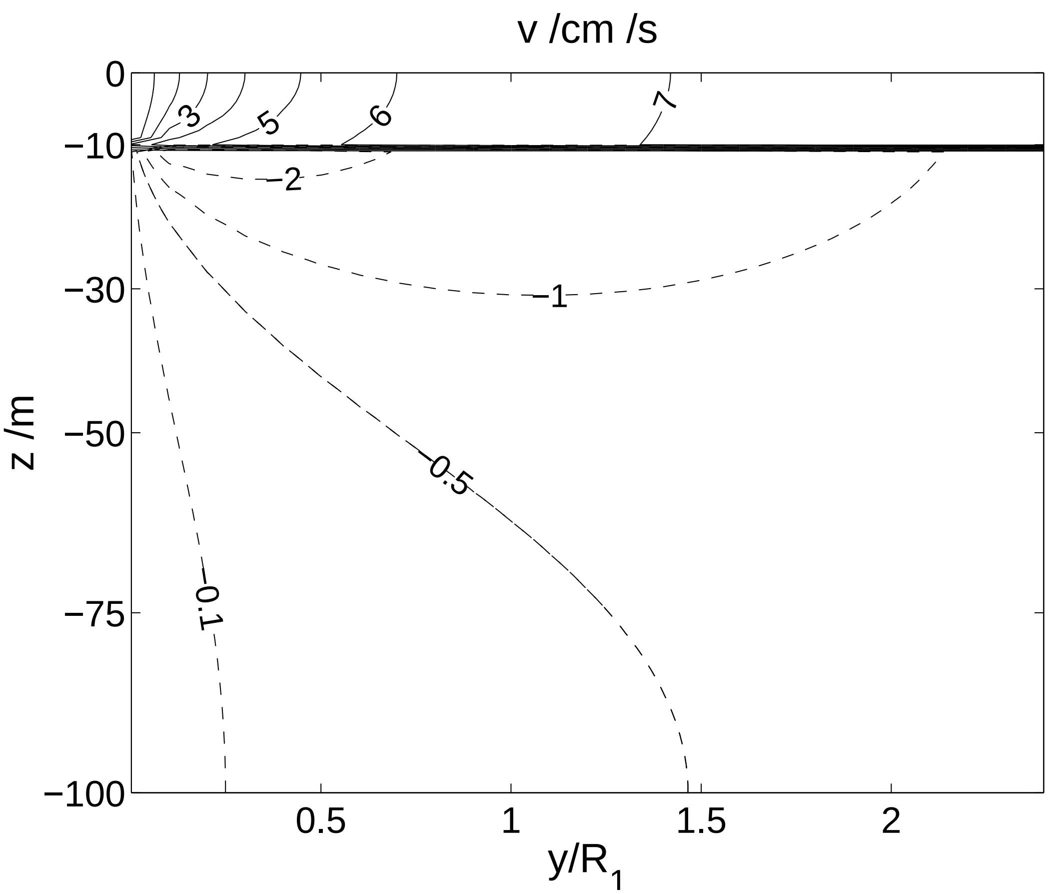

Figure 1.10. The cross shore current

$$\int_{-\infty}^{\infty} \frac{d\omega}{2\pi} e^{-i\omega t} \frac{i\tilde{\omega}}{\tilde{\omega}^2 - f^2} \quad = \quad \theta(t) \cos ft. \tag{1.354}$$

$$u_n(y,t) \quad = \quad \frac{u_*^2}{h_n} \frac{1}{f} \theta(t) \sin ft \tag{1.355}$$

$$v_n(y,t) \quad = \quad \frac{u_*^2}{h_n} \frac{(-1)}{f} \theta(t) \left(1 - \cos ft\right) \tag{1.356}$$

$$p_n(y,t) \quad = \quad 0 \tag{1.357}$$

The sum over the vertical eigenfunctions $\sum_{n=0}^{\infty} F_n(z)(u_n, v_n, p_n)$ just reconstructs the volume force X

$$u(y,z,t) \quad = \quad \frac{1}{f} X \sin ft, \tag{1.358}$$

$$v(y,z,t) \quad = \quad \frac{(-1)}{f} X \left(1 - \cos ft\right), \tag{1.359}$$

$$p(y,z,t) \quad = \quad 0, \tag{1.360}$$

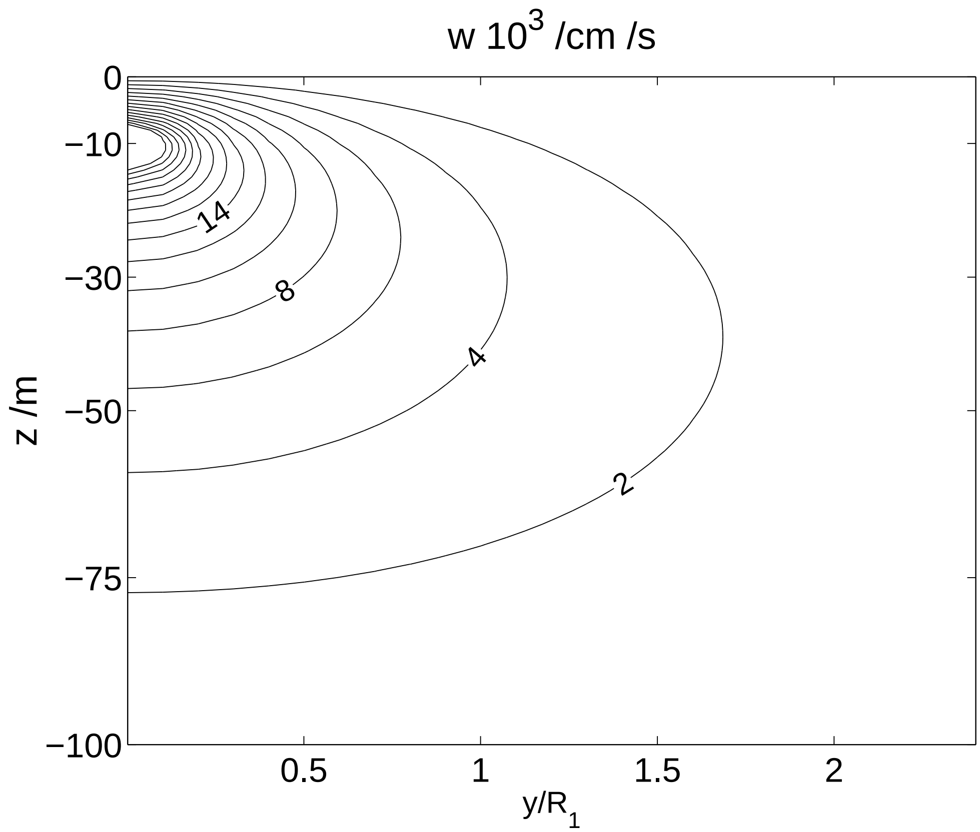

Figure 1.11. The vertical velocity

which is the well known solution for an f-plane ocean forced by a homoheneous wind. The balance of forces (accelerations) is

$$\frac{\partial}{\partial t}u_n - fv_n = X_n, \tag{1.361}$$

$$fu_n(y,t) + \frac{\partial}{\partial y}p_n(y,t) = 0. \tag{1.362}$$

Near the coast, where v is small, the along shore flow u is accelerated by the wind field. More offshore the action of the wind is counteracted by the Coriolis force from the cross shore current, far off shore there remains only the Ekman balance $-fv_n = X_n$. Inertial oscillations will be discussed below. The accelerating current is confined to the coast, therefor it is called coastal jet. Each vertical mode has the baroclinic Rossby radius R_n as its characteristic length scale. The coastal jet is in geostrophic balance with a cross shore pressure gradient.

Note, this part of the solution does not explain how the cross shore current v is driven!

- Branch points at $\alpha = 0$. I simple separate calculation of the contribution of the branch points at $\alpha = 0$ is not possible, but is partly coupled with the asymptotic expresssions discussed previously.

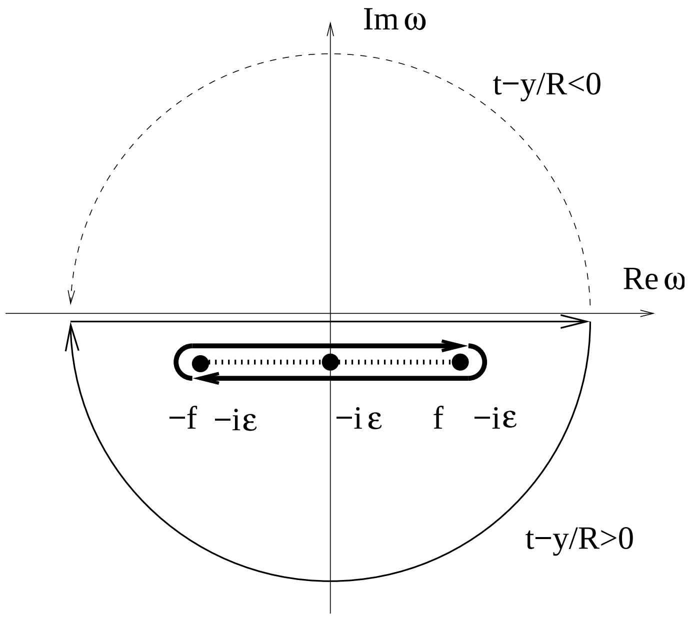

Figure 1.12. Choice of the integration path for the general integrals $C^{(1)}$ and $C^{(2)}$. A separate integration around the singularities is not possible, since α changes sign when crossong the cut in the complex plane (dashed line).

We return to equations 1.314, 1.315 and 1.316, perform the backward Fourier integral with respect to k. Now we transform back into the time domain. Some expression have been discussed before and we use the results.

$$u(x,y,t) = \frac{u_*^2}{h}\left(\theta(t)\frac{\sin ft}{f} + C^{(2)}(y,t)\right) \tag{1.363}$$

$$v(x,y,t) = \frac{u_*^2}{h}\left(\frac{\theta(t)}{f}(\cos ft - 1) + \frac{1}{f}C_t^{(2)}(y,t)\right) \tag{1.364}$$

$$p(x,y,t) = \frac{u_*^2}{h}\frac{f}{\lambda}C^{(1)}(y,t) \tag{1.365}$$

The two integrals $C^{(1)}$ and $C^{(2)}$ are

$$C^{(1)} = \int_{-\infty}^{\infty}\frac{d\omega}{2\pi i}\frac{e^{i\sqrt{\tilde\omega^2-f^2}\lambda y - i\omega t}}{\tilde\omega^2\sqrt{\tilde\omega^2-f^2}}, \tag{1.366}$$

$$C^{(2)} = \int_{-\infty}^{\infty}\frac{d\omega}{2\pi}\frac{f^2 e^{i\sqrt{\tilde\omega^2-f^2}y - i\omega t}}{\tilde\omega^2\left(\tilde\omega^2-f^2\right)}. \tag{1.367}$$

Evaluation of $C^{(1)}$

Following the idea of Fennel, as a first step $C_{tt}^{(1)}$ is transformed into a time integral. $C_{tt}^{(1)}$reads

$$C_{tt}^{(1)} = -\int_{-\infty}^{\infty}\frac{d\omega}{2\pi i}\frac{e^{i\sqrt{\tilde{\omega}^2-f^2}\lambda y-i\omega t}}{\sqrt{\tilde{\omega}^2-f^2}}. \tag{1.368}$$

The integration path can be completed again to a closed contour. Figure 1.12 shows details. For $\lambda y - t > 0$ the semi-circle in the upper half-plane does not contribute to the integral. In this case the inetgration path does not include any singularity and the integral vanishs. For $\lambda y - t < 0$ the integral can be closed in the lower half-plane. Using Cauchy's theorem, the contour can be contracted to the thick closed line. At the upper line the square root $\sqrt{\tilde{\omega}^2 - f^2}$ has the positive sign, at the lower line the negative sign. Hence,

$$\begin{aligned} C_{tt}^{(1)} &= \theta(t-\lambda y) - \int_{-f}^{f}\frac{d\omega}{2\pi i}\frac{e^{i\sqrt{\omega^2-f^2}\lambda y-i\omega t}}{\sqrt{\omega^2-f^2}} - \int_{f}^{-f}\frac{d\omega}{2\pi i}\frac{e^{-i\sqrt{\omega^2-f^2}\lambda y-i\omega t}}{(-1)\sqrt{\omega^2-f^2}} \\ &= \theta(t-\lambda y)\frac{2}{\pi}\int_0^f d\omega\frac{\cosh\sqrt{f^2-\omega^2}\lambda y}{\sqrt{f^2-\omega^2}}\cos\omega t. \end{aligned} \tag{1.369}$$

This integral can be found in standard integral tables leads to a Bessel function of first kind,

$$C_{tt}^{(1)} = \theta(t-\lambda y)J_0\left(f\sqrt{t^2-\lambda^2 y^2}\right). \tag{1.370}$$

The two time integrals can be found either by using the convolution theorem or by direct time integration using a partial integral and the properties of the step function,

$$C_{t}^{(1)} = \int_{-\infty}^{t} dt'\theta(t'-\lambda y)J_0\left(f\sqrt{t'^2-\lambda^2 y^2}\right), \tag{1.371}$$

$$C^{(1)} = \int_{-\infty}^{t} dt'(t-t')\theta(t'-\lambda y)J_0\left(f\sqrt{t'^2-\lambda^2 y^2}\right). \tag{1.372}$$

So far we have replaced only the ω-integral by a time integral. This integral can be carried out numerically, using standard techniques, e.g. a Romberg or Runge-Kutta scheme.

For our purpose analytical approximation may help to understand some more details. The first finding ist, that the integrals vanish for $t < \lambda y$. Hence, considering some special place with a distance y to the coast. The pressure perturbation given by $C^{(1)}$ remains zero until a wave with phase speed λ^{-1}, (remember, this is the upper limit for the group speed), arrrives at this special position. Again, waves are responsible for propagation of pressure signals away from the coast.

To consider the response for large times, $t \gg \lambda y$we search for asymptotic expressions. With the transformation

$$\begin{aligned} t^2 - \lambda^2 y^2 &= q^2, \qquad t^2 = q^2 + \lambda^2 y^2, \\ dt &= \frac{q}{t}dq = \frac{q}{\sqrt{q^2+\lambda^2 y^2}}dq \end{aligned} \tag{1.373}$$

we find

$$C^{(1)} = \theta(t-\lambda y)\int_0^{q_t} dq J_0(fq)\left(\frac{qt}{\sqrt{q^2+\lambda^2y^2}}-q\right),$$
$$q_t = \sqrt{t^2-\lambda^2y^2} \quad (1.374)$$

It is important, that the integrand vanishes at the upper boundary. An approximation for the first term can be found from the integral

$$\int_0^\infty dx\frac{x}{\sqrt{x^2+a^2}}J_0(fx) = \frac{1}{f}e^{-fa}. \quad (1.375)$$

For the second integral we use the relation

$$\int dx x J_0(x) = xJ_1(x), \quad (1.376)$$

and find

$$C^{(1)} = \theta(t-\lambda y)\left(\frac{t}{f}e^{-f\lambda y}-\int_{q_t}^\infty dq\frac{qtJ_0(fq)}{\sqrt{q^2+\lambda^2y^2}}\right)$$
$$-\theta(t-\lambda y)\frac{1}{f}\sqrt{t^2-\lambda^2y^2}J_1\left(f\sqrt{t^2-\lambda^2y^2}\right). \quad (1.377)$$

Obviously, all contribution diverge at for large times t. This is not a satisfying result, away from the coast the response to wind field should vanish. (Remember the original boundary conditions). Hence, we try to reorder the terms. To this end, we use the recurrence relation of the Bessel functions,

$$J_0(x) = J_1(x)+\frac{J_1'(x)}{x}. \quad (1.378)$$

This gives

$$\int_{q_t}^\infty dq\frac{qtJ_0(fq)}{\sqrt{q^2+\lambda^2y^2}} = \int_{q_t}^\infty dq\frac{qt}{\sqrt{q^2+\lambda^2y^2}}\left(\frac{1}{f}\frac{\partial}{\partial q}J_1(fq)+\frac{J_1(fq)}{fq}\right). \quad (1.379)$$

After integrating the first summand by parts we find

$$\int_{q_t}^\infty dq\frac{qtJ_0(fq)}{\sqrt{q^2+\lambda^2y^2}} = -\frac{\sqrt{t^2-\lambda^2y^2}}{f}J_1\left(f\sqrt{t^2-\lambda^2y^2}\right)$$
$$+\int_{q_t}^\infty dqJ_1(fq)\frac{tq^2}{f\sqrt{q^2+\lambda^2y^2}^3} \quad (1.380)$$

The first term cancels exactly the last term of Eq. (1.377), hence these divergent terms cancel out. The remaining term can be processed by using

$$J_1(x) = -J_0'(x). \quad (1.381)$$

Integrating again by parts gives

$$\int_{q_t}^\infty dq\frac{qtJ_0(fq)}{\sqrt{q^2+\lambda^2y^2}} = -\frac{\sqrt{t^2-\lambda^2y^2}}{f}J_1\left(f\sqrt{t^2-\lambda^2y^2}\right)$$
$$-\frac{1}{f^2}J_0\left(f\sqrt{t^2-\lambda^2y^2}\right)\frac{t^2-\lambda^2y^2}{t^2}-\int_{q_t}^\infty dq\frac{J_0(fq)}{q}\mathcal{O}(t/q) \quad (1.382)$$

The last term vanishes faster then t^{-1} for large times t. Hence, we find the following result for the asymptotic behaviour of $C^{(1)}$,

$$C^{(1)} \approx \theta(t-\lambda y)\left(\frac{t}{f}e^{-f\lambda y}+\frac{1}{f^2}J_0\left(f\sqrt{t^2-\lambda^2y^2}\right)\frac{t^2-\lambda^2y^2}{t^2}\right). \quad (1.383)$$

For large arguments the Bessel function shows a slowly decreasing oscillation,

$$\begin{aligned} J_0\left(f\sqrt{t^2-\lambda^2y^2}\right) &\approx \sqrt{\frac{2}{f\pi t}}\cos\left(f\sqrt{t^2-\lambda^2y^2}-\frac{\pi}{4}\right) \\ &= -\sqrt{\frac{2}{f\pi t}}\sin\left(f\sqrt{t^2-\lambda^2y^2}+\frac{\pi}{4}\right) \end{aligned} \quad (1.384)$$

It is important, that we keep the full argument in the *sin*-function. This so called "phase conserving approximation" is needed for the summation over the vertical modes.

$$C^{(1)} \approx \theta(t-\lambda y)\left(\frac{t}{f}e^{-f\lambda y}-\frac{1}{f^2}\sqrt{\frac{2}{f\pi t}}\sin\left(f\sqrt{t^2-\lambda^2y^2}+\frac{\pi}{4}\right)\right). \quad (1.385)$$

Evaluation of $C^{(2)}$

Similarly (Fennel, 1989) we find for $C^{(2)}$ the representation as a time integral,

$$\begin{aligned} C^{(2)} &= \theta(t-\lambda y)\left(t-\lambda y-\frac{\sin f(t-\lambda y)}{f}\right) \\ &\quad -\frac{y}{R}\int_{-\infty}^{t}dt'\left(t-t'-\frac{\sin f(t-t')}{f}\right)\theta(t'-\lambda y)\frac{J_1\left(f\sqrt{t'^2-\lambda^2y^2}\right)}{\sqrt{t'^2-\lambda^2y^2}}. \end{aligned} \quad (1.386)$$

The asymptotic result for large time reads,

$$C^{(2)} \approx \theta(t-\lambda y)\left(te^{-\frac{y}{R}}-\frac{\sin ft}{f}+\frac{y}{R}\sqrt{\frac{2}{f\pi t}}\sin\left(f\sqrt{t^2-\lambda^2y^2}+\frac{\pi}{4}\right)\right), \quad (1.387)$$

$$C_t^{(2)} \approx \theta(t-\lambda y)\left(e^{-\frac{y}{R}}-\cos ft+\frac{y}{Rf}\sqrt{\frac{2}{f\pi t}}\cos\left(f\sqrt{t^2-\lambda^2y^2}+\frac{\pi}{4}\right)\right) \quad (1.388)$$

Switch from Ekman balance to Yoshida balance

We summarize the result in the asymptotic form:

$$\begin{aligned} u(x,y,t) &= \frac{u_*^2}{h}\left(\theta(t)\frac{\sin ft}{f}\right. \\ &\quad \left.+\theta(t-\lambda y)\left(te^{-\frac{y}{R}}-\frac{\sin ft}{f}+\frac{y}{R}\sqrt{\frac{2}{f\pi t}}\sin\left(f\sqrt{t^2-\lambda^2y^2}+\frac{\pi}{4}\right)\right)\right) \end{aligned} \quad (1.389)$$

$$\begin{aligned} v(x,y,t) &= \frac{u_*^2}{h}\left(\frac{\theta(t)}{f}(\cos ft-1)\right. \\ &\quad \left.+\frac{\theta(t-\lambda y)}{f}\left(e^{-\frac{y}{R}}-\cos ft+\frac{y}{Rf}\sqrt{\frac{2}{f\pi t}}\cos\left(f\sqrt{t^2-\lambda^2y^2}+\frac{\pi}{4}\right)\right)\right) \end{aligned} \quad (1.390)$$

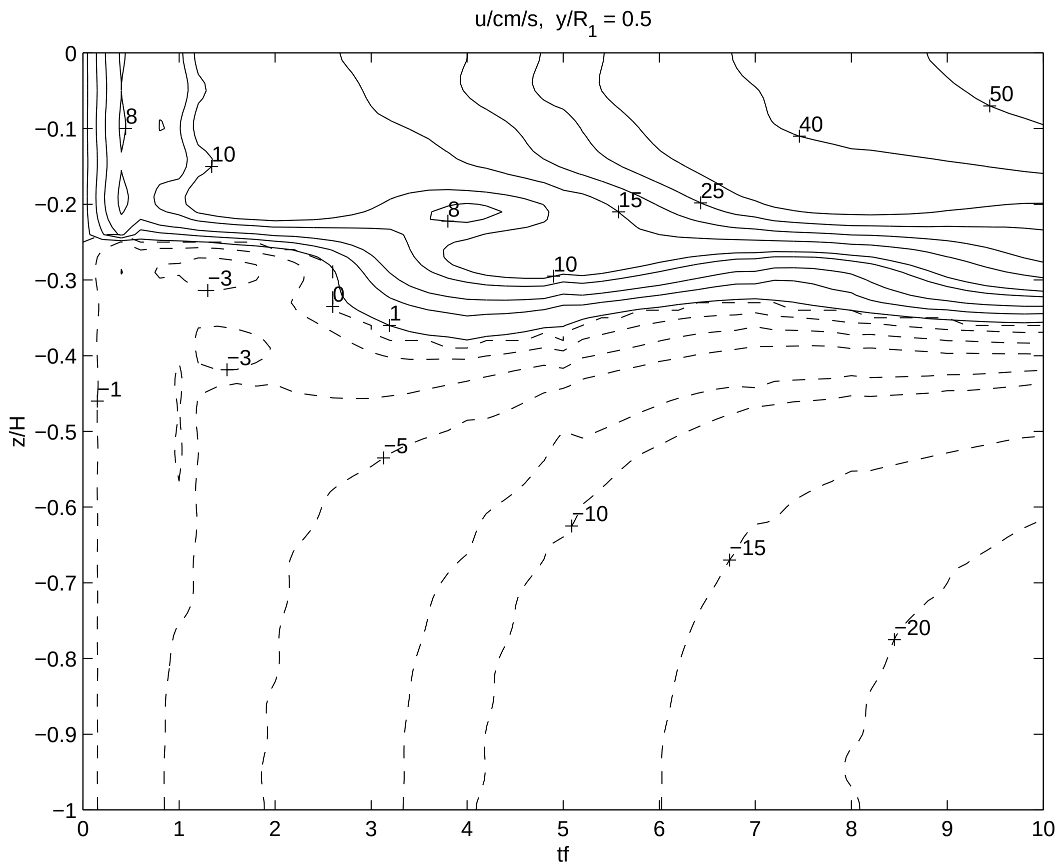

Figure 1.13. Long shore current at $y/R_1 = .5$. After passing through of the first baroclinic mode there develops a coastal jet.

$$p(x,y,t) = \frac{u_*^2}{h}\frac{f}{\lambda}\theta(t-\lambda y)\left(\frac{t}{f}e^{-\frac{y}{R}} - \frac{1}{f^2}\sqrt{\frac{2}{f\pi t}}\sin\left(f\sqrt{t^2-\lambda^2y^2}+\frac{\pi}{4}\right)\right) \quad (1.391)$$

$$w(x,y,t) = \frac{u_*^2}{h}\frac{f}{\lambda}\theta(t-\lambda y)\left(\frac{1}{f}e^{-\frac{y}{R}} - \frac{1}{f}\sqrt{\frac{2}{f\pi t}}\cos\left(f\sqrt{t^2-\lambda^2y^2}+\frac{\pi}{4}\right)\right) \quad (1.392)$$

The vertical velocity is diagnosed form the equation of continuity.

This representation of the solution highlights the role of waves. Assume to be an observer at a fixed position with distance y from the coast. The wind starts blowing and intertial oscillations in the mixed surface layer in combination with Ekman transport can be observed with a current meter. Analysing the balance of forces (accelerations) an Ekman balance is found.

After the time $t_0 = \lambda_0 y$ the current field changes. The oscillations in the surface layer become weaker, instead some oscillation in depth with opposite phase can be observed.

Near the coast the Ekman transport becomes rapidly diminished and the sea level in falling. Vertical movement rises deeper water, which upwells to the surface even seen from space as a band of cold water.

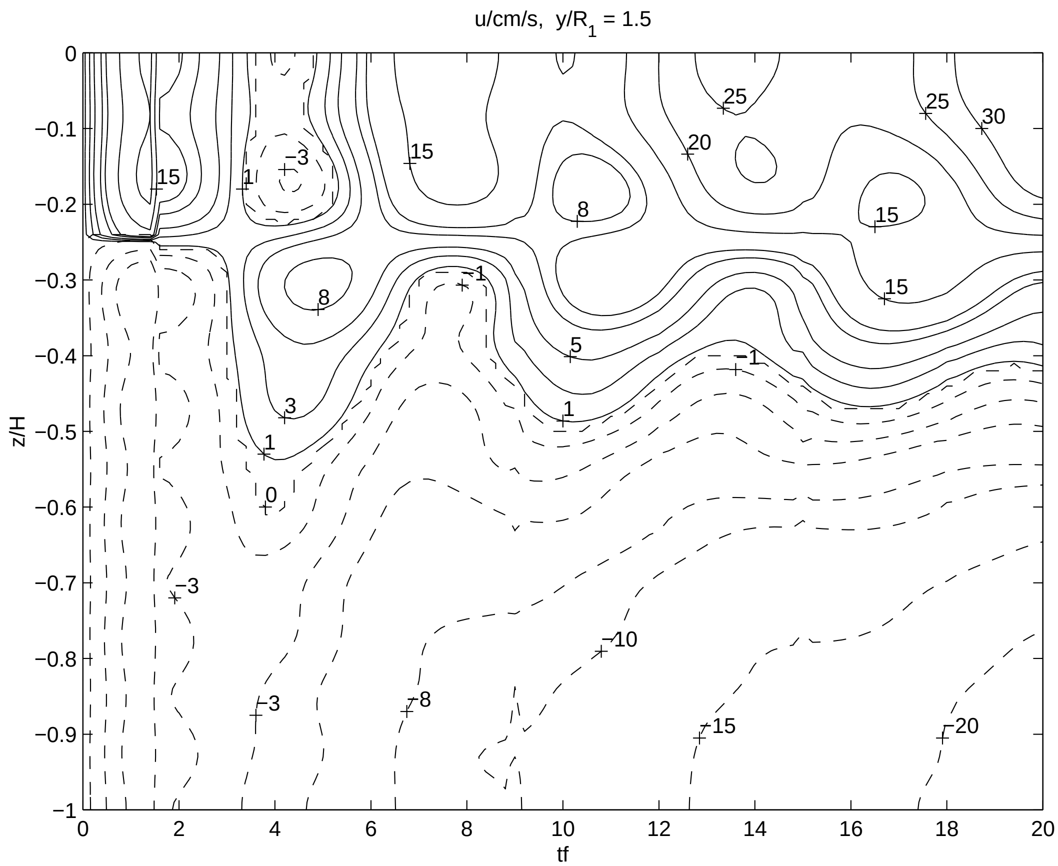

Figure 1.14. Long shore current at $y/R_1 = 1.5$. After passing through of the first baroclinic mode there develops a coastal jet modulated by inertial waves.

For samll time we have an Ekman balance,

$$\begin{aligned} u_t - fv &= X \\ v_t + fu &= 0 \\ p &= 0. \end{aligned}$$

For large times when the inertial waves radiated away a geostrophically balanced pressure perturbation develops and the balance is called a Yoshida balance,

$$\begin{aligned} u_t - fv &= X \\ fu + p_y &= 0 \\ \lambda^2 p_t + v_y &= 0. \end{aligned}$$

1.5.6. A note on the accellerating coastal jet

Near the coast the Ekman balance ist disturbed and a Yoshida balance develops. This implies that the Coriolis force does not balance the acceleration in the direction of the wind stress. Hence, the along-shore current u accelerates linearly. The permanent radiation

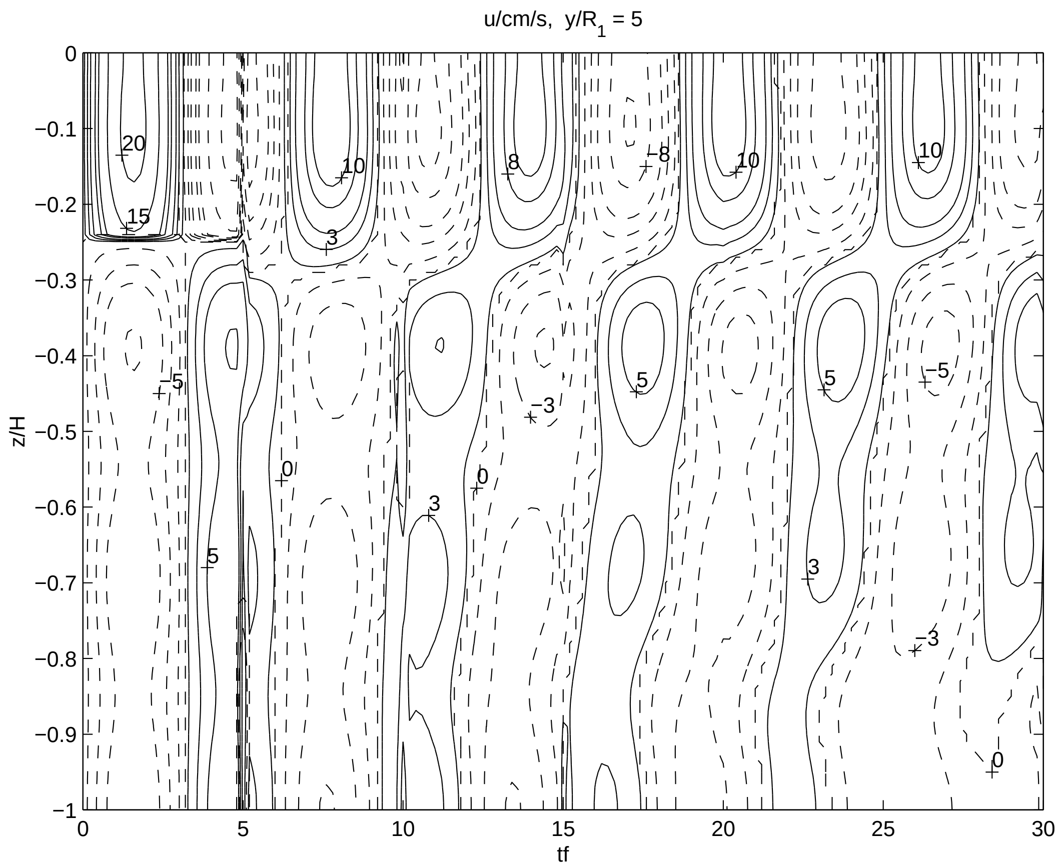

Figure 1.15. Long shore current at $y/R_1 = 5$. Inertial oscillations are modified after passage of the first baroclinic wave but remain still visible.

of inertial waves from the coast establishes a growing pressure gradient in geostrophic balance with the coastal jet. This is not a satisfying result so far. The reason seem to be simple - friction is missing completely. Bottom friction could be considered by an additional stress term. However, experiments show that this term must be proportional to the square of the bottom velocity. Inclusion into our Green's function approach is difficult. In Section 1.2.1 the decomposition into vertical eigenfunction for a special form of vertical vertical friction is described. The result was, that the time derivatives of the velocity are replaced by terms of the form

$$\frac{\partial}{\partial t}u_n \quad\rightarrow\quad \frac{\partial}{\partial t}u_n + A_n u_n, \tag{1.393}$$

or after Fourier transformation

$$i\omega u_n \quad\rightarrow\quad i(\omega + iA_n)u_n, \tag{1.394}$$

Hence, we can replace ω everywhere by $\omega + iA$, except the forcing term X. The linear growth of u and p is replaced by

$$t \quad\rightarrow\quad \frac{1-e^{-At}}{A}. \tag{1.395}$$

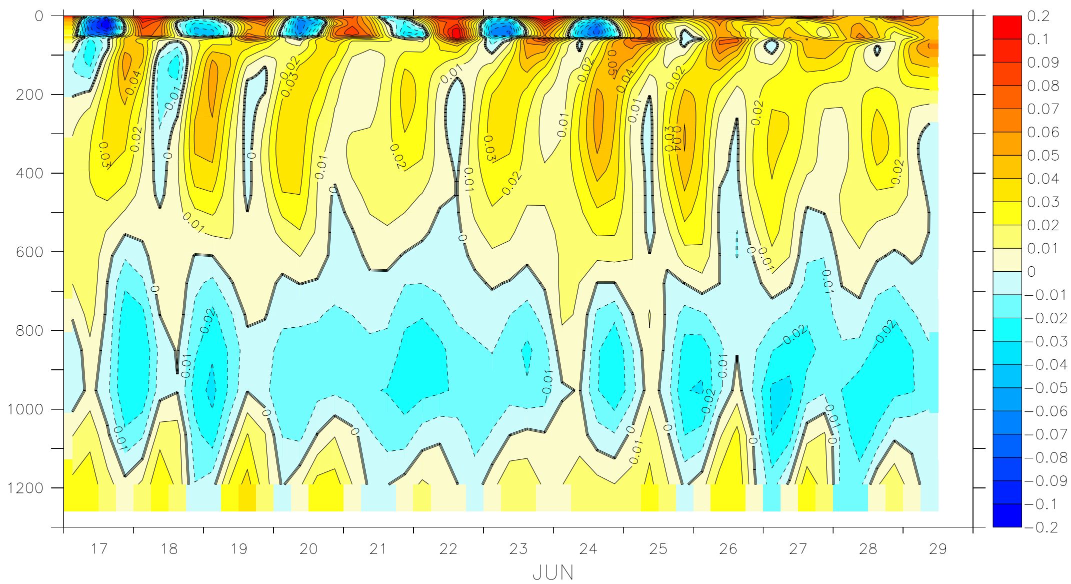

Figure 1.16. Inertial waves in the cross shore current off Namibia seen in model results. Note the phase jump at mixed layer depth.

For small times, $At \ll 1$ the linear accelleration is retained.

Another limitation of the linearly growing coastal jet is shown in the next section. The f-plane approximation, hence the assumption of an infinitely extended ocean driven by a uniform wind field is clearly unrealistic. Laterally limited winds lead to the generation of Kelvin waves propagating along the coast. Behind these wave fronts the linear acceller-ation of the coastal jet will be stopped and a limited solution can be found even for the frictionless case.

1.5.7. Adjustment to inhomogeneous forcing - coastal jets, undercurrents and Kelvin waves

We consider now an alongshore wind field over a half plane. We have seen that coastally trapped waves can only propagate with the coast to the right hand side of the propagation direction (northern hemisphere). Hence, we have to consider two cases,

$$X(xyzt) = \frac{u_*^2}{H_{mix}}\theta(z+H_{mix})\theta(t)\theta(\pm x). \tag{1.396}$$

Fourier transformation of $\theta(x)$ needs a short discussion. It reads

$$\int_{-\infty}^{\infty} dx\theta(\pm x)e^{-i\tilde{k}x} = \frac{i}{\tilde{k}}\begin{cases} e^{-i\tilde{k}x}-1, & x\to\infty \quad : \quad + \\ 1-e^{-i\tilde{k}x}, & x\to-\infty \quad : \quad - \end{cases} \tag{1.397}$$

Hence, $\tilde{k}$ needs to be defined differently in both cases to let the exponential expression vanish,

$$\int_{-\infty}^{\infty} dx\theta(\pm x)e^{-i(k\mp i\varepsilon)x} = \frac{\mp i}{k\mp i\varepsilon} \tag{1.398}$$

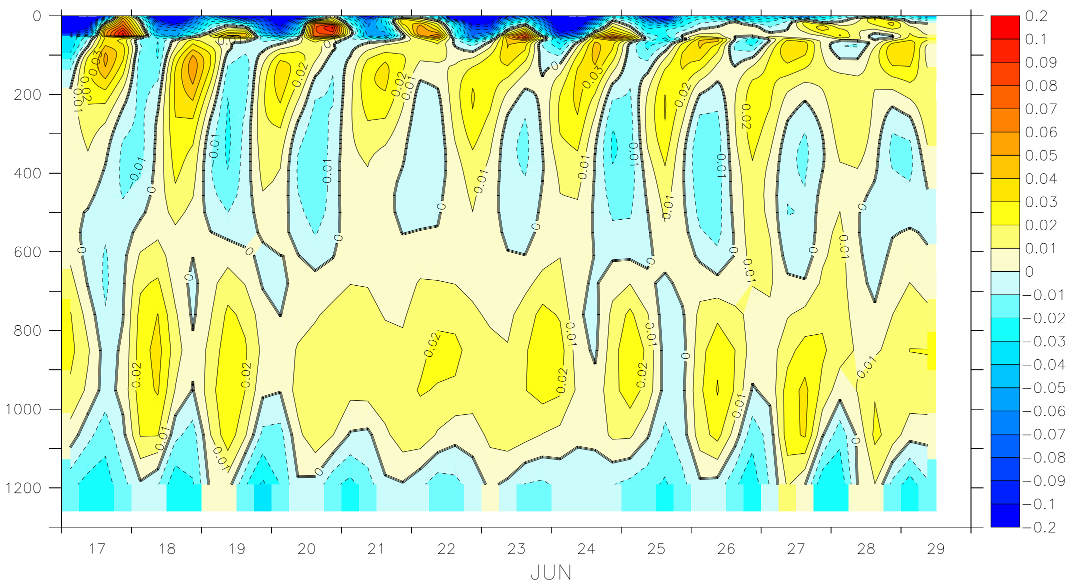

Figure 1.17. Inertial waves in the long shore current off Namibia seen in model results. Note the phase jump at mixed layer depth.

Fourier transformation of X and decomposition into vertical eigenfunctions gives

$$X_n(k\omega) = \frac{u_*^2}{h}\frac{i}{\omega + i\varepsilon}\frac{\mp i}{k \mp i\varepsilon}. \tag{1.399}$$

We return to the formal solution and skip all terms with Y and X_y,

$$u(k,y,\omega) = \frac{u_*^2}{h}\frac{i}{\omega + i\varepsilon}\frac{\mp i}{k \mp i\varepsilon}\frac{i}{\omega^2 - \lambda^{-2}k^2}\left(\tilde{\omega} + \lambda^2 f^2 \tilde{\omega} G * 1 - kfG_y * 1\right) \tag{1.400}$$

$$v(k,y,\omega) = \frac{u_*^2}{h}\frac{i}{\omega + i\varepsilon}\frac{\mp i}{k \mp i\varepsilon}\lambda^2 f G * 1 \tag{1.401}$$

$$p(k,y,\omega) = \frac{u_*^2}{h}\frac{i}{\omega + i\varepsilon}\frac{\mp i}{\omega \mp i\varepsilon}\frac{i\lambda^{-2}}{\tilde{\omega}^2 - \lambda^{-2}k^2}\left(k + k\lambda^2 f^2 G * 1 - \tilde{\omega}\lambda^2 f G_y * 1\right) \tag{1.402}$$

The spectrum has been considered previously, ploes at $\tilde{\omega} = 0$, $\tilde{\omega} = \pm k/\lambda$ and a branche point at $\alpha = 0$. We have seen, that the residuum at $\tilde{\omega} = -k/\lambda$ vanishs (at the northern hemishere for $f > 0$). We have also shown, that the branch point corresponds to inertial waves. Here we consider all contributions except inertial waves and have to find the residuum at $\tilde{\omega} = 0$ and $\tilde{\omega} = k/\lambda$. Repeating the considerations made for the spectrum we find

$$u(k,y,\omega) = \frac{u_*^2}{h}\frac{\pm i}{k \mp i\varepsilon}\frac{\lambda}{k}\left(\frac{e^{-\frac{y}{R}}}{\tilde{\omega} - \frac{k}{\lambda}} - \frac{1}{\omega}\frac{e^{-\sqrt{1+k^2R^2}\frac{y}{R}}}{\sqrt{1+k^2R^2}}\right) \tag{1.403}$$

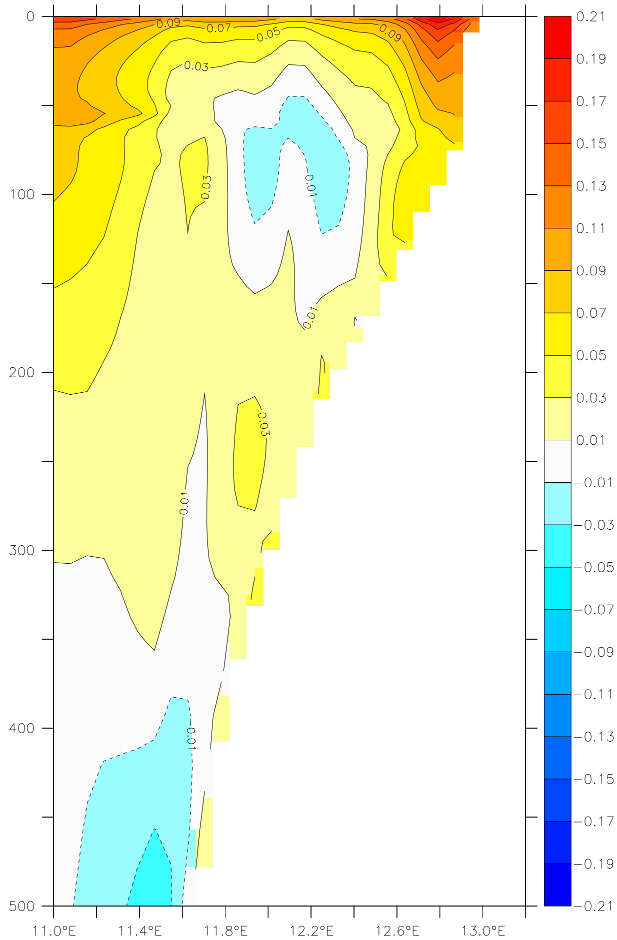

Figure 1.18. Example for a coastal jet seen in model results at 20°S

$$v(k,y,\omega) = \frac{u_*^2}{h}\frac{\mp 1}{k \mp i\varepsilon}\frac{i}{\tilde{\omega}}\left(\frac{1 - e^{-\sqrt{1+k^2R^2}\frac{y}{R}}}{f\left(1+k^2R^2\right)}\right) \tag{1.404}$$

$$p(k,y,\omega) = \frac{u_*^2}{h}\frac{\mp i}{k \mp i\varepsilon}\frac{1}{k}\left(\frac{e^{-\frac{y}{R}}}{\tilde{\omega} - \frac{k}{\lambda}} - \left(\frac{k^2R^2 + e^{-\sqrt{1+k^2R^2}\frac{y}{R}}}{\tilde{\omega}\left(1+k^2R^2\right)}\right)\right) \tag{1.405}$$

Now we apply Cauchy's theorem and find for the inverse Fourier transformed with respect to time

$$u(k,y,t) = \frac{u_*^2}{h}\frac{\mp i}{k \mp i\varepsilon}\frac{i\lambda}{k}\left(e^{-\frac{y}{R}}\left(e^{-\frac{itk}{\lambda}} - 1\right) - \left(\frac{e^{-\sqrt{1+k^2R^2}\frac{y}{R}}}{\sqrt{1+k^2R^2}} - e^{-\frac{y}{R}}\right)\right) \tag{1.406}$$

$$v(k,y,t) = \frac{u_*^2}{h}\frac{\mp i}{k \mp i\varepsilon}\frac{1}{f}\left(\left(e^{-\frac{y}{R}} - 1\right) + \frac{k^2R^2}{1+k^2R^2} + \left(\frac{e^{-\sqrt{1+k^2R^2}\frac{y}{R}}}{1+k^2R^2} - e^{-\frac{y}{R}}\right)\right) \tag{1.407}$$

$$p(k,y,t) \;=\; \frac{u_*^2}{h}\frac{\mp i}{k \mp i\varepsilon}\frac{i}{k}\left(e^{-\frac{y}{R}}\left(e^{-\frac{itk}{\lambda}}-1\right)-\frac{k^2R^2}{1+k^2R^2}-\left(\frac{e^{-\sqrt{1+k^2R^2}\frac{y}{R}}}{1+k^2R^2}-e^{-\frac{y}{R}}\right)\right) \quad (1.408)$$

Now we have to be specific with the meaning of k. The Fourier transformation needs an infinitesimal imaginary part. For a uniform wind field this needs no specification, since only wave processes with wave number $k = 0$ can be excited. Here we make the same choice as for the wind forcing and replace k with $k \mp i\varepsilon$. This guaranties that all Fourier integrals exist where integrands are finite for $x \to \pm\infty$.

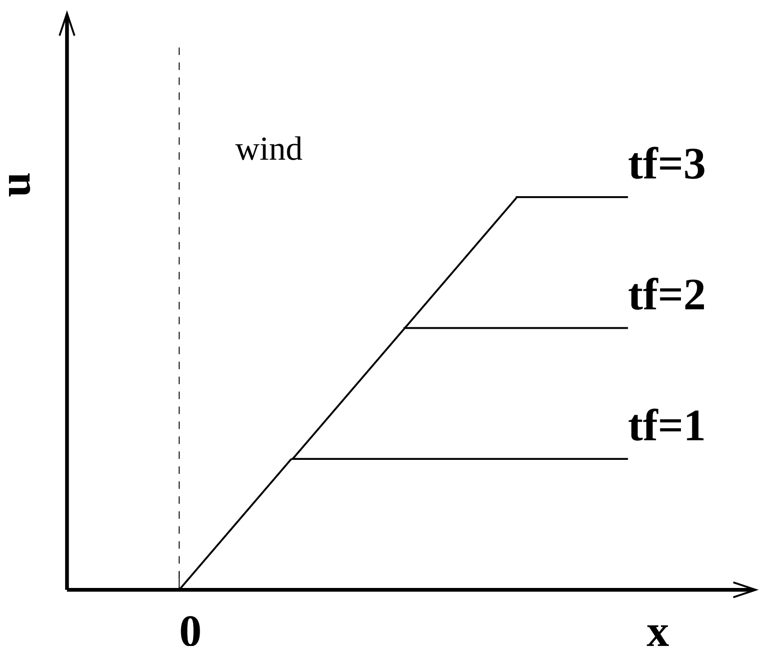

Figure 1.19. Kelvin waves arresting the coastal jet. Distant from the origin, the jet accelerates linearly with time and is independent of the coordinate x. When a wave front has passed through, u remains constant with time. The value depends on the time of arrest and is growing linearly with the distance of the origin.

Performing the inverse Fourier integral over k we consider only the residuum of $k = 0$. For this pole the expression in the last paranthesis has a vanishing contribution. This can be shown by a Taylor series with repect to k where the zero'th order vanishs and the next term is of order k^2. Using the integrals:

$$\int_{-\infty}^{\infty}\frac{dk}{2\pi}\frac{\mp i e^{ikx}}{(k \mp i\varepsilon)} \;=\; \theta(\pm x) \quad (1.409)$$

$$\int_{-\infty}^{\infty}\frac{dk}{2\pi}\frac{-e^{ikx}}{(k \mp i\varepsilon)^2} \;=\; \pm x\theta(\pm x) \quad (1.410)$$

the result is

$$u(k,y,t) \;=\; \frac{u_*^2}{h}e^{-\frac{y}{R}}\left[(t-\lambda x)\theta(\pm(\lambda x - t)) + \lambda x\theta(\pm x)\right] \quad (1.411)$$

$$v(k,y,t) = \frac{u_*^2}{h}\frac{e^{-\frac{y}{R}}-1}{f}\theta(\pm x) \tag{1.412}$$

$$p(k,y,t) = \frac{u_*^2}{h}\frac{1}{\lambda}e^{-\frac{y}{R}}\left[(t-\lambda x)\theta(\pm(\lambda x - t)) + \lambda x\theta(\pm x)\right] \tag{1.413}$$

Upwelling velocity itself is given by the time derivative of the pressure perturbation, $w_n = -p_{n,t}$,

$$w(k,y,t) = -\frac{u_*^2}{h}\frac{1}{\lambda}e^{-\frac{y}{R}}\theta(\pm(\lambda x - t)). \tag{1.414}$$

Comparing with the case of a uniform wind forcing, for small time and within those

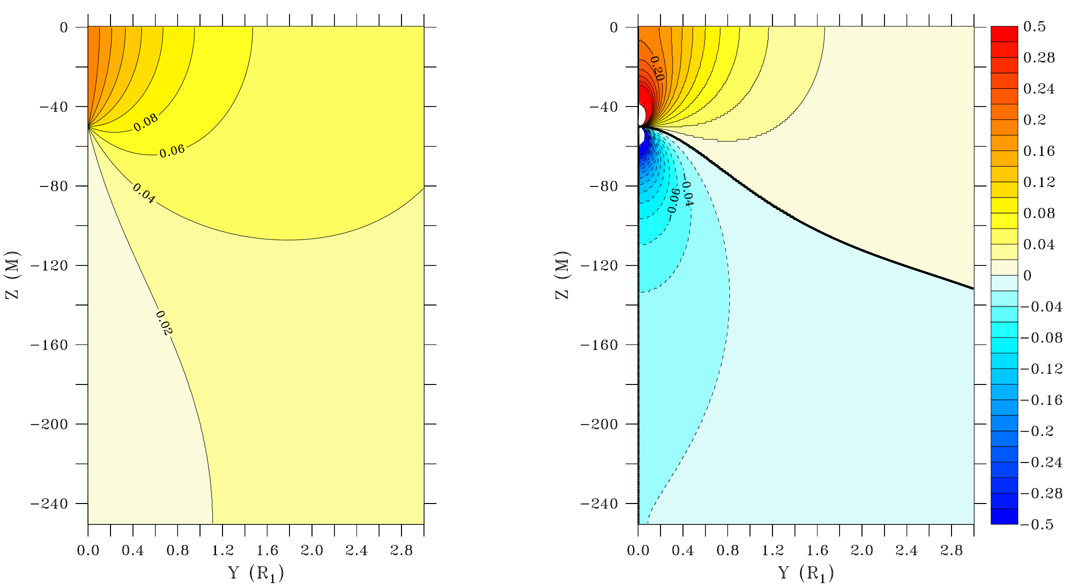

longshore current (m/s) longshore current (m/s)

Figure 1.20. The coastal jet distant from the wind edge (left) and after all vertical model passed through. Note the undercurrent below the coastal jet.

regions where the wind is non-zero, there is again the linearly growing coastal jet. New is that the solution includes a signal propagating with the phase speed λ_n^{-1}. In any case independent of the wind forcing the propagation is directed eastward leaving the coast to the right.

Wind in the right half-plane

If the wind blows in the right half-plane, the cross-shore velocity v is non-zero only in this area. Neither $\theta((\lambda x - t))$ nor $\theta(x)$ become non-zero for negative x. Hence, the ocean remains totally quiescent in the left half-plane. (Inertial waves may propagate into the left half-plane, but are not considered in the approximation $k = 0$.) In the right half plane both θ-functions are switched on for small times. The solution is the same like for uniform forcing. Coastal jet and pressure perturbation are growing linearly with time, the cross-shore velocity is zero at the coast and growth towards the open ocean. The vertical structure of the flow is discussed in the previous section. However, after a period $t = \lambda_n x$ a wave originating from the wind edge at $x = 0$ arives. The speed of the n-th mode of the coastal jet stays constant now. With increasing time more vertical modes become "arrested" in ascending order of the vertical index n.

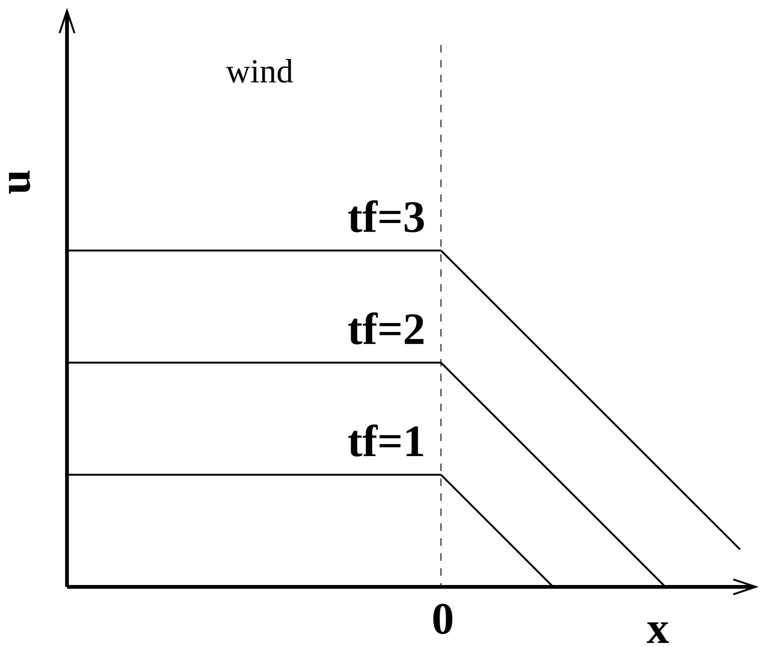

Figure 1.21. Kelvin waves exporting the coastal jet. In the wind forced area the coastal jet is linearly growing with time. The jet is exported to the area without wind. The wave arrives $t = \lambda x$ and the jet is growing linearly after the front has passed through.

Consider the case that the first mode (the barotropic mode) has passed through. Hence, u reads

$$u(k,y,t) = \sum_n F_n(z) \frac{u_*^2}{h_n} e^{-\frac{y}{R_n}} t + (\lambda_0 x - t)\, F_0(z) \frac{u_*^2}{h_0} e^{-\frac{y}{R_0}}. \quad (1.415)$$

Since $t > \lambda_0 x$, the second term is negative and implies a small negative velocity below the coastal jet. After first mode has passed through this current directed against the wind is growing,

$$u(k,y,t) = \sum_n F_n(z) \frac{u_*^2}{h_n} e^{-\frac{y}{R_n}} t + (\lambda_0 x - t)\, F_0(z) \frac{u_*^2}{h_0} e^{-\frac{y}{R_0}} + (\lambda_0 x - t)\, F_1(z) \frac{u_*^2}{h_1} e^{-\frac{y}{R_1}} \quad (1.416)$$

When a wave front corresponding to a vertical mode passes through a similar term arises. Hence, the coastal jet as shown in Fig. 1.9 is replaced step by step by a different pattern as shown if Figure 1.20. There develops an undercurrent flowing into the opposite direction of the coastal jet. Such an undercurrent is observed often in upwelling areas.

The upwelling velocity of the n-th's mode is switched to zero by a passing Kelvin wave front,

$$w(k,y,t) = -\frac{u_*^2}{h}\frac{1}{\lambda}e^{-\frac{y}{R}}\theta(\lambda x - t). \qquad (1.417)$$

This is a very important result. Upwelling does not only depend on the local winds but is strongly influenced by remote inhomogeneities of the wind field. The action is mediated by coastally trapped waves - here Kelvin waves. (If the coast has a shelf and cannot be approximated by perpendicular walls, the wave dispersion relation is more complex, but the basic idea of remotely forced or suppressed upwelling is the same.)

Wind in the left half-plane

In the left half plane both step functions are always “switched on”. There is simply a linearly growing coastal jet in geostrophic balance with the growing pressure perturbation. Hence, in this case the solution in the left half plane is the same like for a uniform wind field. This is a consequence of the fact, that Kelvin waves cannot propagate with the coast at the left hand side. The wind edge does not influence the ocean in the left half plane.

In the right half plane the cross-shore velocity is always zero, but both, the coastal jet and the up- or downwelling are exported from the wind driven half plane. Again, Kelvin waves mediate the remotly forced ocean response. Figure 1.21 shows the extension of the coastal jet into the right half plane. Its velocity is linearly growing with time but it starts the later the Kelvin wave needs to propagate to a given position x. Upwelling velocity,

$$w(k,y,t) = -\frac{u_*^2}{h}\frac{1}{\lambda}e^{-\frac{y}{R}}\theta(t - \lambda x), \qquad (1.418)$$

remains zero until the wave front comes through.

The scenario developed here is highly idealised. It neglects turbulence and friction, more complex winds and the existence of a shelf instead of a perpendicular coastal wall. However, it comprises the basic ideas how coastal flow pattern and upwelling in inhomogeneous wind fields can be understood. It elucidates the role of remote forcing mediated by Kelvin waves. Although known since decades this is not commonly used in the discussion of field experiments. There are many scientific papers discussing upwelling only as the result of local winds. This chapters shows that this is not a sufficient approach.

Chapter 2

Quasi-geostrophic theory for ocean processes

2.1. The quasi-geostrophic approximation

We have seen, that the ocean response to wind forcing changes from an initial Ekman balance to some other dynamic regime governed by a geostrophic balance. In many cases the adjustment process itself is of minor interest, but the final geostrophically balanced state shall be investigated. This rises the question for a simplified set of dynamic equation that excludes the adjustment process from the solution. Using the f-plane approximation, the set of geostrophic equations,

$$
\begin{aligned}
-fv + p_x &= 0, && (2.1)\\
fu + p_y &= 0, && (2.2)
\end{aligned}
$$

is of little help, since the geostrophically balanced field is non-divergent,

$$u_x + v_y = f^{-1}\left(p_{yx} - p_{xy}\right) = 0, \tag{2.3}$$

and the related vertical velocity vanishes. Another point is, that the two geostrophic equations are not sufficient to define the three variables u, v and p.

Here a systematic method is shown to find the asymptotic geostrophic solution but without the detailed calculation of the transient states. We start with the non-linear Boussinesq equations 1.19, but in hydrostatic approximation

$$
\begin{aligned}
\frac{d}{dt}u - fv + \frac{\partial}{\partial x}p &= F_u + F_x^{ext}, && (2.4)\\
\frac{d}{dt}v + fu + \frac{\partial}{\partial y}p &= F_v + F_y^{ext}, && (2.5)\\
\frac{\partial}{\partial z}p - b &= F_w + F_z^{ext}, && (2.6)\\
\frac{d}{dt}b + wN^2 &= 0. && (2.7)\\
\nabla \cdot \overrightarrow{v} &= 0. && (2.8)
\end{aligned}
$$

We have already discussed, that the order of the different terms can be estimated by scale parameters, namely the Rossby number, Burger number and Ekman number (see

Pedlosky). Here we line out the principle and do not discuss the detailed form of these scale parameters. We assume, that all dynamic quantities q have the form

$$q = q^{(0)} + \epsilon q^{(1)}, \tag{2.9}$$

where ϵ is a dimensionless small number $\epsilon \ll 1$. We have

$$\begin{aligned} u &= u^{(0)} + \epsilon u^{(1)}..., & (2.10)\\ v &= v^{(0)} + \epsilon v^{(1)}..., & (2.11)\\ p &= p^{(0)} + \epsilon p^{(1)}..., & (2.12)\\ w &= w^{(0)} + \epsilon w^{(1)}..., & (2.13)\\ b &= b^{(0)} + \epsilon b^{(1)}.... & (2.14) \end{aligned}$$

The superscript (0) should mark the geostrophic solution. For this reason we decompose also the Coriolis parameter f,

$$f = 2\Omega \sin\varphi = 2\Omega \sin\varphi_0 + \beta y = f_0 + \beta y. \tag{2.15}$$

For the earth the value of β is:

$$\beta = \frac{2\Omega}{a} \cos\varphi_0 \approx 2.287\, 10^{-11}\, (\mathrm{ms})^{-1} \cos\varphi_0. \tag{2.16}$$

So we start with the statement: **A frictionless ocean on a rotating planet without external forces is in geostrophic and hydrostatic balance.**

$$\begin{aligned} -f_0 v^{(0)} + p_x^{(0)} &= 0, & (2.17)\\ f_0 u^{(0)} + p_y^{(0)} &= 0, & (2.18)\\ \frac{\partial}{\partial z} p^{(0)} - b^{(0)} &= 0. & (2.19) \end{aligned}$$

For a known density distribution, the hydrostatic pressure and the geostrophic velocity can be calculated. However, there is no way to find the density distribution (except measuring it) in terms of the zero order velocities. The reason is, that $w^{(0)}$ is zero. Hence, the system of geostrophic and hydrostatic equations is incomplete and does not provide enough information on ocean dynamics. Considering the next order of equations in the limit $\epsilon \to 0$ under the assumption the friction and external forces are of order ϵ, we get

$$\begin{aligned} \frac{d^{(0)}}{dt} u^{(0)} - f_0 v^{(1)} - \beta y v^{(0)} + \frac{\partial}{\partial x} p^{(1)} &= F_u + F_x^{ext}, & (2.20)\\ \frac{d^{(0)}}{dt} v^{(0)} + f_0 u^{(1)} + \beta y u^{(0)} + \frac{\partial}{\partial y} p^{(1)} &= F_v + F_y^{ext}, & (2.21)\\ \frac{\partial}{\partial z} p^{(1)} - b^{(1)} &= F_w + F_z^{ext}, & (2.22)\\ \frac{d^{(0)}}{dt} b^{(0)} + w^{(1)} N^2 &= 0. & (2.23)\\ \nabla \cdot \overrightarrow{v^{(1)}} &= 0. & (2.24) \end{aligned}$$

The buoyancy equation relates a first order quantity $w^{(1)}$ to a zero order quantity. Hence, we try to eliminate first order quantities to get a closed system for zero order quantities. Knowing that geostrophic adjustment conserves potential vorticity, we consider the curl of the first two equations,

$$\frac{d^{(0)}}{dt}\chi^{(0)} + \beta v^{(0)} = f_0 w_z^{(1)} + curl\mathcal{F}, \tag{2.25}$$

$$\chi^{(0)} = \frac{\partial}{\partial x}v^{(0)} - \frac{\partial}{\partial y}u^{(0)} \tag{2.26}$$

With

$$\frac{d^{(0)}}{dt}\beta y = \beta v^{(0)} \tag{2.27}$$

this reads

$$\frac{d^{(0)}}{dt}\left(\chi^{(0)} + \beta y\right) = f_0 w_z^{(1)} + curl\mathcal{F}. \tag{2.28}$$

$w^{(1)}$ is the only quantity of first order in this equation. $w^{(1)}$ can be substitute by $\frac{d^{(0)}}{dt}b^{(0)}$,

$$w^{(1)} = -\frac{1}{N^2}\frac{d^{(0)}}{dt}b^{(0)} = -\frac{1}{N^2}\frac{d^{(0)}}{dt}\frac{\partial}{\partial z}p^{(0)}. \tag{2.29}$$

We need the vertical derivative,

$$\frac{\partial}{\partial z}w^{(1)} = -\frac{d^{(0)}}{dt}\frac{\partial}{\partial z}\frac{1}{N^2}\frac{\partial}{\partial z}p^{(0)}. \tag{2.30}$$

(Show that $\frac{d^{(0)}}{dt}$ commutes with $\frac{\partial}{\partial z}$. Hence, we have got an equation in terms of zero order quantities.

$$\frac{d^{(0)}}{dt}\left(\chi^{(0)} + \beta y + \frac{\partial}{\partial z}\frac{f_0}{N^2}\frac{\partial}{\partial z}p^{(0)}\right) = curl\mathcal{F}. \tag{2.31}$$

Finally we introduce the quasi-geostrophic stream function Ψ,

$$v^{(0)} = \Psi_x, \tag{2.32}$$

$$u^{(0)} = -\Psi_y \tag{2.33}$$

$$\Psi = \frac{p}{f_0}, \tag{2.34}$$

and end up with a single equation for the quasi-geostrophic stream function,

$$\frac{d^{(0)}}{dt}\left(\Delta_h\Psi + \beta y + \frac{\partial}{\partial z}\frac{f_0^2}{N^2}\frac{\partial}{\partial z}\Psi\right) = curl\mathcal{F}. \tag{2.35}$$

This is the equation of motion for the quasi-geostrophic potential vorticity Q_{qg},

$$Q_{qg} = \Delta_h\Psi + \beta y + \frac{\partial}{\partial z}\frac{f_0^2}{N^2}\frac{\partial}{\partial z}\Psi, \tag{2.36}$$

$$\frac{d^{(0)}}{dt} Q_{qg} = curl \mathcal{F}. \tag{2.37}$$

Hence, the asymptotic state developing for large time scales is governed by a conservative quantity quasi-geostrophic potential vorticity Q_{qg}. The source and sink of this quantity is the curl of the external force (wind stress and bottom friction) accelerating the horizontal flow velocity and the curl of the internal frictional forces. I the quasi-geostrophic potential vorticity is known a stream function can be diagnosed to deliver velocity and density distribution. (It should be mentioned, that diabatic effects (compressibility, steric effects) contribute to the quasi-geostrophic potential vorticity with a force term. This is important for the long development of global circulation, by is not considered here.)

2.2. Planetary geostrophic motion

A more general geostrophic approximation considers the zonal variability of f as well as friction and external drivers

$$-fv + p_x = \mathcal{F}_u, \tag{2.38}$$

$$fu + p_y = \mathcal{F}_v. \tag{2.39}$$

Neglecting friction for the moment, the divergence of (fu, fv) gives

$$f(u_x + v_y) + \beta v = 0. \tag{2.40}$$

Together with the continuity equation this gives the so called **Sverdrup balance**,

$$f \frac{\partial}{\partial z} w = \beta v. \tag{2.41}$$

It is valid for the frictionless ocean interior and relates the meridional movement of water with a vertical velocity. The background is again conservation of potential vorticity and the change of relative vorticity from changing planetary vorticity. This equation in principle permits the estimate of vertical motion from measured density fields - v is diagnosed with the geostrophic method and w from the vertical integral of βv.

2.3. Planetary waves

In this section we introduce a wave type governed by the meridional variability of the Coriolis force. To find the dispersion relation of these waves we consider the linearized frictionless equation for the quasi-geostrophic stream function,

$$\frac{\partial}{\partial t} \left(\Delta_h \Psi + \frac{\partial}{\partial z} \frac{f_0^2}{N^2} \frac{\partial}{\partial z} \Psi \right) + \beta \frac{\partial}{\partial x} \Psi = 0. \tag{2.42}$$

2.3.1. The basic restoring mechanism

To understand the restoring force we consider an idealized case of the conservation of angular momentum on the rotating earth, no forcing, no zonal flow, no vertical advection, linearized equations (Olbers et al. (2012), p 227)

$$\frac{\partial}{\partial t}\chi^{(0)} + \beta v^{(0)} = 0, \tag{2.43}$$

$$\chi^{(0)} = \frac{\partial}{\partial x}v^{(0)} - \frac{\partial}{\partial y}u^{(0)} \tag{2.44}$$

Northward moving water means increasing planetary vorticity f. Conservation of vorticity implies decreasing relative vorticity χ. Hence the flow shear v_x must be decreasing. The faster the northward flow the stronger its reduction. We consider an initial flow field directed northward with

$$v_0(x) = V\sin(x/L), \qquad \chi_0(x) = \frac{V}{L}\cos(x/L). \tag{2.45}$$

Integrating over time gives

$$\chi = \chi_0(x) - t\beta v_0(x) = \frac{V}{L}\cos(x/L) - t\beta V\sin(x/L) \approx \frac{V}{L}\cos\left(\frac{x}{L} + \beta L t\right) \tag{2.46}$$

Integrating over x gives v oscillating with a sin-function.

$$v \approx V\sin\left(\frac{x}{L} + \beta L t\right) \tag{2.47}$$

Remarkably the wave has the shape of the initial disturbance spreading westward, since $\beta L > 0$. It moves faster near the equator and slowly at high latitudes. Any initial rotational flow, for example a coastal jet or an undercurrent within the eastern boundary current system has the tendency to decay slowly by radiation of planetary waves. The phase speed depends on the horizontal scale L of the flow pattern, the planetary waves are dispersive.

2.3.2. The dispersion relation

As in the previous sections we decompose into vertical modes F_n and apply a Fourier transformation with respect to time and horizontal coordinates:

$$\Psi_n = \Psi_{n0}e^{ik_1x+k_2y-\omega t}. \tag{2.48}$$

This gives the dispersion relation

$$\omega = -\frac{\beta k_1}{k_1^2 + k_2^2 + R^{-2}}. \tag{2.49}$$

Remarkably, these waves can especially exist near the equator but are of minor importance at high latitudes where β becomes small.

The **phase velocity** is always negative, hence, the phase propagates westward and southward.

We investigate the analytical properties of the group velocity. Considering a fixed k_2 there is a maximum of ω from

$$\frac{\partial\omega}{\partial k_1} = -\frac{\beta}{k_1^2 + k_2^2 + R^{-2}} + \frac{2k_1^2\beta}{(k_1^2 + k_2^2 + R^{-2})^2} = 0. \quad k_1 = -\sqrt{k_2^2 + R^{-2}}. \tag{2.50}$$

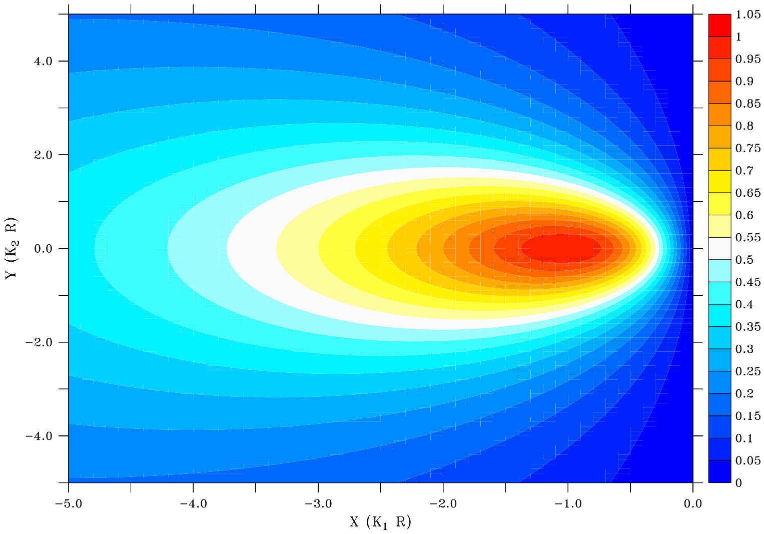

Figure 2.1. The frequency, scaled with the maximum frequency in dependency on the wave numbers.

The maximum frequency is

$$\omega_m = +\frac{\beta}{2\sqrt{k_2^2 + R^{-2}}}. \tag{2.51}$$

The global maximum is found for $k_2 = 0$,

$$\omega_{max} = +\frac{\beta R}{2}. \tag{2.52}$$

If there is a maximum frequency in dependency on k_1 the group velocity changes change its sign here. The group velocity vector is,

$$c_g = \begin{pmatrix} c_g^x \\ c_g^y \end{pmatrix} = \begin{pmatrix} \frac{\beta\left(k_1^2 - k_2^2 - R^{-2}\right)}{(k_1^2+k_2^2+R^{-2})^2} \\ \frac{2\beta k_1 k_2}{(k_1^2+k_2^2+R^{-2})^2} \end{pmatrix} \tag{2.53}$$

Hence, short waves ($k_1 R \gg 1$), propagate eastward, but long waves ($k_1 R \ll 1$) always propagate westward. Remarkably, for short waves phases and energy spread into the opposite direction. Long waves $k_1 R \ll 1$,$k_2 R \ll 1$ obey the asymptotic dispersion relation

$$\omega = -\beta k_1 R^2. \tag{2.54}$$

Long waves have the largest group velocity and are approximately non-dispersive.
Exercise
Consider the spreading of a wave packet, defined by the superposition of waves with different wave number and frequency,

$$\Psi(x,t) = \int \frac{dk}{2\pi} \int \frac{d\omega}{2\pi} a_k e^{ikx-\omega t} f(k,\omega) \tag{2.55}$$

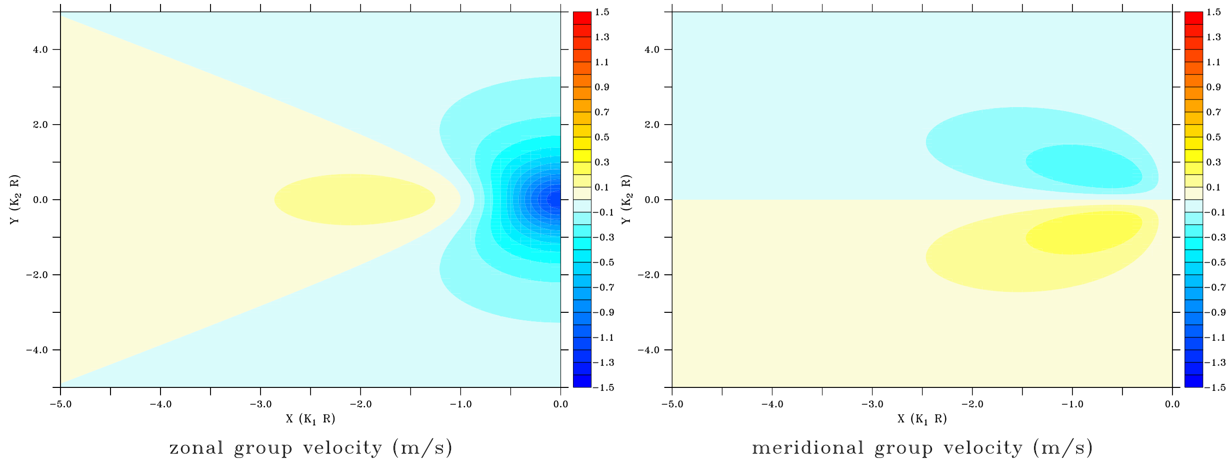

Figure 2.2. Zonal and meridional group velocity. Blue means westward (southward) propagation.

R_n	c_g	time (5000 km)
1000 km	10 m/s	5.8 d
30 km	$9 \cdot 10^{-3}$ m/s	17.6 y
15 km	$2 \cdot 10^{-3}$ m/s	70.6 y
10 km	$1 \cdot 10^{-3}$ m/s	158.5 y

Table 2.1
Maximum group speed of planetary Rossby waves and time to spread of 5000 km distance for different values of the Rossby radius

a_k is the amplitude of partial waves with wave number k, $f(k,\omega)$ describes the spectral density of the partial waves. It reads for for Poincare waves

$$\begin{aligned} f(k,\omega) &= 2\pi\delta(\omega-\omega_k), \\ \omega_k^2 &= f^2(1+k^2R^2). \end{aligned} \tag{2.56}$$

- How should the spectral density look like for planetary Rossby waves?

Consider spreading of a wave packet starting from an initial condition that looks like

$$\Psi_0(x,t) = \sin(k_0 x)e^{-x^2/x_0^2} \tag{2.57}$$

To this end, the amplitudes a_k must be found by Fourier analysis.

- Use the matlab script to perform the Fourier analysis and make a plot of a_k as function of k.

- If the a_k are known, $\Psi(x,t)$ can be calculated for a sequence of time steps. Use the given matlab-script as a template to generate an AVI-movie that illustrates the wave spreading. Investigate the wave spreading for typical wave numbers k_0 for Rossby waves with eastward and westward group velocity. Investigate the special case of zero group velocity, $k_0^2 = R^{-2}$.

- Consider also a superposition like

$$\Psi_0(x,t) \;=\; \left(\sin(k_1 x) + \sin(k_2 x)\right) e^{-x^2/x_0^2} \tag{2.58}$$

where k_1 and k_2 are below and above the wave number R^{-2} corresponding to zero group velocity.

2.4. Planetary circulation adjustment to large scale winds

If a wind field acts on the ocean surface a local balance is rapidly established. Within the open ocean it consists of inertial oscillations. The subtropical gyres are established by Ekman pumping in relation from the wind stress curl. At the coasts up- or down welling is established by radiation of inertial waves, Kelvin waves tend to modify this flow pattern arresting the coastal jets and generating undercurrents. All these wave and flow pattern can be understood with a f-plane theory. However, considering the meridional variability of f, these flow pattern cannot be stable but are source of Rossby waves starting an adjustment to the external forcing on a planetary scale by planetary Rossby waves.

Here we try to understand this adjustment process without considering the waves on frequencies $\omega > f$. We assume a pure zonal wind field (again a volume force)

$$X(y,t) = -X_0 \cos\frac{\pi y}{L}\theta(t) \tag{2.59}$$

which reflects roughly the band of the westward directed trade winds. The ocean is a rectangular basin $0 < x < B$, the wind band is non-zero at $0 < y < L$. Assuming a flat bottom, we may decompose into vertical eigenfunctions and find for the components of the stream function

$$\frac{\partial}{\partial t}\left(\Delta_h \Psi + \frac{\partial}{\partial z}\frac{1}{R^2}\frac{\partial}{\partial z}\Psi\right) + \beta\frac{\partial}{\partial x}\Psi \;=\; \frac{\partial}{\partial x}Y - \frac{\partial}{\partial y}X. \tag{2.60}$$

With the Ansatz

$$\Psi(x,y,t) \;=\; -\Phi(x,t)\frac{u_*^2}{h} l \sin(ly), \quad l = \frac{\pi}{L}, \tag{2.61}$$

we find an equation for Φ,

$$\frac{\partial}{\partial t}\left(\frac{\partial^2 \Phi}{\partial x^2} - \left(l^2 + \frac{1}{R^2}\right)\Phi\right) + \beta\frac{\partial}{\partial x}\Phi \;=\; \theta(t). \tag{2.62}$$

The forcing is independent of x, hence, away from the coast Φ should be also independent of x,

$$\Phi \;=\; \Phi_{loc} = -\frac{t}{l^2 + \frac{1}{R^2}} = \frac{t c_g}{\beta}. \tag{2.63}$$

c_g is the zonal group velocity for $k_1 = 0$,

$$c_g = -\frac{\beta}{l^2 + \frac{1}{R^2}}. \tag{2.64}$$

Starting at $t = 0$ the response is a linearly growing stream function with time. The horizontal velocities are

$$\begin{aligned} v &= \Psi_x = 0, \\ u &= -\Psi_y = \frac{u_*^2}{h} l^2 \cos(ly) \frac{tc_g}{\beta}, \end{aligned} \tag{2.65}$$

the current follows the wind and its amplitude is linearly growing. Note, that the Ekman transport is not part of this solution, it is not in geostrophic balance and must be considered separately!
At the coasts this solution is not valid, since $u(x = 0, B) = 0$.
Eastern coast
At the east coast waves must propagate westward, hence they must be long planetary waves. The total solution has the form

$$\Phi^E = \Phi_{loc} + \Phi^E_{wave} \tag{2.66}$$

For theses waves we neglect the second derivative (long waves) and find

$$-\left(l^2 + \frac{1}{R^2}\right)\frac{\partial}{\partial t}\Phi^E_{wave} + \beta\frac{\partial}{\partial x}\Phi^E_{wave} = 0. \tag{2.67}$$

The solution is a wave front,

$$\Phi^E_{wave}(x,t) = F(x - c_g t). \tag{2.68}$$

At the coast $x = B$, for the boundary condition $u(B) = 0$, the total stream function must always vanish, and we get

$$\Phi^E_{wave}(B,t) = -\frac{tc_g}{\beta}, \tag{2.69}$$

and

$$\Phi^E_{wave}(x,t) = -\frac{B - x + tc_g}{\beta}, \tag{2.70}$$

The time a wave front needs to move from the coast b to a position x is

$$t_f = \frac{B - x}{c_g}. \tag{2.71}$$

If a wave front arrives at position x,a contribution Φ^E_{wave} is added to the linearly growing part Φ_{loc},

$$\Phi^E(x,t) = \Phi_{loc} + \Phi^E_{wave} = \begin{cases} \frac{tc_g}{\beta} & t < t_f \\ -\frac{B-x}{\beta} & t > t_f \end{cases} \tag{2.72}$$

(Note, $c_g < 0$!) From the first point of view this is a very satisfying result. For large time, when all wave fronts have passed, Φ is independent of the mode index. This will take centuries since the group velocity for higher vertical modes becomes very small, see Table 2.1. The vertical mode sum can be carried out and the meridional current is simply

$$\beta v = \beta\Psi_x = curl X. \tag{2.73}$$

This is the well known Sverdrup balance, which is believed (and validated for some cases) to be valid in the mid-latitude ocean. Here we can understand the Sverdrup balance as the result of an adjustment process of the ocean to the large scale wind field by planetary Rossby waves radiating away from the eastern boundary. Again, waves are the key to understand the origin of steady flow pattern. Notably, the adjustment takes place without any friction (except in the surface, where small scale turbulence establishs the volumn force).

A closer look on the result reveals a serios problem. $curl X$ is confined to the surface layer and the ocean interior is at rest (Sverdrup catastrophy). This is not observed and the theory needs extension and refinement.

Western coast

Waves generated at the west coast may spread only eastward. Hence these waves must be Rossby waves with short wave length (high wave number). The east-ward group velocity is very slow which justifies to neglect these waves considering the boundary condition at the east coast. The influence of these waves must be confined to a boundary layer at the west.

$$\Phi^W = \Phi_{loc} + \Phi^E_{wave} + \Phi^W_{wave} \tag{2.74}$$

Inserting into Eq. 2.62 the equation for Φ^W_{wave} reads

$$\frac{\partial}{\partial t}\frac{\partial^2 \Phi^W_{wave}}{\partial x^2} + \beta\frac{\partial}{\partial x}\Phi^W_{wave} = 0. \tag{2.75}$$

Integrating once gives

$$\frac{\partial}{\partial t}\frac{\partial}{\partial x}\Phi^W_{wave} + \beta\Phi^W_{wave} = c(t). \tag{2.76}$$

However, since Φ^W_{wave} (and the derivatives) is confined to a boundary layer at the west and vanishs outside, $c(t)$ must be zero. Analysing this equation it turns out that the assumption

$$\Phi^W_{wave} = A\left(\frac{t\beta B^2}{x}\right)^{m/2} G\left(2\sqrt{xt\beta}\right) \tag{2.77}$$

results in a differential equation for G

$$z^2G'' + zG' + (z^2 - m^2)G = 0. \tag{2.78}$$

This Bessel's differential equation, the solutions are Bessel functions of the first (J_m) and second kind (Y_m). The Bessel functions of second kind diverge at $z \to 0$, Bessel functions of first kind have the form

$$J_m(z) = \frac{1}{m!}\left(\frac{z}{m}\right)^m \quad \text{for} \quad z \to 0. \tag{2.79}$$

Hence, Φ^W_{wave} has the form

$$\Phi^W_{wave} = A\left(\frac{t\beta B^2}{x}\right)^{m/2} J_m\left(2\sqrt{xt\beta}\right) \tag{2.80}$$

Now we can use the boundary condition

$$\Phi^W(x=0) = 0, \tag{2.81}$$

to specify the amplitude A and the unknown index m. For $t < t_f$ the local solution is linearly growing with time and Φ^W_{wave} must be,

$$\Phi^W_{wave} = A\left(\frac{t\beta B^2}{x}\right)^{m/2} J_m\left(2\sqrt{xt\beta}\right) = -\frac{tc_g}{\beta} \quad \text{for} \quad x \to 0. \tag{2.82}$$

This can be satisfied only for $m = 1$ and gives

$$A = -\frac{c_g}{\beta^2 B} \quad \text{for} \quad t < t_f. \tag{2.83}$$

For $t > t_f$ the long wave have passed and the boundary condition is

$$\Phi^W_{wave} = A\left(\frac{t\beta B^2}{x}\right)^{m/2} J_m\left(2\sqrt{xt\beta}\right) = \frac{B-x}{\beta} \quad \text{for} \quad x \to 0. \tag{2.84}$$

Here the choice $m = 0$ and

$$A = \frac{B}{\beta} \quad \text{for} \quad t > t_f \tag{2.85}$$

satisfies the western boundary condition. The final result is

$$\Phi^W(x,t) = \Phi_{loc} + \Phi^E_{wave} + \Phi^W_{wave} = \begin{cases} \frac{tc_g}{\beta} - c_g\left(\frac{t}{x\beta^3}\right)^{1/2} J_1\left(2\sqrt{xt\beta}\right) & t < t_f \\ -\frac{B-x}{\beta} + \frac{B}{\beta} J_0\left(2\sqrt{xt\beta}\right) & t > t_f. \end{cases} \tag{2.86}$$

For large arguments the Bessel function oscillates with decreasing amplitude,

$$J_m(z) = \sqrt{2/(\pi z)}\cos(z - m\pi/2 - \pi/4) \text{for} \quad z \to \infty. \tag{2.87}$$

Hence, for large time the oscillating solution near the western boundary becomes more and more trapped to the coast (within $1/\beta t$) but changes rapidly in sign. It's derivative (velocity) is growing in time and friction needs to be included to avoid a divergence. This is subject of Stommel's theory of western boundary currents.

Chapter 3

Wind driven equatorial currents

3.1. The basic equations

Near the equator the Coriolis force becomes negligibly small. So one may expect that the cross wise coupling of meridional and zonal motion by the Coriolis acceleration does not play any role here. Indeed, one may assume a simple balance: In the surface layer zonal wind stress accelerates a zonal current. Since there are continents intersecting this current, pressure gradients build up. In the surface layer the wind stres becomes balanced by a gradient of the sea surface heigt η,

$$\rho_1 g \frac{\partial}{\partial x}\eta = \rho_s X, \tag{3.1}$$

an east wind (blowing westward, negative X) is balanced by a negative (high sea level in the west) sea surface elevation gradient. Below the wind driven surface layer the surface pressure gradient is compensated by an opposite gradient of the thermocline,

$$\rho_1 g \frac{\partial}{\partial x}\eta \quad = \quad (\rho_2 - \rho_1)\, g \frac{\partial}{\partial x} h. \tag{3.2}$$

As a result the acceleration becomes small throughout the water column. Indeed, measurements of temperature and salinity in the equatorial area show westward enhanced mixed layer depth and westward enhanced sea level elevation. However, this simplistic view does not show, how this balance is established. Morevoer, it does not reveal any information on the currents except that the acceleration is zero.

In the last chapter we have seen that the zonal variation of the Coriolis parameter permits wave like current patterns from the conservation of potential vorticity. This conservation is also valid at the equator with zero Coriolis force, any zonal movement corresponds to changing relative (local) vorticity. To understand these waves we start here a detailed analysis of the dispersion relation of equatorial wavs and the corresponding wind driven flow pattern.

We start with the linearised frictionless Boussinesq equations

$$\frac{\partial}{\partial t}u - \beta y v + \frac{\partial p}{\partial x} \quad = \quad X \tag{3.3}$$

$$\frac{\partial}{\partial t}v + \beta y u + \frac{\partial p}{\partial y} \quad = \quad Y \tag{3.4}$$

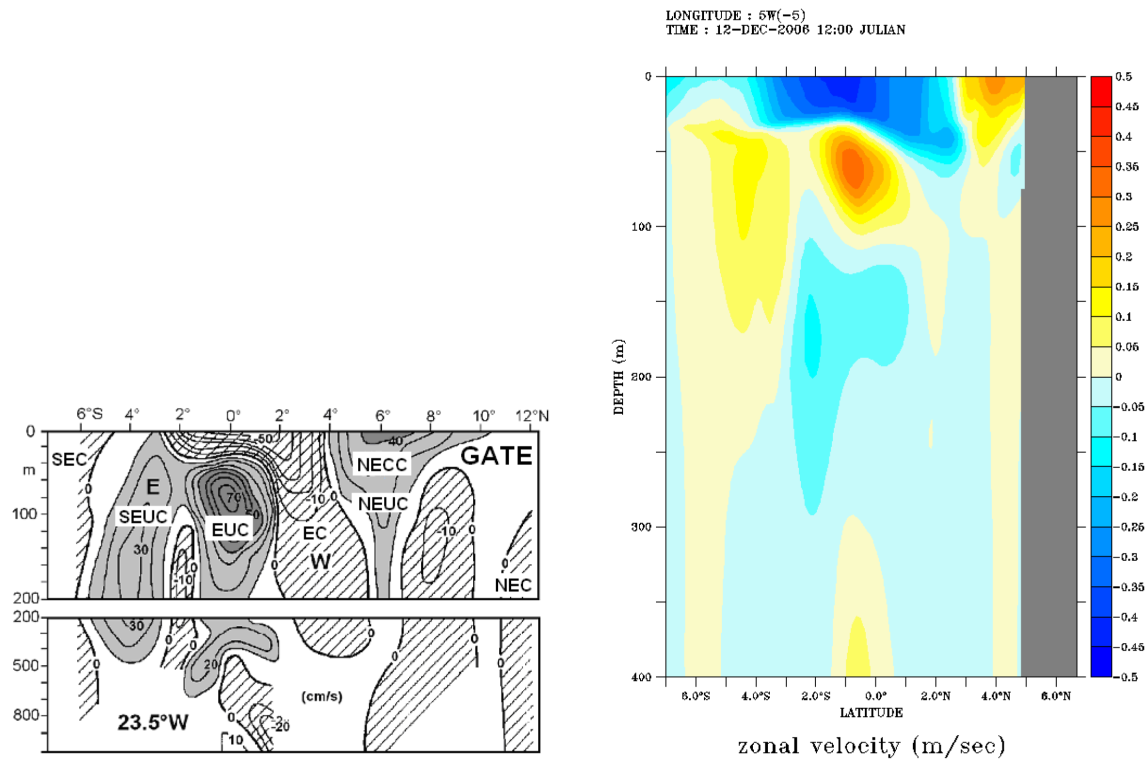

Figure 3.1. The equatorial currents found during the GATE experiment in the 60th (left) and seen in a numerical simulation (right).

$$\frac{\partial u}{\partial x} + \frac{\partial v}{\partial y} = \mathcal{Z}\frac{\partial}{\partial t}p. \tag{3.5}$$

The operator $\mathcal{Z}$ stands for

$$\mathcal{Z} = \frac{\partial}{\partial z}\frac{1}{N^2}\frac{\partial}{\partial z}. \tag{3.6}$$

and implies as usual the decomposition into vertical eigenfunctions F_n. The index n will be dropped below. After Fourier transformation over x and t we find

$$-i\bar{\omega}u - \beta y v + ikp = X, \tag{3.7}$$

$$-i\bar{\omega}v + \beta y u + \frac{\partial p}{\partial y} = Y, \tag{3.8}$$

$$iku + \frac{\partial v}{\partial y} - i\bar{\omega}\lambda^2 p = 0, \tag{3.9}$$

with $\bar{\omega} = \omega + i\varepsilon$. After a little algebra this can be resolved to single equation for v,

$$\frac{\partial^2 v}{\partial s^2} + \left(q + \frac{1}{2} - \frac{s^2}{4}\right)v = i\frac{(\bar{\omega}^2\lambda^2 - k^2)\,Y}{2\lambda\beta\bar{\omega}} + \sqrt{\frac{\lambda}{2\beta}}\frac{s}{2}X + \frac{k}{\bar{\omega}\sqrt{2\lambda\beta}}X_s, \tag{3.10}$$

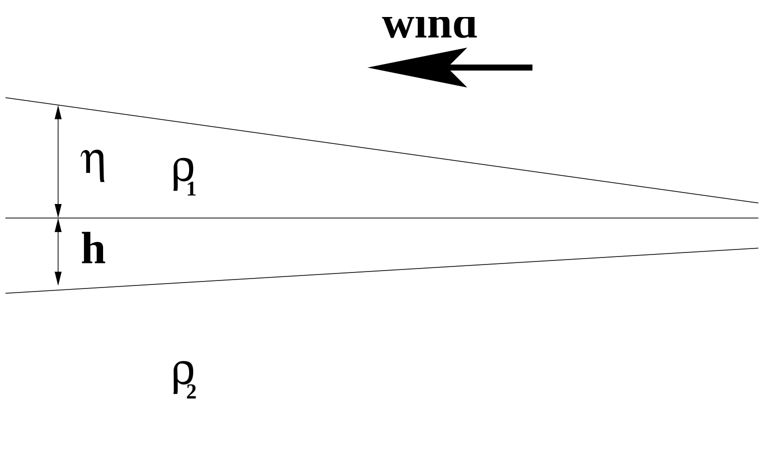

Figure 3.2. The wind induced surface elevation and the thermocline elevation.

with the scaled coordinate $s = \sqrt{2\lambda\beta}y$ and

$$2q+1 \;=\; \frac{\bar{\omega}^2\lambda^2 - k^2}{\lambda\beta} - \frac{k}{\lambda\bar{\omega}}. \tag{3.11}$$

We assume the boundary conditions

$$v \;\rightarrow\; 0 \quad \text{for} \quad y \rightarrow \pm\infty. \tag{3.12}$$

3.2. Green's function

The Green's function is defind by the equation

$$\frac{\partial^2}{\partial s^2}G(s,s') + \left(q + \frac{1}{2} - \frac{s^2}{4}\right)G(s,s') \;=\; \delta(s-s'). \tag{3.13}$$

The homogeneous equation has the so called parabolic cylinder functions $Dq(s$ and $D_q(-s)$ as solution. Without a proof we note, that the Wronskian of the D is

$$W \;=\; D_q(s)\frac{\partial}{\partial s}D_q(-s) - D_q(-s)\frac{\partial}{\partial s}D_q(s) = -\frac{\sqrt{2\pi}}{\Gamma(-q)}. \tag{3.14}$$

Hence, as described in Section 1.5.2 the resulting Green's function reads

$$G_q(s,s') \;=\; \theta(s-s')G^{>}(q,s,s') + \theta(s'-s)G^{<}(q,s,s'), \tag{3.15}$$

with

$$G^{>}(q,s,s') \;=\; -\frac{\Gamma(-q)}{\sqrt{2\pi}}D_q(s)D_q(-s') = G^{<}(q,s',s) \tag{3.16}$$

The function Γ has poles for integer values of q and reads approximately,

$$\Gamma(-q) \;\approx\; \frac{(-1)^m}{m!(m-q)}, \tag{3.17}$$

Hence, we consider the Green's function near these poles for integer values of $q = n$. In this case the parabolic cylinder functions simplify to Hermite polynominals

$$D_n(s) = \frac{1}{\sqrt{2^m}} e^{-\frac{s^2}{4}} H_m\left(\frac{s}{\sqrt{2}}\right), \tag{3.18}$$

and the Green's function becomes a sum over all residuals of the poles of the Γ-function

$$G_q(s, s') = \sum_{n=0}^{\infty} \frac{e^{-\frac{s^2+s'^2}{4}}}{2^m m! \sqrt{2\pi}(q-m)} H_m\left(\frac{s}{\sqrt{2}}\right) H_m\left(\frac{s'}{\sqrt{2}}\right) \tag{3.19}$$

The Hermite polynominals are either symmetric or antisymmetric,

$$\begin{aligned} H_0(x) &= 1, \\ H_1(x) &= 2x, \\ H_2(x) &= 4x^2 - 2, \\ H_3(x) &= 8x^3 - 12x. \end{aligned} \tag{3.20}$$

Here we can derive our first result. The solution is localised at the equator and decays exponentially with y. The typical scale is

$$R_n = \sqrt{\beta\lambda}^{-1}, \tag{3.21}$$

the so called equatorial Rossby radius. The special waves described by the Green's function are confined to the so called equatorial wave guide.

3.3. Formal solution

The formal solution for this Green's function is found like in the previous examples.

$$v(\bar{\omega}, k, s) = i\frac{(\bar{\omega}^2\lambda^2 - k^2)\, G_q \star Y}{2\lambda\beta\bar{\omega}} + \sqrt{\frac{\lambda}{2\beta}} G_q \star \frac{s'}{2} X + \frac{k}{\bar{\omega}\sqrt{2\lambda\beta}} G_q \star X'_s, \tag{3.22}$$

the zonal velocity and the perssure read

$$\begin{aligned} u(\bar{\omega}, k, s) &= \sqrt{\frac{\lambda}{2\beta}} \left(\frac{k}{\bar{\omega}\lambda}\frac{\partial}{\partial s} - \frac{s}{2}\right) G \star Y \\ &+ \frac{i\bar{\omega}\lambda^2}{\bar{\omega}^2\lambda^2 - k^2} \left(X + \left(\frac{s}{2} - \frac{k}{\bar{\omega}\lambda}\frac{\partial}{\partial s}\right)\left(G \star \frac{s'}{2} X + \frac{k}{\bar{\omega}\lambda} G \star X'_s\right)\right), \end{aligned} \tag{3.23}$$

$$\begin{aligned} p(\bar{\omega}, k, s) &= \sqrt{\frac{1}{2\beta\lambda}} \left(\frac{\partial}{\partial s} - \frac{k}{\bar{\omega}\lambda}\frac{s}{2}\right) G \star Y \\ &+ \frac{ik}{\bar{\omega}^2\lambda^2 - k^2} \left(X + \left(\frac{s}{2} - \frac{\bar{\omega}\lambda}{k}\frac{\partial}{\partial s}\right)\left(G \star \frac{s'}{2} X + \frac{k}{\bar{\omega}\lambda} G \star X'_s\right)\right) \end{aligned} \tag{3.24}$$

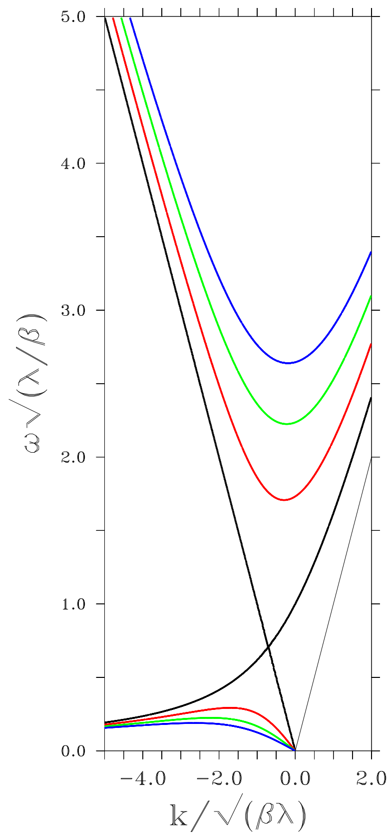

Figure 3.3. The positive frequency part of the dispersion relation for equatorial waves. Black is the result for $m = 0$, the so called Yanai-wave. Red the Rossby and gravity waves for $m = 1$ and so on. The thin black curve is a Kelvin wave that does not result from the dispersion relation (3.26).

3.4. The dispersion relation

The dispersion relation is given by the integer values of q, or,

$$2n + 1 \quad = \quad \frac{\bar{\omega}^2\lambda^2 - k^2}{\lambda\beta} - \frac{k}{\lambda\bar{\omega}}. \tag{3.25}$$

This defines a third order polynominal

$$\bar{\omega}^3 - \left(\frac{k^2}{\lambda^2} + \frac{\beta}{\lambda}(2m+1)\right)\bar{\omega} - \frac{\beta k}{\lambda^2} \quad = \quad 0, \tag{3.26}$$

that is the dispersion relation for equatorial waves. An explicit solution does not exist and we will discuss approximations. To this end we introduce the scaling

$$\tilde{\omega} \quad = \quad \bar{\omega}\sqrt{\frac{\lambda}{\beta}}, \quad \tilde{k} = \frac{k}{\sqrt{\lambda\beta}} \tag{3.27}$$

$$\tilde{\omega}^3 - \left(\tilde{k}^2 + 2m + 1\right)\tilde{\omega} - \tilde{k} \quad = \quad 0. \tag{3.28}$$

This is a reduced cubic equation of the general form

$$y^3 + 3py + 2q \;=\; 0, \tag{3.29}$$

The discriminant $D = p^3 + q^2$ is

$$D \;=\; \frac{k^2}{4} - \left(\frac{1}{3}\left(k^2 + 2m + 1\right)\right) < 0 \tag{3.30}$$

is negative and 3 reals roots of the dispersion relation must exist. Figure 3.3 shows the positive frequency branches for the equatorial ocean. The thick black lines are the curves for $m = 0$, the so called Yanai-wave. Equation 3.26 can be solved for the wave number and has two roots

$$\begin{aligned}\tilde{k}_{0;1/2} \;&=\; -\frac{1}{2\tilde{\omega}} \pm \sqrt{\frac{1}{4\tilde{\omega}^2} + \tilde{\omega}^2 - 1} = -\frac{1}{2\tilde{\omega}} \pm \left(\frac{1}{2\tilde{\omega}} - \tilde{\omega}\right) \\ \tilde{k}_{01} \;&=\; \tilde{\omega} - \frac{1}{\tilde{\omega}}, \quad k_{02} = -\tilde{\omega}.\end{aligned} \tag{3.31}$$

The second root k_{02} corresponds to a Kelvin wave. We will show below, that this wave cannot propagate within an unbounded ocean. For large negative wave numbers the Yanai wave is similar to short wave Rossby waves with east-ward propagating phases. For large positive wave numbers is behaves similarly to gravity waves.

For $m \geq 1$ there is a large frequency gap between Rossby waves with low frequency and gravity waves with high frequency. For low frequency the dispersion relation reads approximately

$$\bar{\omega} \;\approx\; -\frac{\beta k}{k^2 + (2m+1)\beta\lambda}, \tag{3.32}$$

which is similar to that of mid-latitude Rossby waves, but now with the equatorial Rossby radius $R^2 = 1/(\beta\lambda)$. The phase velocity is also west-ward, the groop velocity changes sign and is negative for small wave number (long waves) and positive for large (negative) wave numbers. For large frequency we find

$$\bar{\omega}^2 \;\approx\; \frac{\beta}{\lambda}(2m+1) + \frac{k^2}{\lambda^2}, \tag{3.33}$$

similar to gravity waves. But note, the different limit $k \to 0$ (dependent on λ_n) for the different vertical modes.

The zonal velocity u as well as the pressure p have additional poles at

$$\tilde{\omega} \;=\; \pm\frac{k}{\lambda}, \tag{3.34}$$

corresponding to Kelvin waves spreading along the equator. One Kelvin pole coincides with one of the Yanai wave modes, the other one is a simple Kelvin pole to be discussed below.

3.5. The equatorial Kelvin wave

We consider the residuum of the poles at $\bar{o}mega = \pm k$ and $\bar{o}mega = 0$. These poles can be found in the expression for the zonal velocity u and the pressure p. It is of some help to separate the poles using the relations

$$\frac{k}{\omega^2 - \left(\frac{k}{\lambda}\right)^2} = \frac{\lambda}{2}\left(\frac{1}{\omega - \frac{k}{\lambda}} - \frac{1}{\omega + \frac{k}{\lambda}}\right), \tag{3.35}$$

$$\frac{\omega}{\omega^2 - \left(\frac{k}{\lambda}\right)^2} = \frac{1}{2}\left(\frac{1}{\omega - \frac{k}{\lambda}} + \frac{1}{\omega + \frac{k}{\lambda}}\right), \tag{3.36}$$

$$\frac{1}{\omega\left(\omega^2 - \left(\frac{k}{\lambda}\right)^2\right)} = \frac{\lambda^2}{k^2}\left(\frac{1}{\omega} - \frac{1}{2}\left(\frac{1}{\omega - \frac{k}{\lambda}} + \frac{1}{\omega + \frac{k}{\lambda}}\right)\right). \tag{3.37}$$

We sort contribution of the different poles for the zonal velocity,

$$\begin{aligned} u(\bar{\omega}, k, s) &= \sqrt{\frac{\lambda}{2\beta}}\left(\frac{k}{\bar{\omega}\lambda}\frac{\partial}{\partial s} - \frac{s}{2}\right) G \star Y \\ &+ \frac{i}{2}\frac{1}{\omega - \frac{k}{\lambda}}\left(X + X \star \Lambda^-(s)\Lambda^-(s')G\right) && (3.38) \\ &+ \frac{i}{2}\frac{1}{\omega + \frac{k}{\lambda}}\left(X + X \star \Lambda^+(s)\Lambda^+(s')G\right) && (3.39) \\ &+ \frac{i}{\omega}\frac{\partial}{\partial s} G \star X_{s'}. && (3.40) \end{aligned}$$

To achieve this result the term with $G \star X_{s'}$ has been integrated by parts. The operator $\Lambda^{\pm}$ is short for

$$\Lambda^{\pm}(s) = \left(\frac{\partial}{\partial s} \pm \frac{s}{2}\right). \tag{3.41}$$

The choice of this operator is motivated by the property of the parabolic cylinder functions

$$\Lambda^+(s) D_q(\pm s) = \pm q D_{q-1}(\pm s), \tag{3.42}$$

$$\Lambda^-(s) D_q(\pm s) = \mp D_{q+1}(\pm s). \tag{3.43}$$

Applying Λ to the Green's function yields

$$\Lambda^+(s) G(q, s, s') = -\frac{\Gamma(-q)}{\sqrt{2\pi}} q \left(\theta(s - s') D_{q-1}(s) D_q(-s') - \theta(s' - s) D_{q-1}(-s) D_q(s')\right). \tag{3.44}$$

and

$$\begin{aligned} \Lambda^+(s)\Lambda^+(s') \quad & G_q(s, s') \\ = \; & -\frac{\Gamma(-q)}{\sqrt{2\pi}} q^2 \left(-\theta(s - s') D_{q-1}(s) D_{q-1}(-s') - \theta(s' - s) D_{q-1}(-s) D_{q-1}(s')\right) \\ + \; & \frac{\Gamma(-q)}{\sqrt{2\pi}} q \delta(s - s') \left(D_{q-1}(s) D_q(-s) + D_{q-1}(-s) D_q(s)\right), && (3.45) \end{aligned}$$

With the help of the Wronskian and the property of the Γ-function

$$z\Gamma(z) \;=\; \Gamma(z+1), \quad \text{or} \quad (-q)\Gamma(-q) = \Gamma(-q+1), \tag{3.46}$$

we find

$$\Lambda^+(s)\Lambda^+(s')G_q(s,s') \;=\; -\delta(s-s') + qG_{q-1}(s,s') \tag{3.47}$$
$$\Lambda^-(s)\Lambda^-(s')G_q(s,s') \;=\; -\delta(s-s') + (q+1)G_{q+1}(s,s') \tag{3.48}$$
$$\tag{3.49}$$

and finally

$$u(\bar\omega,k,s) \;=\; \sqrt{\frac{\lambda}{2\beta}}\left(\frac{k}{\bar\omega\lambda}\frac{\partial}{\partial s} - \frac{s}{2}\right)G_q \star Y$$
$$+ \;\frac{i}{2}\frac{1}{\omega-\frac{k}{\lambda}}\left((q+1)G_{q+1}\star X\right) \tag{3.50}$$
$$+ \;\frac{i}{2}\frac{1}{\omega+\frac{k}{\lambda}}\left(qG_{q+1}\star X\right) \tag{3.51}$$
$$+ \;\frac{i}{\omega}\frac{\partial}{\partial s}G_q\star X_{s'}. \tag{3.52}$$

Remains the determination of q from

$$2q+1 \;=\; \frac{\bar\omega^2\lambda^2 - k^2}{\lambda\beta} - \frac{k}{\lambda\bar\omega}. \tag{3.53}$$

For $\omega = 0$ this results in a singularity and the k-integrals have to be calculated first. For $\omega = k/\lambda$ we find $q = -1$ and $q = 0$ for $\omega = -k/\lambda$. Hence, with

$$-(q+1)\Gamma(-(q+1)) \;=\; \Gamma(-(q+1)+1) \to \Gamma(1) \tag{3.54}$$

we find for the $\omega = k/\lambda$-contribution

$$\frac{i}{2}\frac{1}{\omega-\frac{k}{\lambda}}\left((q+1)G_{q+1}\star X\right) \;\to\; \frac{i}{2}\frac{1}{\omega-\frac{k}{\lambda}}\left(\frac{1}{\sqrt{2\pi}}e^{-\frac{s^2+s'^2}{4}}\star X\right). \tag{3.55}$$

The $\omega = -k/\lambda$ does not contribute, since $\Gamma(-(q-1))$ remains finite for $q = 0$ and the explicit factor $q \to 0$ cancels this contribution out,

$$u(\bar\omega,k,s) \;=\; \sqrt{\frac{\lambda}{2\beta}}\left(\frac{k}{\bar\omega\lambda}\frac{\partial}{\partial s} - \frac{s}{2}\right)G_q \star Y + \frac{i}{\omega}\frac{\partial}{\partial s}G_q\star X_{s'}$$
$$+ \;\frac{i}{2}\frac{1}{\omega-\frac{k}{\lambda}}\left(\frac{1}{\sqrt{2\pi}}e^{-\frac{s^2+s'^2}{4}}\star X\right). \tag{3.56}$$

Similarly we get for the pressure

$$p(\bar\omega,k,s) \;=\; \sqrt{\frac{1}{2\lambda\beta}}\left(\frac{\partial}{\partial s} - \frac{k}{\bar\omega\lambda}\frac{s}{2}\right)G_q \star Y - \frac{i}{\lambda\omega}\frac{s}{2}G_q\star X_{s'}$$
$$- \;\frac{i}{2\lambda}\frac{1}{\omega-\frac{k}{\lambda}}\left(\frac{1}{\sqrt{2\pi}}e^{-\frac{s^2+s'^2}{4}}\star X\right) \tag{3.57}$$

In summary:

- the equator serves as a wave guide. The characteristic meridional extension is the equatorial Rossby radius $R_n = \sqrt{\beta\lambda}^{-1}$.
- Several wave types may be excited in this wave guide. Rossby waves may spread (group velocity) east- and west-ward. Kelvin waves are non-dispersive, localized in the equatorial wave guide and can spread only east-ward.
- From a uniform zonal wind even in absence of the Coriolis acceleration a meridional flow can be driven. It can be shown, that this flow is antisymmetric across the equator and drives upwelling confined to the equatorial wave guide.

3.6. Kelvin waves and equatorial currents

Considering a zonal wind patch over the equator with large meridional extension,

$$X = -\frac{u_*^2}{H_{mix}}\theta(t)\theta\left(z + H_{mix}\right)\theta(a - |x|). \qquad (3.58)$$

We will discuss only the contribution of the Kelvin waves. In this case the velocity and the pressure simplifies to

$$\begin{aligned} v(\bar{\omega}, k, s) &= \sqrt{\frac{\lambda}{2\beta}} G_q \star \frac{s'}{2} X = 0, \\ u(\bar{\omega}, k, s) &= \frac{i}{2}\frac{1}{\omega - \frac{k}{\lambda}}\left(\frac{1}{\sqrt{2\pi}} e^{-\frac{s^2+s'^2}{4}} \star X\right), \\ p(\bar{\omega}, k, s) &= -\frac{i}{2\lambda}\frac{1}{\omega - \frac{k}{\lambda}}\left(\frac{1}{\sqrt{2\pi}} e^{-\frac{s^2+s'^2}{4}} \star X\right). \end{aligned} \qquad (3.59)$$

Calculating the inverse Fourier transforms and the residuum around the $\omega - \frac{k}{\lambda}$-pole the result for u is

$$\begin{aligned} u(x, y, t) &= -\frac{u_*^2}{h}\Psi_0(y) \\ & \quad [\theta(t)\theta(a - |x|)t \\ &- \theta(x + a)\theta(t - \lambda(x + a))(t - \lambda(x + a)) \\ &+ \theta(x - a)\theta(t - \lambda(x - a))(t - \lambda(x - a))] \\ p(x, y, t) &= \frac{1}{\lambda} u(x, y, t) \\ w(x, y, t) &= -p_t = \frac{1}{\lambda} u_t = \frac{u_*^2}{h\lambda}\Psi_0(y) \\ & \quad [\theta(t)\theta(a - |x|) - \theta(x + a)\theta(t - \lambda(x + a)) + \theta(x - a)\theta(t - \lambda(x - a))] \end{aligned} \qquad (3.60)$$

The response is confined to a stripe near the equator described by the function $\Psi_0(y)$ from the convolution of the wind field with $e^{-\frac{s^2+s'^2}{4}}$. For u the result is a superposition of three components - a linearly growing jet within the wind patch and two eastward spreading Kelvin waves starting from $x = a$ and $x = -a$. The waves adjust the growing equatorial jet to a fixed value.

Performing the mode sum yields the following picture:

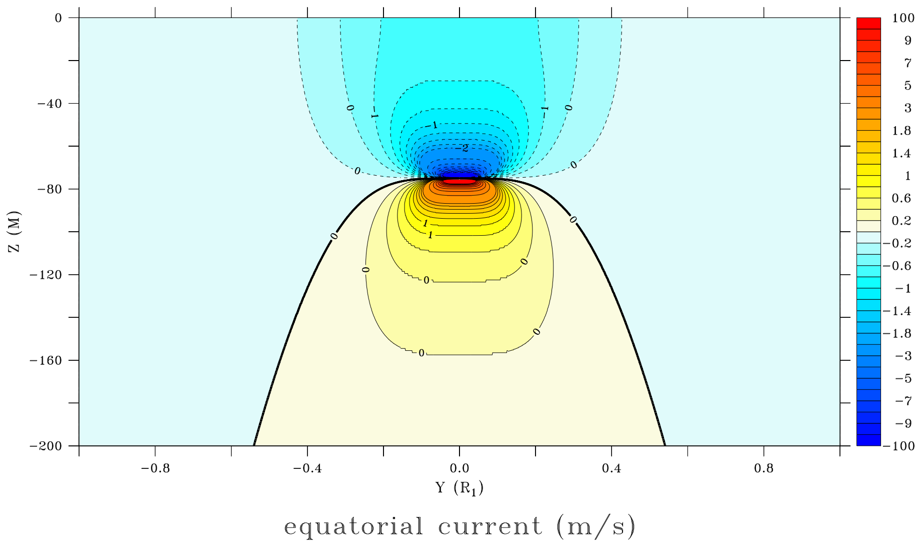

Figure 3.4. The analytical solution for the system of equatorial currents.

- There exists a strong west-ward surface current with an underlying strong east-ward under-current.
- The under-current is established by the Kelvin waves starting from the edges of the wind patch.
- Kelvin waves export the wind response from the area of the wind patch.

Chapter 4

The Antarctic Circumpolar current

4.1. ACC as a zonally periodic system

The Antarctiv Circumpolar Current (ACC) is one of the largest circulation systems of the world. It encircles Antarctica and connects this way all major oceans except the Arctic Ocean. Although the flow is basically a closed stream band, it exhibits strong lateral elevations and embedded eddies. It is strongest in narrow straits between continents, easpecially between the souther tip of South Americal and the Antarctic Peninsula. Here ADCP measurments reveal a permanent east-ward current, see Fig. 4.1. The ACC is approximately in geostrophic balance and can be seen as band with permanent gradient in the sea surface elevation around Antarctica, see Fig. 4.2. Its transport is about 120 Sv. However, snapshots reveal a strong eddy component of the flow, see Fig. 4.3. These eddies are drifting mainly westward and seem to obey Rossby wave dynamics. Differently from the subtropical gyres where the flow is confined to the surface layer, (see Sverdrup's catastrophy), the flow in the ACC extends to deep areas, partly over 2000 m depth. As the result the stratification is more "horizontal" than vertical and Antarctica is surrounded by a complex system of fronts. The northern boundary of the ACC is the so called "Polar front", the southern boundary the "Antarctic front", Fig. 4.4.

The dynamics of the ACC has been subject of intense reasearch and partly controversal discussions during the last decades. Especially its momentum balance is not finally understand yet. Nevertheless, the key processes seem to be clear now and some basic ideas will be outlined here. The ACC is situated within a belt of strong westerly (east-ward) wind around Antarctica. Actually this wind pattern is a sequence of localised low pressure areas born frequentyl in the permanent polar gyres. Those appear in the climatology as a contineous low pressure band with corresponding westerly winds. The first effect of the east-ward wind is an equatorward Ekman transport in the surface layer,

$$-fv_E = X. \tag{4.1}$$

Integrating this Ekman flow over a circle round Antarctica, say following the Polar front, it implies a permanent loss of water from the ACC system. This is not the case and the equator-ward Ekman transport must be compensated by a pole-ward flow in the ocean interiour, v_g or v_b. Here v_g is the approximately qeostrophically balanced flow in the ocean interiour and v_b the flow within a turbulent bottom boundary layer similarly to the Ekman transport in the surface layer. Averaging over a sufficient time period the total

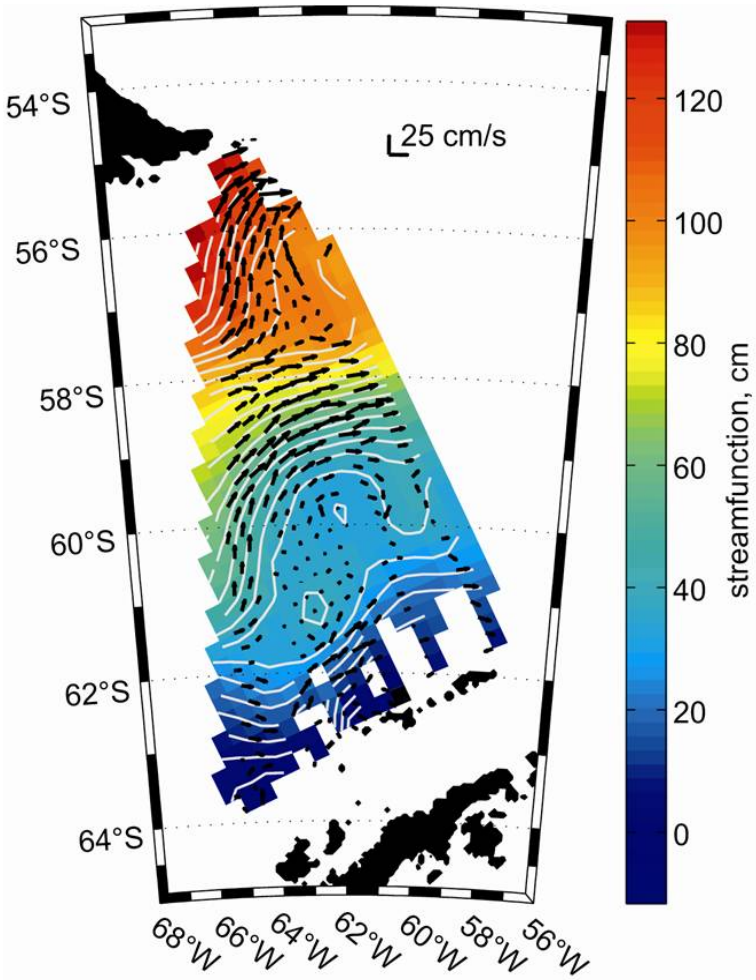

Figure 4.1. The surface component of the ACC in ADCP measurements in the Drake passage.

volume of the water within the ACC area must be constant,

$$\int_{-H}^{0} dz \left(< v >_E + < v >_g + < v >_b \right) \;=\; 0. \tag{4.2}$$

Here the brackets denote a zonally averaged quantity. This special and unique form of a budget - zonally periodic and meridionally semi-closed seems to be a key to understand the ACC. We will follow this idea with step-wise increased complexity of the analysis. We start from following system of Boussinesq equations

$$\frac{\partial}{\partial t}u + \nabla \cdot (\mathbf{u}u) - fv + \frac{\partial}{\partial x}p \;=\; \frac{\partial}{\partial z}\tau^x, \tag{4.3}$$

$$\frac{\partial}{\partial t}v + \nabla \cdot (\mathbf{u}v) + fu + \frac{\partial}{\partial y}p \;=\; \frac{\partial}{\partial z}\tau^y, \tag{4.4}$$

$$\frac{\partial}{\partial x}u + \frac{\partial}{\partial y}v + \frac{\partial}{\partial z}w \;=\; 0, \tag{4.5}$$

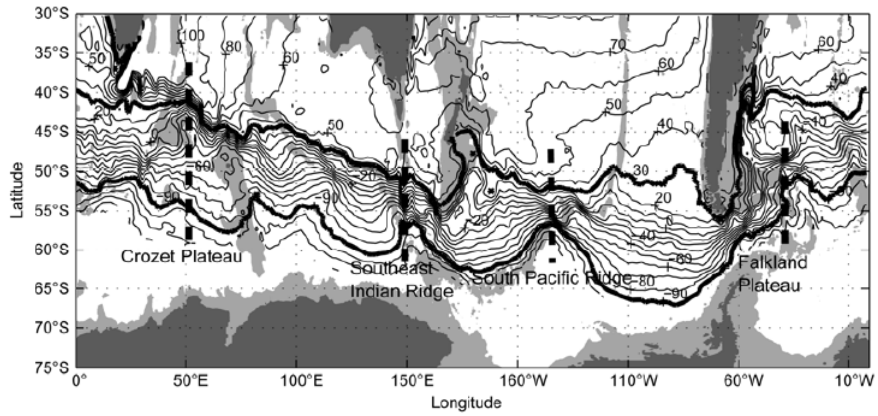

Figure 1 Mean SSH (cm) during 1993–2011 from AVISO (contours). Bold contours represent the northernmost and southernmost streamlines that pass through Drake Passage. Depths less than 3000 m are gray shaded. Dashed lines indicate four regions where the ACC strength has large interannual variations, as described in section 3.

Figure 4.2. The ACC seen in altimeter data. (Zhang et. al, 2012)

$$\frac{\partial}{\partial z} p = -g \tag{4.6}$$

τ is the turbulent vertical momentum flux. We assume, that the sea level elevation $\eta \ll H$ and neglect the upper part between $0 - \eta$ in vertical integrals. For consistency we use the rigid lid approximation $w(z = 0) = 0$. A more general derivation with variable sea surface height is possible. $< .. >$ denotes the zonal average, for vertically integrated quatities we use capital letters.

4.2. Flat bottom, low lateral friction

For an ocean with flat bottom the Boussinesq equations can be averaged zonally and integrated vertically. Since the flow is zonally periodic, some terms are eliminated this way,

$$\frac{\partial}{\partial t} < U > + \int_{-H}^{0} dz \frac{\partial}{\partial y} < vu > - f < V > = \tau_s^x - \tau_b^x, \tag{4.7}$$

$$\frac{\partial}{\partial t} < V > + \int_{-H}^{0} dz \left(\frac{\partial}{\partial y} < vv > + \frac{\partial}{\partial y} < p > \right) + f < U > = \tau_s^y - \tau_b^y, \tag{4.8}$$

$$\frac{\partial}{\partial y} < V > = 0, \tag{4.9}$$

$$p(z) = g\eta + \int_{z}^{0} dz' \frac{\rho(z')}{\rho_0}. \tag{4.10}$$

The remaining term of the continuity equation means, that the total meridional flow is independent off y and, hence, a constant. The existence if the rigid southern boundary Antarctica implies, that

$$< V > = 0. \tag{4.11}$$

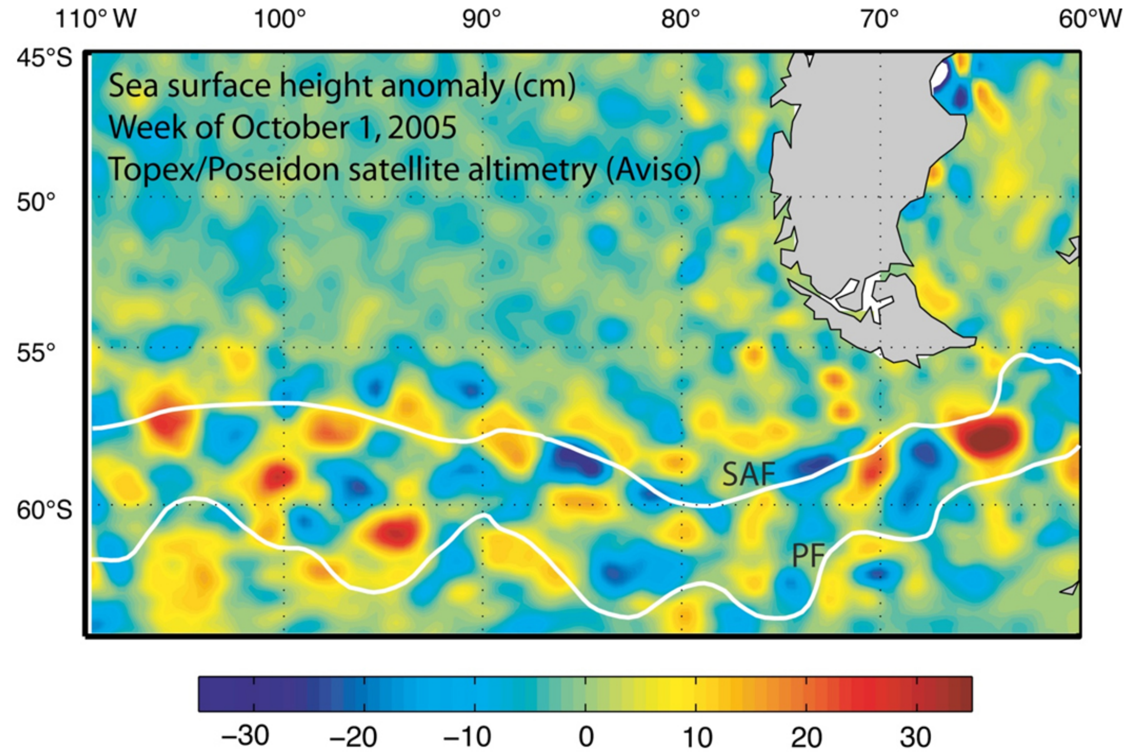

Figure 4.3. The ACC variability seen in altimeter data.

Considering a steady limit and neglecting the nonlinear terms for the moment, we find simple momentum budgets promising to reveal the basic physics behind governing the ACC,

$$-f < V > \; = \; 0 = \tau_s^x - \tau_b^x, \tag{4.12}$$

$$f < U > + gH \frac{\partial}{\partial y} < \eta > \; = \; \tau_s^y - \tau_b^y. \tag{4.13}$$

The first equation is simply the statement, that the momentum flux into the ocean from wind stress is balanced by a momentum flux out of the ocean from bottom friction. Although this equation is the zonal moentum equation, is does not simply define the velocity of the ACC. The second equation is the general geostrophic balance of the ACC valid in the ocean interiour except for the surface and the bottom boundary layers. Assuming a pure zonal wind, this equation defines the total transport of the ACC,

$$< U > \; = \; -\frac{gH}{f} \frac{\partial}{\partial y} \eta - \frac{\tau_b^y}{f}. \tag{4.14}$$

τ_s results from the wind field. The flow in the ACC will grow to such an extend, that bottom friction compensates exactly the momentum input from the wind.

The find the bottom friction we employ the classical Ekman theory of frictional boundayr layers in a rotating system. We consider the steady state solution only, since we are

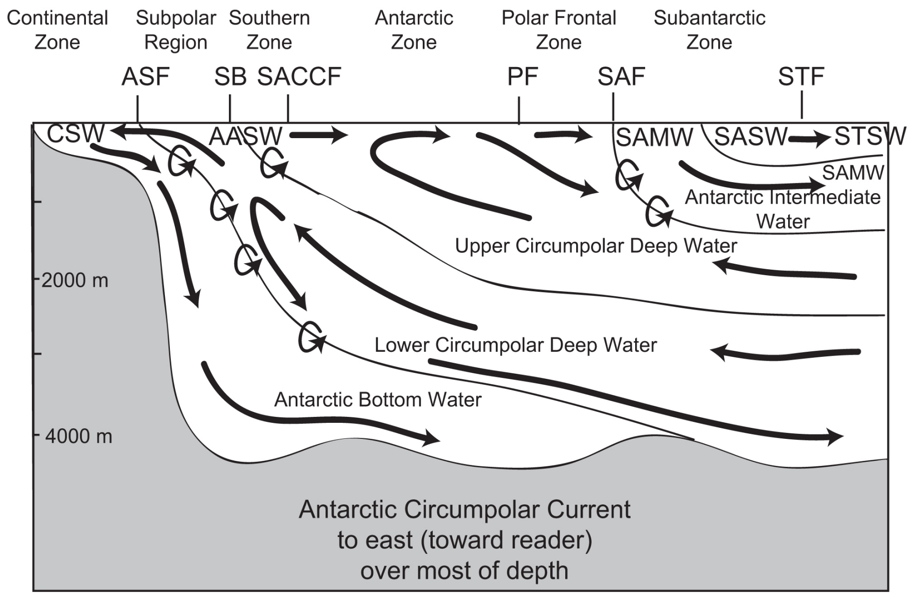

Figure 4.4. The system of fronts between water masses around Antarctica.

not interested in the high frequency inertial oscillations. A missing ingredient is the relation between the vertical momentum flux τ and the horizontal flow. We use the standard approximation

$$\tau = \nu \frac{\partial}{\partial z} \mathbf{u} \tag{4.15}$$

where ν is the turbulent viscosity. Omitting the nonlinear terms we get

$$-f < v > = \frac{\partial}{\partial z} \nu \frac{\partial}{\partial z} < u >, \tag{4.16}$$

$$f < u > + g \frac{\partial}{\partial y} < \eta > = \frac{\partial}{\partial z} \nu \frac{\partial}{\partial z} < v >, \tag{4.17}$$

$$\frac{\partial}{\partial y} < v > + \frac{\partial}{\partial z} < w > = 0. \tag{4.18}$$

From the Ekman boundary layer theory we know, that the friction terms are important only within thin boundary layers near the sea surface and the sea floor. Here the wind entrains turbulence or turbulence is formed from the shear between the flow in the ocean interiour and the bottom, where the horizontal flow vanishes,

$$< v > = 0, \quad < u >= 0 \quad \text{for} \quad z = -H. \tag{4.19}$$

This allows to split the total flow into a geostropic part and an ageostrophic part in the boundary layers,

$$< u > = u_g + u_b \tag{4.20}$$

$$< v > = v_g + v_b. \tag{4.21}$$

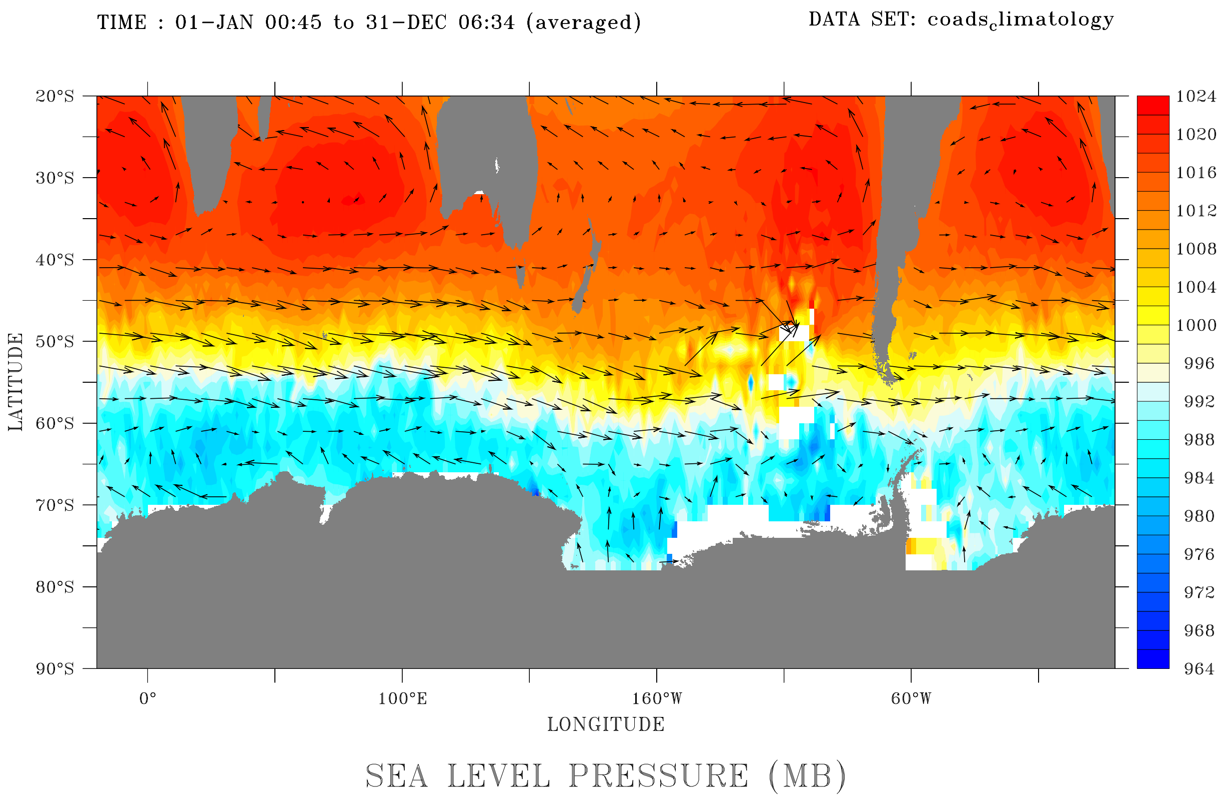

Figure 4.5. The west wind belt encircling Antarctica seen in the time averaged climatology. Actually this wind pattern is a sequence of localised low pressure areas encircling Antartica.

u_b and v_b are confined to a thin bottom layer, hence we require

$$< u > \; = \; u_g, \quad < v >= v_g \quad \text{for} \quad z \gg -H. \tag{4.22}$$

The geostrophic meridional flow vanishs, and we have $v_b =< v >$. The geostrophic zonal flow is balanced (per definition) with the meridional pressure gradient,

$$-f < v > \; = \; \frac{\partial}{\partial z}\nu\frac{\partial}{\partial z} < u >, \tag{4.23}$$

$$f < u > \; = \; f u_g + \frac{\partial}{\partial z}\nu\frac{\partial}{\partial z} < v > . \tag{4.24}$$

This system of equations is solved with the ansatz

$$< u(z) > \; = \; u_g + a e^{\lambda(z+H)}, \tag{4.25}$$

$$< v(z) > \; = \; b e^{\lambda(z+H)}. \tag{4.26}$$

Inserting gives an equation for λ,

$$\lambda^4 \; = \; -\frac{f^2}{\nu^2}, \tag{4.27}$$

i.e.

$$\lambda = \pm(1 \pm i)\frac{1}{d}, \tag{4.28}$$

$$d = \sqrt{\frac{2\nu}{|f|}} \tag{4.29}$$

From the boundary condition all solutions growing exponentially with z must have vanishing coefficients. The remaining part can be written as

$$< u(z) > = u_g \left(1 - e^{-\frac{z+H}{d}} \cos \frac{z+H}{d}\right), \tag{4.30}$$

$$< v(z) > = sig(f)\, u_g\, e^{-\frac{z+H}{d}} \sin \frac{z+H}{d}. \tag{4.31}$$

To find the vertical momentum flux we calculate the first derivative,

$$\tau^x = \nu \frac{\partial}{\partial z} < u(z) >= \frac{\nu u_g}{d} e^{-\frac{z+H}{d}} \left(\cos \frac{z+H}{d} + \sin \frac{z+H}{d}\right), \tag{4.32}$$

$$\tau^y = \nu \frac{\partial}{\partial z} < v(z) >= -sig(f)\frac{\nu u_g}{d} e^{-\frac{z+H}{d}} \left(\sin \frac{z+H}{d} - \cos \frac{z+H}{d}\right). \tag{4.33}$$

With this finding we can express the bottom stress in terms of the geostrophic flow in the ocean interiour,

$$\tau_b^x = \frac{\nu u_g}{d} = u_g \frac{d|f|}{2}, \tag{4.34}$$

$$\tau_b^y = sig(f)\frac{\nu u_g}{d} = u_g \frac{d\, f}{2}. \tag{4.35}$$

In the next step we use the exact balance of the wind stress and the bottom friction in zonal direction. Note, it is a consequence of the volume conservation in the ACC-area! Solving for the geostrophic quantities “zonal flow” and “ sea level elevation” we find,

$$u_g = \frac{2\tau_s^x}{d|f|}, \quad \frac{\partial}{\partial y}\eta = -sig(f)\frac{2\tau_s^x}{dg}. \tag{4.36}$$

The geostrophic flow is proportional to the wind stress and the inverse thickness ofthe bottom boundary layer as a measure for bottom friction. The sea level is rising north-ward at the southern hemisphere.

This result is interesting and suggests the possibility of geostrophic adjustment by bottom friction instead of inertial waves, Kelvin- or Rossby waves. It would explain the extension of the ACC into deep layers. From typical parameters like the observed width and depth of the ACC and friction parameters results a zonal transport and meridional overturning with a reasonable magnitude, but the surface tilt is much to small compared with altimeter observations. Choosing a smaller value for d enhances the tilt, but also the transport. Hence the theory is not complete and some important ingredient seems to be missing.

4.3. Lateral friction, Hidarkas dilemma

Some areas of the ACC exhibit a large eddy acitivity, hence, many mesoscale eddies are embedded in the mean current. These eddies may drift into the area north of the ACC and carry some momentum of the ACC. In turn water with low zonal momentum may enter the ACC with the tendency of slowing down the amin current. This way the exchange of eddies between the ACC and the adjacent seas acts like a meridional diffusion of momentum, or like friction between the ACC and the adjacent sea. This meridional momentum flux becomes part of the total momentum budget an is an alternative for the bottom friction to balance the wind driven acceleration.

Adding the therm

$$A_h \frac{\partial^2 u}{\partial y^2} \tag{4.37}$$

to the right hand side of the zonal momentum equation gives the balance equations

$$-f < V > \; = \; 0 = \tau_s^x - \tau_b^x + A_h \frac{\partial^2 < U >}{\partial y^2}, \tag{4.38}$$

$$f < U > + gH \frac{\partial}{\partial y} < \eta > \; = \; \tau_s^y - \tau_b^y. \tag{4.39}$$

For zero bottom stress, the system can be solved for simple assumptions on the form of the wind field. Choosing realistic value for $A_h = 10^4 \mathrm{m}^2 \mathrm{s}^{-1}$ derived from the observed eddy size and probability the calculated transport of the ACC amounts $\approx$ 2500 Sv which is completely unrealistic. Increasing A_h may give realistic transport values, but the resulting tilt of the sea surface becomes much to high. This finding is called in the literature "Hidarkas dilemma" - it is impossible to find a momentum budget of the ACC based on friction, that is compatible with the measurements for the transport of the ACC, the meridional surface tilt and the observed eddy size and activity within the ACC.

4.4. Topographic form stress

Figure 4.6 shows the position of the polar front as the northern rim of the ACC derived from microwave sea surface temperature data. Obviously it follows the bottom topography which suggests the hypothesis, that the ACC interacts strongly with the bottom topography. Indeed the ACC is not confined to the surface but extends into the depth.

Introducing a zonally variable bottom topography

$$z \; = \; -H(x,y), \tag{4.40}$$

the vertical and zonal average of the pressure gradient reads,

$$< P > \; = \; \int dx \int_{-H}^{0} dz \, p_x = \int dx \left(\frac{\partial}{\partial x} \int_{-H}^{0} dz \, p - p(x,y,-H) \frac{\partial}{\partial x} H(x,y) \right). \tag{4.41}$$

The first term vanishes for a periodic integral, the second term

$$\tau_f \; = \; - < p \frac{\partial}{\partial x} H > = < H \frac{\partial}{\partial x} p > \tag{4.42}$$

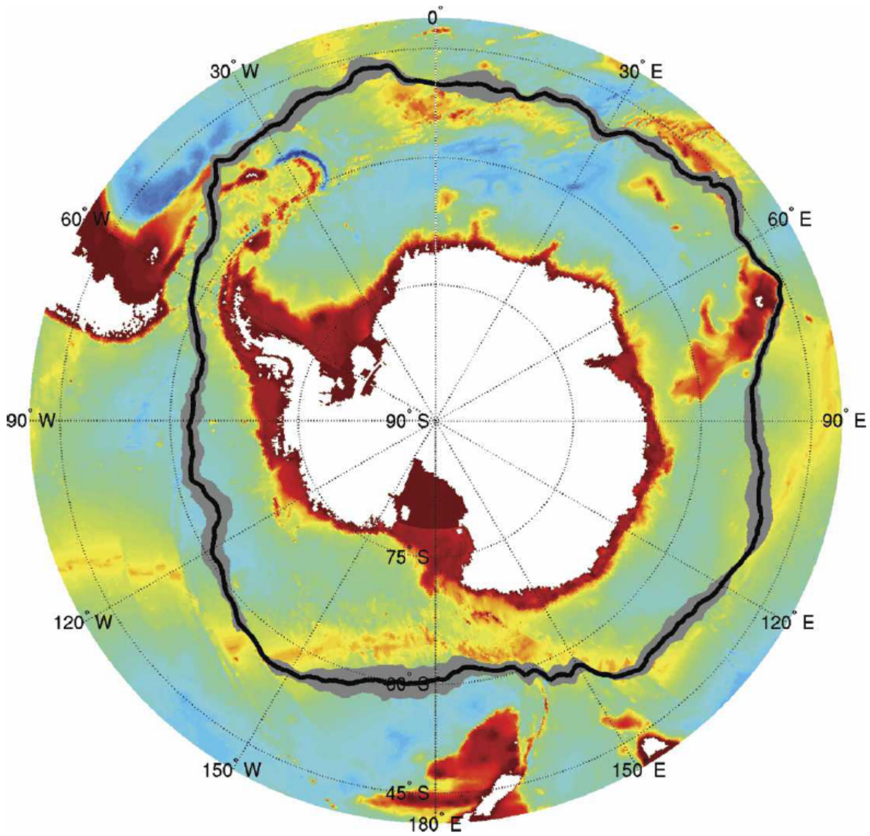

FIG. 5. Mean PF (black line) from the 3 yr of AMSR-E SST measurements and bottom topography (colors). The shaded area shows one std dev of the PF location.

Figure 4.6. The polar front seen in microwave data and its relation to bottom topography. (Dong et. al, 2005)

is called the bottom form stress. Hence, the momentum balance for the ACC with variable bottom topography reads

$$\tau_f - A_h \frac{\partial^2 < U >}{\partial y^2} = \tau_s^x - \tau_b^x, \tag{4.43}$$

$$f < U > + gH \frac{\partial}{\partial y} < \eta > = \tau_s^y - \tau_b^y. \tag{4.44}$$

So far we have introduced a new term into the balance equations, but the calculation of this term is not simple. Neither the bottom presssure nor its derivative can be experssed in one of the zonally averaged quantities. Our system of equations is not complete and the determination of the bottom form stress requires the detailed knowledge of the current (pressure) field.

The calculation of the bottom pressure field for realistic topography is a complex task and is solved mostly numerically. Even for very simple topography like a ridge or symmetric obstacle the solution reveals as complex. A first guess for the solution can be derived from the fact, that a steady geostrophic vertically averaged flow follows approximately contours of f/H. Hence, the stream function must be some function of f/H. Neglecting for a moment the meridional variability of f, we find

$$\tau_f \approx < g(H)\frac{\partial}{\partial x}H >=< \frac{\partial}{\partial x}G(H) >= 0. \tag{4.45}$$

Hence, a purely topographically steered flow does not produce any form stress. Some mechanism must be taken into account that generates a zonal shift of the pressure field against the topography causing a “phase shift” between the pressure and the topography. Candidates for processes generating this shift is bottom friction and lateral friction, but also Rossby waves propagating west-ward within the eastward ACC. The design of such so called “low order models” to find solutions of this problem exceeds the frame of these lecture.

Chapter 5

The oceanic wave guide

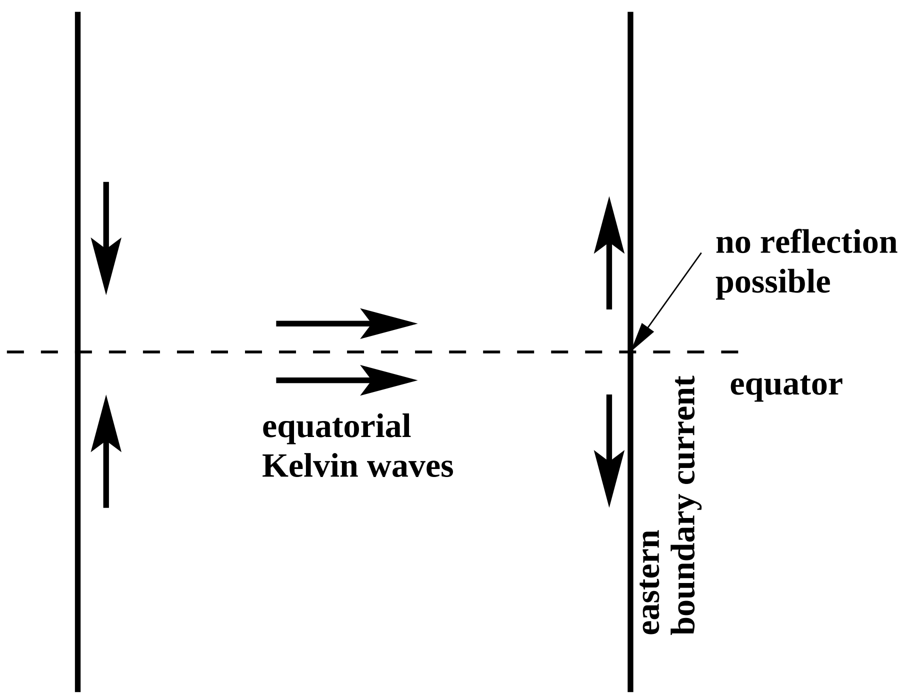

Figure 5.1. The equatorial wave guide and the eastern boundary currents.

In the previous chapters the ocean response to wind forcing was governed by waves. These waves may carry signals on wind events into areas far away from the wind forcing. Examples are coastal or equatorial Kelvin waves exporting up- or downwelling signals, adjusting jet-like surface currents or generating undercurrents. Rossby waves may cross the oceans generating strong western boundary currents. Putting all these pieces together there emerges a new view on the ocean. There are several wave guides connecting distant areas of the ocean. The group speed of the waves defines times scales for the connectivity.

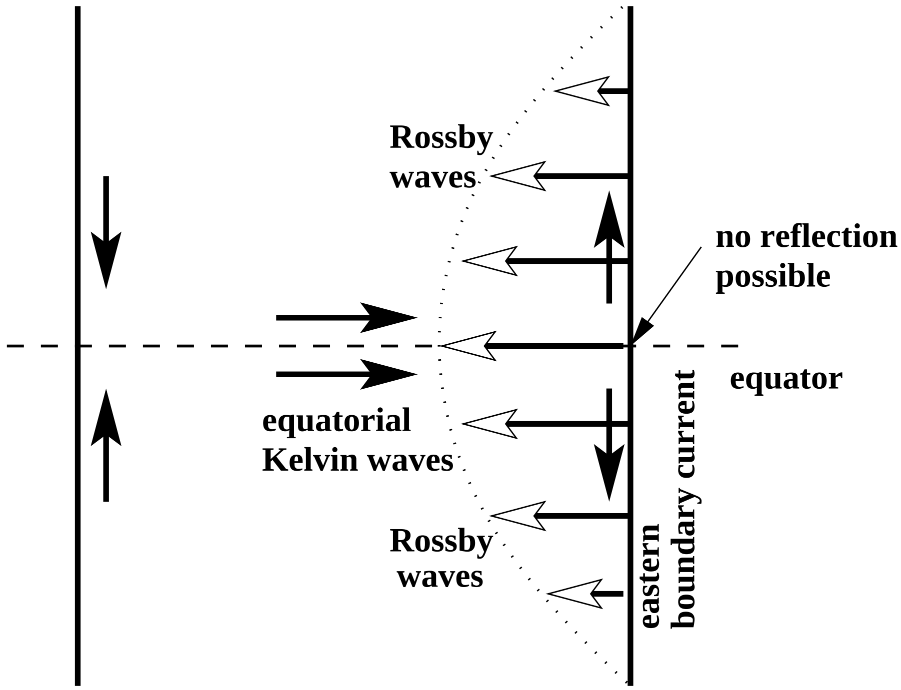

Figure 5.2. The equatorial wave guide, eastern boundary currents and Rossby waves closing the cycle.

This transport of signals and energy over long distances may have consequences for the state of the ocean on long time scales, hence, may be relevant for the ocean component of the earth climate. Fig. 5.1 shows the equatorial wave guide. Kelvin waves propagating equator-wards at the west coast cannot cross the equator but may bend east-ward and cross the ocean toward the east coast. Similarly, signals generated in the equatorial ocean propagate toward the east coast. At the east coast, Kelvin waves cannot be reflected because they have only east-ward phase and group velocity. Moreover, it can be shown that west-ward moving Rossby wave cannot be excited. Hence, the wave energy accumulates at the east coast and is the source of pole-ward moving Kelvin waves, now trapped at the oceans east coast.

This mechanism is one driver of the El Niño phenomenon observed in the Pacific ocean. Weaken trade winds over the equator disturb the balance of the barotropic (sea level) and baroclinic (tilt of the thermocline) gradients. As a result a wave is generated that goes along with an pulse of warm water in the east-ward undercurrent. Hence, at the coast of South America a a warm temperature anomaly can be observed. The undercurrent bends pole-ward and can propagate the warm water north- and south-ward. A result is reduced upwelling and a thick layer of warm nutrient depleted surface water with far reaching consequences for the food chain at the coast of Peru. There is a strong feedback to the atmosphere circulation altering the weather for months or even longer.

This so called El Niño Southern Oscillation (ENSO) is subject of climate research since many years. One key for the understanding are Kelvin waves in the equatorial and coastal wave guides which convey the directed transfer of energy and matter between the western and the eastern part of the Pacific. A similar, but less energetic phenomenon is known for the Atlantic ocean, the so called Benguela Niños.

As it was shown previously, a disturbance at an eastern coast generates Rossby waves that propagate west-ward. Without a proof or derivation we note that after a much longer time than the Kelvin waves need to cross the Pacific, the Rossby waves arrive at the west-coast and generate Kelvin waves there that move again equator-ward and cross the equator within the equatorial wave guide, but now carrying a signal in the oposite direction. Hence, we have a closed cycle of signal propagation. There is a phase shift from the finite wave group velocity. Positive feedbacks to the atmosphere may counteract to wave damping and the ocean with its system of wave guides may behave like some oscillator. Although the Kelvin- and Rossby waves can be described with linear Boussinesq equations the coupling to the atmosphere with positive feedback introduce non-linearity. This way we stumble into the wide field of the theory of non-linear systems with possibly chaotic or unpredictable behaviour. To deal with such systems requires an approach beyond this lecture.

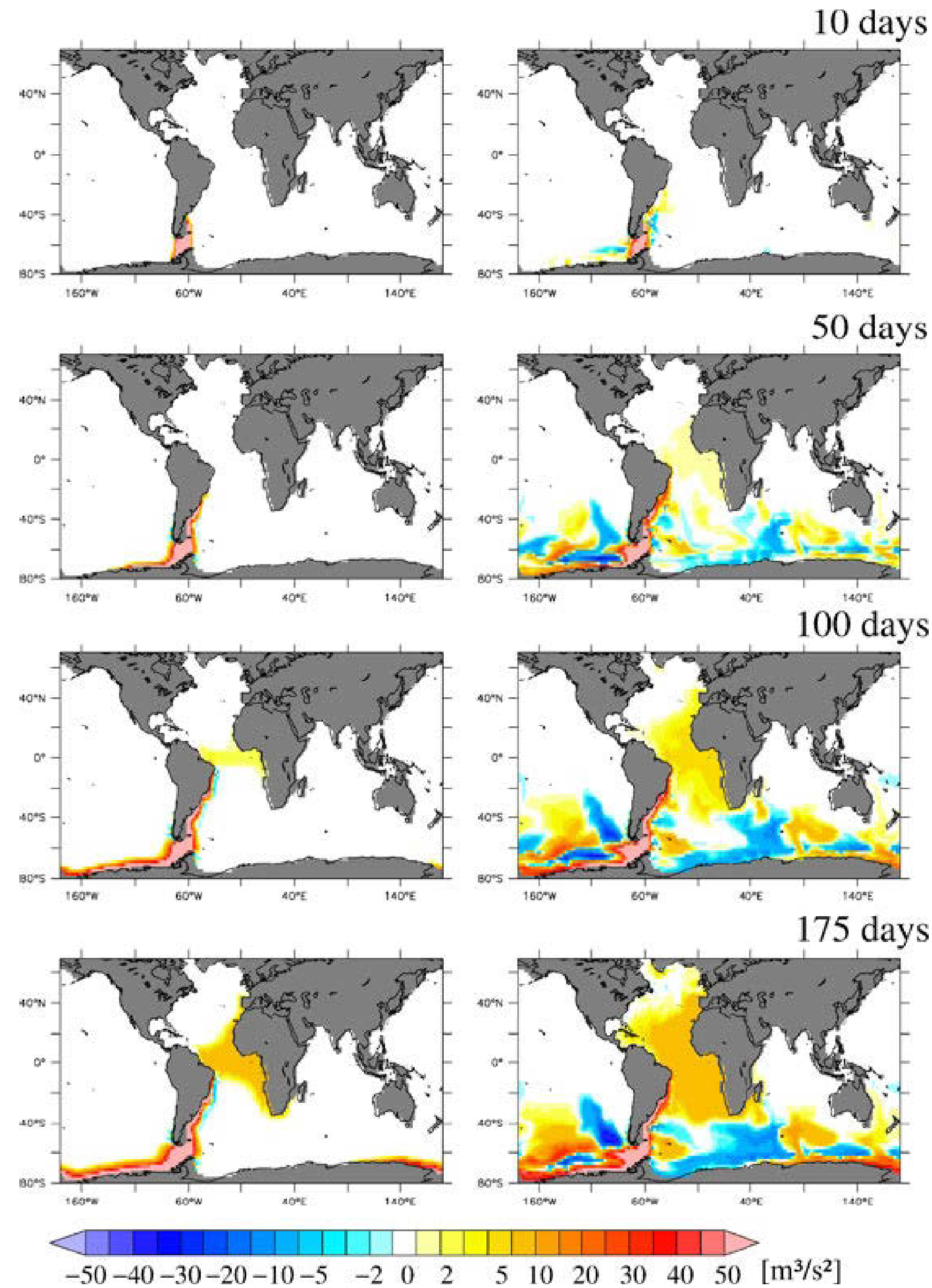

Fig. 8.22 Aspects of oceanic wave propagation, as simulated with the BARBI model (see Ap pendix B.2). The wave is initiated in Drake Passage by a baroclinic perturbation and propagates i the ocean wave guide around the globe. Left without topography, right with realistic topography Both simulations are for a mean state with prescribed Brunt–Väisälä frequency without any mea flow

Appendix A

Einige in der Vorlesung häufig verwendete Fourierintegrale

$$F(t) \quad = \quad \int\limits_{-\infty}^{\infty} \frac{d\omega}{2\pi} e^{-i\omega t} \tilde{F}(\omega) \; , \; \tilde{F}(\omega) = \int\limits_{-\infty}^{\infty} dt e^{i\omega t} F(t)$$

$F(t)$	$\tilde{F}(\omega)$
1	$2\pi\delta(\omega)$
e^{ift}	$2\pi\delta(\omega+f)$
$\cos(ft)$	$\pi\left(\delta(\omega+f)+\delta(\omega-f)\right)$
$\sin(ft)$	$\frac{\pi}{i}\left(\delta(\omega+f)-\delta(\omega-f)\right)$
t^n	$\frac{2\pi}{i^n}\frac{d^n}{d\omega^n}\delta(\omega)$
$\theta(t)$	$\frac{i}{\omega+i\epsilon}$
$\theta(t)\sin(ft)$	$\frac{-f}{(\omega+i\epsilon)^2-f^2}$
$\theta(t)\cos(ft)$	$\frac{i\omega}{(\omega+i\epsilon)^2-f^2}$
$\theta(t)t$	$\frac{-1}{(\omega+i\epsilon)^2}$

Für die entsprechenden räumlichen Integrale ist $x = t$ und $k = -\omega$ zu wählen.

Fennel, W., Lass, H.U., 1989. *Analytical theory of forced oceanic waves.* Akademie-Verlag.